1983

Simulation of plenum thermo-hydraulics in a liquid metal fast breeder reactor under a buoyancy-affected condition

Min-jen Chen
Iowa State University

INFORMATION TO USERS

This reproduction was made from a copy of a document sent to us for microfilming. While the most advanced technology has been used to photograph and reproduce this document, the quality of the reproduction is heavily dependent upon the quality of the material submitted.

The following explanation of techniques is provided to help clarify markings or notations which may appear on this reproduction.

1. The sign or "target" for pages apparently lacking from the document photographed is "Missing Page(s)". If it was possible to obtain the missing page(s) or section, they are spliced into the film along with adjacent pages. This may have necessitated cutting through an image and duplicating adjacent pages to assure complete continuity.

2. When an image on the film is obliterated with a round black mark, it is an indication of either blurred copy because of movement during exposure, duplicate copy, or copyrighted materials that should not have been filmed. For blurred pages, a good image of the page can be found in the adjacent frame. If copyrighted materials were deleted, a target note will appear listing the pages in the adjacent frame.

3. When a map, drawing or chart, etc., is part of the material being photographed, a definite method of "sectioning" the material has been followed. It is customary to begin filming at the upper left hand corner of a large sheet and to continue from left to right in equal sections with small overlaps. If necessary, sectioning is continued again—beginning below the first row and continuing on until complete.

4. For illustrations that cannot be satisfactorily reproduced by xerographic means, photographic prints can be purchased at additional cost and inserted into your xerographic copy. These prints are available upon request from the Dissertations Customer Services Department.

5. Some pages in any document may have indistinct print. In all cases the best available copy has been filmed.

University
Microfilms
International
300 N. Zeeb Road
Ann Arbor, MI 48106

Chen, Min-jen

SIMULATION OF PLENUM THERMO-HYDRAULICS IN A LIQUID METAL FAST BREEDER REACTOR UNDER A BUOYANCY-AFFECTED CONDITION

Iowa State University PH.D. 1983

Simulation of plenum thermo-hydraulics in a liquid metal fast breeder reactor under a buoyancy-affected condition

by

Min-jen Chen

A Dissertation Submitted to the
Graduate Faculty in Partial Fulfillment of the
Requirements for the Degree of
DOCTOR OF PHILOSOPHY

Major: Nuclear Engineering

Approved:

Signature was redacted for privacy.

In Charge of Major Work

Signature was redacted for privacy.

For the Major Department

Signature was redacted for privacy.

For the Graduate College

Iowa State University
Ames, Iowa

1983

TABLE OF CONTENTS

NOMENCLATURE

C_p	heat capacity at constant pressure
g_r	gravitational acceleration in r direction
g_θ	gravitational acceleration in θ direction
g_z	gravitational acceleration in Z direction
H	heat, basic dimension for dimensional analysis
h	heat transfer coefficient
k	thermal conductivity
k_t	turbulent thermal conductivity
L	characteristic length
	length, basic dimension for dimensional analysis
M	mass, basic dimension for dimensional analysis
P	pressure
$\bar{p}$	dimensionless dynamic pressure
Pe	Peclet Number
Pr	Prandtl Number
Q	volumetric flow rate
$\dot{Q}$	volumetric heat source
R	ratio of conduction to convection

Re	Reynolds Number
Ri	Richardson Number
r	radial coordinate ratio
T	temperature
	temperature, basic dimension for dimensional analysis
T_o	initial temperature
t	time
u	velocity in r direction
v	velocity in θ direction
w	velocity in z direction
w_o	initial velocity in z direction
z	axial coordinate
α	thermal diffusivity
η	dimensionless position variable in radial direction
ζ	dimensionless position variable in azimuthal direction
ξ	dimensionless position variable in axial direction
Θ	temperature, basic dimension for dimensional analysis
θ	azimuthal coordinate
μ	viscosity
μ_t	turbulent viscosity

π Pi term of the dimensional analysis

ρ density of fluid

ρ initial density of fluid

τ dimensionless time

ϕ normalized temperature

I. INTRODUCTION

An accurate prediction of Liquid Metal Fast Breeder Reactor (LMFBR) upper plenum thermal response is essential for reliable thermal design of plenum and primary components. The main concern is that upper plenum flow stratification following a reactor scram may cause severe thermal shock to the components, especially the outlet nozzles. The establishment of a hot-cold interface may also cause fatigue damage to the vessel and the components exposed to thermal discontinuity. In addition, upper plenum stratification may also introduce problems for a reactor to restart after a scram.

During a normal scram, the outlet plenum experiences an abrupt decrease in the entering sodium temperature along with a flow coastdown. The entering cool dense sodium fluid does not have sufficient momentum to overcome the negative buoyant forces and flow stratification is created. Instead of penetrating into the plenum and mixing with the hot sodium fluid therein, the entering sodium fluid is deflected downward and outward toward the exit nozzles in a mushroom-shaped stratified flow pattern.

The investigation of this safety issue consists of both experimental and analytical studies. Both studies start with governing equations for mass, momentum and energy with requisite boundary and initial conditions.

A series of studies were conducted to evaluate the problem of flow stratification [1, 2, 3, 4, 5]. Those programs were directed

toward: (a) studying the temperature response within the plenum during reactor scrams, with emphasis on exit nozzle transients; (b) correlating water and sodium behavior; and (c) computer code validation. The basis is shown graphically in Figure 1.

After extensive study on this issue, it was found that the largest uncertainties and the most critical phenomena which needs to be resolved are the adequacy of extrapolating the test data to the full scale prototype behavior for low flow, stratification conditions [3].

Several tests at a reduced scale were conducted at the Argonne National Laboratory and the Battelle - Columbus Laboratory. The tests were used to demonstrate the adequacy of using water in place of sodium as a test fluid [4, 5]. It was concluded that water could be used to accurately stimulate sodium for normal and full flow scram transients [6]. It was also concluded that highly convective flow at normal reactor scrams completely overshadowed the conductive heat transfer within the fluid. These tests, coupled with the laws of similitude, established the bases of all ANL water tests [7].

However, extending this finding to include water simulation at natural circulation may be inadequate. For example, at extremely low velocities and under thermal stratification conditions, the heat conduction between the hot and cold layers of sodium could alter the temperature field within the plenum. There is a possibility that as the heat transfer within the plenum becomes more conductive in

nature, water may become inappropriate as a test medium. The concept of using a small scale sodium test facility was subsequently introduced [3].

The purpose of this study is to provide the method to resolve this issue. A three dimensional thermo-hydraulic computer code PREMIX which is a simplified version of COMMIX-1A [8] has been developed for analyzing important factors which affect the flow and temperature fields in a reactor plenum. Scaling requirements have also been examined. The computer code was validated through comparisons with measured temperature distributions in a plenum simulation test. It was also shown that the adequacy of scaling laws can be determined by analytical tools despite the complexity of physical phenomena involved.

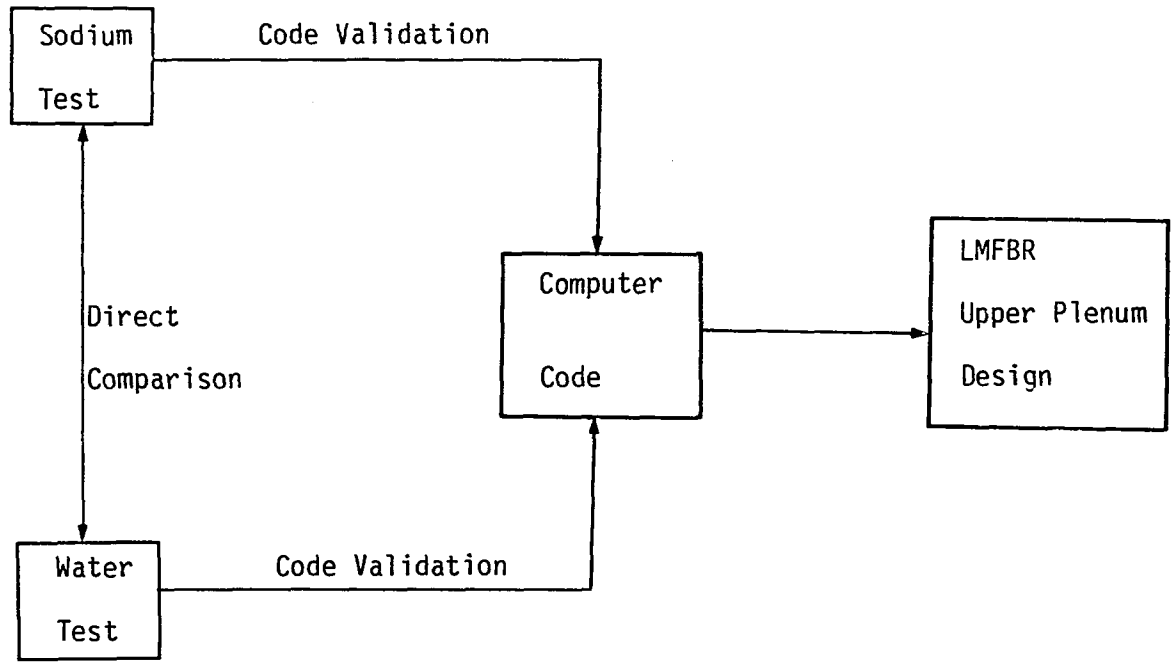

Figure 1. Basis for the upper plenum thermohydraulic simulation

II. ANALYTICAL MODEL

A. Code Development

Previous analytical models available for analyzing a reactor plenum were mostly one-dimensional or two-dimensional models [9, 10]. The applicability of these models is limited as three-dimensional effects in a reactor plenum become important. The shortcomings of the one-dimensional and two-dimensional models are particularly serious in that these models fail to account for effects of thermal stratification, the plenum height-to-diameter ratio and the inlet/outlet flow rates.

For the purpose of understanding the thermo-hydraulic behavior inside a reactor plenum, and for the sake of identifying and evaluating important parameters which affect the advanced plenum design, a rigorous and flexible computer code was developed. PLENMIX is a simplified version of COMMIX-1A [8], a rigorous, three-dimensional, single-phase, transient, thermal-hydraulic analysis computer code. It was developed for continuum analysis (e.g., tanks, pipes, etc.) in general, and for plenum analysis in particular, while COMMIX-1A was for general-purpose components analysis (e.g. fuel bundles, heat exchangers, pipes, etc.). A set of governing equations for the conservation of mass, momentum, and energy is solved as a boundary value problem in space and as an initial value problem in time. The model can handle both

cylindrical and Cartesian coordinates. Thermal interactions are taken into account between fluid and structure material. A simple effective viscosity turbulence model was employed in this code to account for turbulence viscosity and turbulence conductivity.

B. Governing Equations

The governing equations of conservation of mass, momentum, and energy for transient, three-dimensional flow in cylindrical coordinates are given as follows:

1. The Continuity Equations

$$\frac{\partial \rho}{\partial t} + \frac{1}{r}\frac{\partial}{\partial r}(\rho r u) + \frac{1}{r}\frac{\partial}{\partial \theta}(\rho v) + \frac{\partial}{\partial z}(\rho w) = 0 \qquad (1)$$

where t = time

r, θ, z = radial, azimuthal, and axial coordinates, respectively;

u, v, w = velocities in r, θ, and z directions, respectively;

ρ = density of fluid.

2. The Momentum Equations

r - Momentum Equation

$$\frac{\partial}{\partial t}(\rho u) + \frac{1}{r}\frac{\partial}{\partial r}(\rho r u^2) + \frac{1}{r}\frac{\partial}{\partial \theta}(\rho u v) + \frac{\partial}{\partial z}(\rho u w) - \frac{\rho v^2}{r}$$

$$= -\frac{\partial P}{\partial r} + \left[\frac{1}{r}\frac{\partial}{\partial r}\left(\mu r \frac{\partial u}{\partial r}\right) + \frac{1}{r^2}\frac{\partial}{\partial \theta}\left(\mu \frac{\partial u}{\partial \theta}\right) + \frac{\partial}{\partial z}\left(\mu \frac{\partial u}{\partial z}\right)\right.$$

$$\left. - \frac{2\mu}{r^2}\frac{\partial v}{\partial \theta} - \mu \frac{u}{r^2}\right] + \rho g_r \qquad (2)$$

θ - Momentum Equation

$$\frac{\partial}{\partial t}(\rho v) + \frac{1}{r}\frac{\partial}{\partial r}(\rho r u v) + \frac{1}{r}\frac{\partial}{\partial \theta}(\rho v^2) + \frac{\partial}{\partial z}(\rho v w) + \frac{\rho u v}{r}$$

$$= -\frac{1}{r}\frac{\partial P}{\partial \theta} + \left[\frac{1}{r}\frac{\partial}{\partial r}\left(\mu r \frac{\partial v}{\partial r}\right) + \frac{1}{r^2}\frac{\partial}{\partial \theta}\left(\mu \frac{\partial v}{\partial \theta}\right)\right.$$

$$\left. + \frac{\partial}{\partial z}\left(\mu \frac{\partial v}{\partial z}\right) + \mu \frac{2}{r^2}\frac{\partial u}{\partial \theta} - \mu \frac{v}{r^2}\right] + \rho g_\theta \qquad (3)$$

z - Momentum Equation

$$\frac{\partial}{\partial t}(\rho w) + \frac{1}{r}\frac{\partial}{\partial r}(\rho r u w) + \frac{1}{r}\frac{\partial}{\partial \theta}(\rho v w) + \frac{\partial}{\partial z}(\rho w^2)$$

$$= -\frac{\partial P}{\partial z} + \left[\frac{1}{r}\frac{\partial}{\partial r}\left(\mu r \frac{\partial w}{\partial r}\right) + \frac{1}{r^2}\frac{\partial}{\partial \theta}\left(\mu \frac{\partial w}{\partial \theta}\right) + \frac{\partial}{\partial z}\left(\mu \frac{\partial w}{\partial z}\right)\right]$$

$$+ \rho g_z \qquad (4)$$

where P = pressure;

g_r, g_θ, g_z = component of gravitational acceleration in the r, θ, z direction

μ = effective viscosity consisting of laminar and turbulent components

3. Energy Equation

$$\frac{\partial}{\partial t}(\rho h) + \frac{1}{r}\frac{\partial}{\partial r}(\rho ruh) + \frac{1}{r}\frac{\partial}{\partial}(\rho vh) + \frac{\partial}{\partial z}(\rho wh)$$

$$= \frac{\partial P}{\partial t} + \frac{1}{r}\frac{\partial}{\partial r}(kr\frac{\partial T}{\partial r}) + \frac{1}{r^2}\frac{\partial}{\partial \theta}(k\frac{\partial T}{\partial \theta}) + \frac{\partial}{\partial z}(k\frac{\partial T}{\partial z}) + \dot{Q} \qquad (5)$$

where h = enthalpy

k = thermal conductivity of fluid

$\dot{Q}$ = volumetric heat source.

4. Thermal Interaction Between Fluid and Structures

A one-dimensional model presented below has been developed to simulate the convective heat transfer between structure material (e.g. wall) and the contained fluid. Heat transfer within the wall structure is neglected in the axial and peripheral directions. The only thermal interaction allowed within the wall structure is from the coolant in the vicinity of the wall.

Such a simplification greatly facilitates computations and reduces computer storage requirements while still allowing essential

physical processes to be represented.

Consider a wall element having volume V and heat transfer area A, the energy balance for this wall element can be written:

$$\rho_W C_W V \frac{\partial T_W}{\partial t} = \frac{1}{\frac{1}{h} + R_W^{\cdot}} (T_f - T_W) + VQ_W \tag{6}$$

where ρ = density of wall

C_W = heat capacity of wall

T_W = temperature of wall

t = time

h = heat transfer coefficient between wall and fluid

R_W = thermal resistance of wall

T_r = temperature of fluid

Q_W = volumetric heat source of wall

Define $\bar{h} = \frac{1}{\frac{1}{h} + R_W}$ (7)

$$\lambda = \frac{\rho_W C_W V}{\bar{h} A} \tag{8}$$

Eq. (6) gives

$$\frac{\partial T_W}{\partial t} + \frac{1}{\lambda} T_W = \frac{1}{\lambda} \left(T_f + \frac{V}{\bar{h} A} Q_W\right) \tag{9}$$

Solving eq. (9) for $T_W (t + \Delta t)$ with known $T_W (t)$ yields

$$T_W(t + \Delta t) = \left(T_f + \frac{V}{\bar{h} A} Q_W\right) + T_W(t)$$

$$- \left(T_f + \frac{V}{\bar{h}A} Q_w\right) \exp\left(-\frac{\Delta t}{\lambda}\right) \tag{10}$$

The heat flux from the wall to the coolant is

$$q = -\bar{h}\left[T_f - T_w\,(t + \Delta t)\right]$$

$$= \bar{h}\left[T_w\,(t) - \left(T_f + \frac{V}{\bar{h}A} Q_w\right) \exp\left(\frac{\Delta t}{\lambda}\right)\right] + \frac{V}{A} Q_w \tag{11}$$

5. Sodium Properties

The sodium properties used in the code were taken from the works by Golden and Tokar [11] . The properties are given in the following expressions:

Density (kg/m^3)

$$\rho\,(T) = 9.50076 \times 10^2 + T\left[-2.2976 \times 10^{-1} + T(-1.46049 \times 10^{-5} + 5.63788 \times 10^{-9}\,T)\right] \tag{12}$$

Viscosity (Pa / s)

$$\mu\,(T) = 3.2419 \times 10^{-3} \exp\left[5.080 \times 10^2 / (T + 273.15) - 0.4925 \ln (T + 273.15)\right] \tag{13}$$

Specific Heat (J/kg · K)

$$C_p(T) = 1.43605 \times 10^3 + T\left[-5.802 \times 10^{-1} + 4.62506 \times 10^{-4}T\right] \tag{14}$$

Conductivity (W/M · K)

$$k(T) = 92.948 - 5.809 \times 10^{-2}T + 1.1727 \times 10^{-5}T^2 \tag{15}$$

where T is temperature, in degrees Celsius.

6. Water Properties

The water properties in the liquid phase are taken from the works of Keenan et al. [12]. Curve fitting techniques were used to develop the following expressions:

Density (kg/m^3)

$$\rho(T) = 1000 - .3456T \tag{16}$$

Viscosity ($Pa \cdot s$)

$$\mu(T) = \begin{cases} 1.75 \times 10^{-3} \exp\ -0.0259T\ , & T\epsilon(0,40\ ) \\ 1.177 \times 10^{-3} \exp\ -0.0148T\ , & T\epsilon(40,100) \end{cases} \tag{17}$$

Specific Heat ($J/kg \cdot K$)

$$C_p(T) = 4190.0 \tag{18}$$

Conductivity ($W/M \cdot K$)

$$k(T) = 0.569 + 1.11 \times 10^{-3}T \tag{19}$$

where T is temperature, in degrees Celsius.

7. Effective Turbulence Viscosity Model

The effective viscosity μ which occurs in Eqs. (2), (3), and (4) and the effective thermal conductivity which occurs in Eq. (5) are regarded as consisting of two parts, the laminar and turbulent parts; i.e.,

$$\mu = \mu_\ell + \mu_t \tag{20}$$

and $$k = k_\ell + k_t \tag{21}$$

μ_ℓ and k_ℓ are included in the fluid property package.

μ_t and k_t are estimated as [13]:

$$\mu_t = 0.007\ C_\mu\ U_{max} L \tag{22}$$

$$\text{Where } C_\mu = \begin{cases} 0.1 & Re_{max} > 2000 \\ 0.1\ (0.001\ Re_{max} - 1) & 2000 \geq Re_{max} \geq 1000 \\ 0.0 & Re_{max} < 1000 \end{cases}$$

$$U_{max} = \max\ (u,v,w)$$

$$Re_{max} = \max\ (Re_r,\ Re_\theta,\ Re_z)$$

and $L = \max\ (\Delta r,\ r\Delta^\theta,\ \Delta z)$

Once μ_t is known k_t can be estimated from

$$k_t = \frac{C_p \mu_t}{Pr_t} \tag{23}$$

where Pr_t = turbulent Prandtl number

The turbulent Prandtl number may be evaluated as [14].

$$Pr_t = 0.8\ [1 - \exp(-6 \times 10^{-5}\ Re_{max}\ Pr^{1/3})\ ]^{-1} \tag{24}$$

It should be noted that Eqs. (22) and (23) merely provide an estimate for normal LMFBR operating conditions. In this study, it is believed this model is adequate because the flow conditions being studied are mainly low flow conditions, consequently the magnitude of turbulence is relatively small. Also sensitivity studies were done by varying turbulent viscosity and turbulent conductivity. The results gave no significant difference.

C. Solution Procedure

The PLENMIX code is a simplified version of COMMIX-1A. Many features of COMMIX-1A are not available in the PLENMIX to save computer storage. However, their main solution procedures are the same.

The governing equations are finite-differenced in a staggered mesh system. The procedure of solving these finite difference equations is given in Figure 2. The program begins by specifying the geometry and the mesh. Next, the initial conditions and the boundary conditions are specified.

The solution sequence is then performed to determine the first approximation of the velocity components for the next time step from the momentum equations. The next sequence involves an implicit iteration between mass and momentum. Since the mass is not identically conserved during this iteration, the mass residue is introduced. Then, the new pressure distribution is calculated. In order to reduce the mass residue, the new velocity components are generated to account for the pressure distribution. Upon completion of this step, the mass equation convergence criteria are examined. If satisfied, the iterative process terminates. If not converged, the iteration proceeds until it converges or the specified number of iterations have been performed.

Finally, the enthalpy is calculated explicitly from the energy equation. After enthalpy has been evaluated, temperature and density are obtained from the equation of state.

Since the solution of the momentum equations involves Poisson type equations, several numerical techniques are introduced to speed up the convergence. Those techniques involve Jacobi iteration, successive over-relaxation, selective over-relaxation, and mass rebalancing. A detailed description of these techniques can be found in Reference [8].

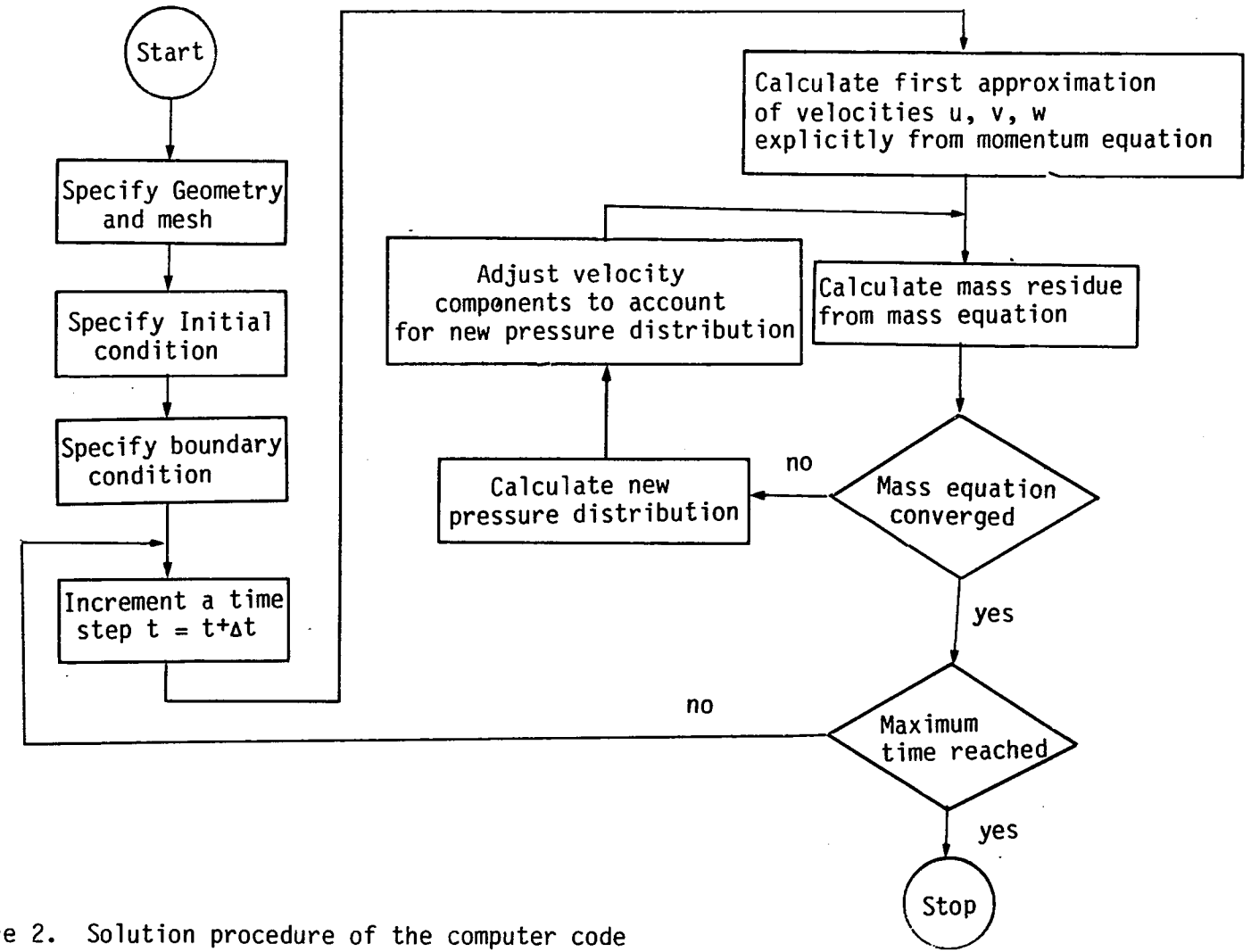

Figure 2. Solution procedure of the computer code

D. Initial Conditions and Boundary Condition

1. Initial Conditions

The enthalpy and density are calculated in the code from the equation of state and the prescribed pressure and temperature distribution.

Only one pressure value at a point and the values of the gravity vector are needed for the pressure initialization. The entire temperature field is generated from the input temperature information. The density field is computed by the equation of state. Using this density field and the point pressure, a pressure field is generated to account for the static head.

A constant pressure gradient in any coordinated direction can be added to the initial hydraulic pressure by specifying the desired pressure gradient values.

2. Boundary Conditions

Each surface has two boundary conditions associated with it, one for velocity and the other for temperature.

Five velocity boundary conditions are available in the code, they are (a) constant velocity, (b) transient velocity, (c) free-slip surface, the boundary tangent velocity is set equal to its corresponding adjacent internal velocity so that the wall shear stress is zero, (d) continuation velocity outlet, the boundary normal velocity set equal to the corresponding adjacent internal velocity, and (e) continuative-momentum outlet, the boundary normal

velocity is set such that the boundary normal momentum is equal to the corresponding adjacent internal momentum.

Five temperature boundary conditions are also available in the code. They are (a) constant temperature, (b) uniform transient temperature, (c) uniform constant normal heat flux, (d) uniform transient normal heat flux, and (e) adiabatic boundary conditions. For each of these boundary conditions, density and enthalpy are assigned from equations of the state after the boundary temperature has been determined.

E. Similitude Analysis

The design of a scale model requires that all important phenomena be preserved. Many workers, who make extensive use of scale models, have a preferred method of determining the appropriate scaling laws for a given system. The most extensively used method is the Buckingham Pi theroem. In this method, the input information required is a list of the relevant physical quantities including one dependent quantity and a sufficient list of independent physical quantities. Application of the Pi theorem leads to a set of governing Pi groups which needs to be matched for both the model and the prototype. If a complete set of physical quantities is chosen, the result will be complete. Another method is through the use of governing differential equations [15]. Each variable is normalized so that the magnitudes of both itself and its derivatives are 0

(1). The normalized equations contain non-dimensional parameters whose relative magnitude in full scale determines physical effects which must be preserved in the scale model. The normalized variables also are preserved, making it possible to employ data from a small scale model and determine full size behavior. If one begins from the correct equations and performs each step correctly, one can be sure that all appropriate variables have been included. Both methods should be able to reach the same conclusion. If any disagreement is found, further investigation is needed to determine which parameter is being ignored or can be ignored.

1. Buckingham Pi Theroem

The pertinent parameters for buoyancy affected flows can be expressed in functional form as:

$$\Delta T = F\ (\Delta T_o,\ r,\ \theta,\ z,\ L,\ u,\ v,\ w,\ w_o,\ g_z,\ \rho, \rho_o,\ \mu,\ k,\ C_p,\ t,\ P)$$

The corresponding dimensions of these parameters are:

ΔT	temperature change with respect to reference temperature	Θ
ΔT_o	maximum temperature with respect to reference temperature	Θ
r	radial coordinate	L
θ	azimuthal coordinate	dimensionless
z	axial coordinate	L
L	characteristic length	L
u	velocity in r direction	LT^{-1}

v	velocity in θ direction	LT^{-1}
w	velocity in z direction	LT^{-1}
w_o	reference velocity, initial inlet velocity in z direction	LT^{-1}
g_z	gravitational acceleration in z direction	LT^{-2}
ρ	fluid density	ML^{-3}
ρ_o	initial fluid density	ML^{-3}
μ	viscosity	$ML^{-1}T^{-1}$
k	thermal conductivity	$HT^{-1}L^{-1}\Theta^{-1}$
t	time	T
C_p	heat capacity	$H\Theta^{-1}$
P	pressure	$ML^{-1}T^{-2}$

It is justified to use four basic dimensions, H, T, M, L, as well as Θ, since there is no transformation of kinetic energy to thermal, or vice versa.

With eighteen parameters and five dimensions involved, there must be thirteen Pi terms. One possible set is:

$$\pi 1 = \eta = \frac{r}{L} \tag{25}$$

$$\pi 2 = \zeta = \theta \tag{26}$$

$$\pi 3 = \xi = \frac{z}{L} \tag{27}$$

$$\pi 4 = u = \frac{u}{w_o} \tag{28}$$

$$\pi 5 = V = \frac{v}{w_o} \tag{29}$$

$$\pi 6 = W = \frac{w}{w_o} \tag{30}$$

$$\pi 7 = \bar{P} = \frac{P - \rho_o g_z z}{\rho_o w_o^2} \tag{31}$$

$$\pi 8 = \tau = \frac{t\, w_o}{L} \tag{32}$$

$$\pi 9 = \phi = \frac{T - T_o}{\Delta T_o} \tag{33}$$

$$\pi 10 = Ri = \frac{(\rho - \rho_o)\, g_z\, L}{\rho_o w_o^2} \tag{34}$$

$$\pi 11 = Pe = \frac{\rho_o C_p w_o L}{k} \tag{35}$$

$$\pi 12 = Re = \frac{\rho_o w_o L}{\mu} \tag{36}$$

$$\pi 13 = \frac{\rho}{\rho_o} \tag{37}$$

The first three terms pertain to geometrical characteristics; the next three represent velocity similarity. Eq. (31) indicates the dynamic pressure similarity. Eq. (32) is the time scale. Eq. (33) gives the temperature characteristics. Eq. (34) is the Richardson Number representing buoyant to inertia force. Eq (35) is the Peclet Number which represents the convection to conduction heat transfer ratio. The Reynolds Number in Eq. (36) represents the ratio of inertia to viscous force. Eq. (37) is the requirement of equality of density ratio.

Eqs. (25) to (27) can be matched if the geometries of the model and the prototype are similar. Eqs. (28) to (30) can be matched if the velocities are measured by the normalized magnitude w_o. Eq. (31) can be matched with the unit dynamic pressure if it equals $\rho_o w_o^2$. Eq. (32) can be satisfied if the results are compared in the dimensionless time scale tw_o/L. Similarly, Eq. (33) can be satisfied if the temperature difference is measured by ΔT_o. The remaining four design conditions that need to be satisfied are the Richardson Number, the Peclet Number, the Reynolds Number, and the density ratio.

With these thirteen parameters for the model satisfied, the thermohydraulic behavior for the prototype can be extrapolated from the data of the model.

2. Dimensionless Governing Equations

The basic similitude laws for buoyancy affected flows can also be derived from Eqs. (1) to (5). These Equations can be made dimensionless by redefining the variables:

$$\eta = \frac{r}{L} \tag{38}$$

$$\zeta = \theta \tag{39}$$

$$\xi = \frac{z}{L} \tag{40}$$

$$U = \frac{u}{w_o} \tag{41}$$

$$V = \frac{v}{w_o} \tag{42}$$

$$W = \frac{w}{w_o} \tag{43}$$

$$W = \frac{w}{w_o} \tag{43}$$

$$\overline{P} = \frac{P - \rho_o g_z z}{\rho_o w_o^2} \tag{44}$$

$$\tau = \frac{t w_o}{L} \tag{45}$$

$$\phi = \frac{T - T_o}{\Delta T_o} \tag{46}$$

$$Ri = \frac{(\rho - \rho_o)\, g_z\, L}{\rho_o w_o^2} \tag{47}$$

$$Pe = \frac{\rho_o C_p w_o L}{K} \tag{48}$$

$$Re = \frac{\rho_o w_o L}{\mu} \tag{49}$$

Assume (1) $g_r = g_\theta = 0$; $g_z = -g$

(2) $\partial\rho/\partial t = \partial P/\partial t = 0$

(3) No heat source

(4) Constant heat capacity, heat conductivity and viscosity

Substituting Eqs. (38)-(49) into Eqs. (1)-(5) yields:

$$\frac{1}{\eta}\frac{\partial}{\partial \eta}(\eta U) + \frac{1}{\eta}\frac{\partial}{\partial \zeta}(V) + \frac{\partial}{\partial \xi}(W) = 0 \tag{50}$$

$$\frac{\partial}{\partial \tau} U + \frac{1}{\eta}\frac{\partial}{\partial \eta}(\eta U^2) + \frac{1}{\eta}\frac{\partial}{\partial \zeta}(UV) + \frac{\partial}{\partial \xi}(UW) - \frac{V^2}{\eta}$$

$$= -\frac{\partial \bar{P}}{\partial \eta} + \frac{1}{Re}\left[\frac{1}{\eta}\frac{\partial}{\partial \eta}\left(\eta \frac{\partial U}{\partial \eta}\right) + \frac{1}{\eta^2}\frac{\partial}{\partial \zeta}\frac{\partial U}{\partial \zeta} + \frac{\partial}{\partial \xi}\frac{\partial U}{\partial \xi}\right.$$

$$\left. - \frac{2}{\eta^2}\frac{\partial V}{\partial \zeta} - \frac{U}{\eta^2}\right] \tag{51}$$

$$\frac{\partial V}{\partial \tau} + \frac{1}{\eta}\frac{\partial}{\partial \eta}(\eta UV) + \frac{1}{\eta}\frac{\partial}{\partial \zeta}(V^2) + \frac{\partial}{\partial \xi}(UV) + \frac{UV}{\eta}$$

$$= -\frac{1}{\eta}\frac{\partial P}{\partial \zeta} + \frac{1}{Re}\left[\frac{1}{\eta}\frac{\partial}{\partial \eta}\left(\eta\frac{\partial V}{\partial}\right) + \frac{1}{\eta^2}\frac{\partial}{\partial \zeta}\left(\frac{\partial V}{\partial \xi}\right)\right.$$

$$\left. + \frac{\partial}{\partial \xi}\left(\frac{\partial V}{\partial \xi}\right) + \frac{2}{\eta^2}\frac{\partial U}{\partial \zeta} - \frac{V}{\eta^2}\right] \tag{52}$$

$$\frac{\partial W}{\partial \xi} + \frac{1}{\eta}\frac{\partial}{\partial \eta}(\eta UW) + \frac{1}{\eta}\frac{\partial}{\partial \zeta}(VW) + \frac{\partial}{\partial \xi}(W^2)$$

$$= -\frac{\partial \bar{P}}{\partial \xi} + \frac{1}{Re}\left[\frac{1}{\eta}\frac{\partial}{\partial \eta}\left(\eta\frac{\partial W}{\partial \eta}\right) + \frac{1}{\eta^2}\frac{\partial}{\partial \zeta}\left(\frac{\partial W}{\partial \zeta}\right) + \frac{\partial}{\partial \xi}\left(\frac{\partial W}{\partial \xi}\right)\right]$$

$$-Ri_{\phi} \tag{53}$$

$$\frac{\partial \phi}{\partial \tau} + \frac{1}{\eta}\frac{\partial}{\partial \eta}(\phi \eta U) + \frac{1}{\eta}\frac{\partial}{\partial \zeta}(V\phi) + \frac{\partial}{\partial \xi}(W\phi)$$

$$= \frac{1}{Pe}\left[\frac{1}{\eta}\frac{\partial}{\partial \eta}\left(\eta\frac{\partial \phi}{\partial \eta}\right) + \frac{1}{\eta^2}\frac{\partial}{\partial \zeta}\left(\frac{\partial \phi}{\partial \zeta}\right) + \frac{\partial}{\partial \xi}\left(\frac{\partial \phi}{\partial \xi}\right)\right] \tag{54}$$

Eqs. (50) to (54) reveal that if twelve design conditions given in Eqs. (38) to (49) are met, then both systems are described by identical dimensionless differential equations. If, in addition, the dimensionless initial and boundary conditions are the same, then the two systems are mathematically identical; that is, the dimensionless velocity distribution, dimensionless pressure distribution, and dimensionless temperature distribution are the same in each.

It can be seen that the requirements from the dimensional analysis and the dimensionless governing equations are the same except the density ratio term. In dimensional analysis, the density ratio needs to be matched independently. Those terms will be discussed in the following sections.

3. Essential Laws

In the upper plenum mixing problem, we begin with a selected and simplified part of nature by eliminating most of the marginal and non-essential laws to arrive at a useful approximation. But even then, we may find that we have too many laws, and that scaling is difficult or impossible. When this happens, further relaxations are necessary.

As a first step in relaxation, as Schuring [16] has pointed out, it is helpful to determine whether the laws, causing scaling conflicts, are governing the given system with equal or unequal strength. If they are governing with unequal strength, the weakest

laws can perhaps be disregarded within segments of the investigation if not throughout its entire range. If their influences are equally strong, none can be nelgected outright, but adequate results may still be attained by skillful circumvention of the most disturbing law.

When the effect of a law on the total performance is uncertain, tests with a model may supply misleading data. In model simulation, a law will be revealed as weak or strong by checking its effects on the similarity between model results and prototype results. As Murphy [17] has pointed out, true models reproducing all governing laws will always give accurate predictions. Only if scaling requirements are violated - e.g. neglecting weak governing laws - would the prediction accuracy suffer.

As has been seen, with the geometry, initial conditions, and boundary conditions satisfied, there are three or four design requirements to be satisfied: Ri, Re, Pe, and/or ρ/ρ_o. It is impossible to match all the parameters simultaneously at reduced scale. The discussion of these parameters are given in the following sections.

a. Richardson Number Of these parameters, the Richardson Number is the most important; it is fundamental to all the stratified flow and can never be neglected. It has been proven experimentally [6] in forced convection that with equal Richardson numbers in both the model and the prototype, a slight deviation of

the other parameters has little influence upon plenum mixing. Hence, the conservation of the Richardson number is the strongest law.

Physically, the Richardson number represents the ratio between the entering fluid's negative buoyancy and its momentum. Negative buoyancy is a transient condition that exists when the entering fluid is colder than the ambient fluid within the upper plenum; this condition exists immediately after a reactor scram.

This force balance determines the flow and temperature patterns within the upper plenum. The ratio of the Richardson numbers will then be unity:

$$Ri_r = \frac{Ri_m}{Ri_p} = \left(\frac{\Delta\rho}{\rho}\right)_r \frac{L_r g_r}{V_r^2} = 1 \tag{55}$$

where subscripts r, m, and p represent ratio, model and prototype, respectively.

Since both model and prototype will be operated under the same gravitational influence,

$$g_r = 1$$

and Eq. (55) becomes

$$Ri_r = \left(\frac{\Delta\rho}{\rho}\right)_r \frac{L_r}{V_r^2} = 1 \tag{55}$$

If both model and prototype are operated over the same temperature range and the same fluid is used, then

$$\left(\frac{\Delta\rho}{\rho}\right)_r = 1$$

Eq. (55) can be further reduced to

$$V_r = L_r \tag{56}$$

The discharge for the model and the prototype can be obtained from the continuity equation

$$Q = VA \tag{57}$$

where A = cross-sectional flow area

$$Q_r = \frac{Q_m}{Q_p} = \frac{V_m A_m}{V_p A_p} \tag{58}$$

Since $\frac{A_m}{A_p} = \left(\frac{L_m}{L_p}\right)^2$

hence $$V_r = \frac{Q_r}{L_r^2} \tag{59}$$

Inserting Eq. (59) into Eq. (55) one obtains

$$\left(\frac{\Delta\rho}{\rho}\right)_r = \frac{Q_r^2}{L_r^5} \tag{61}$$

A time scale between model and prototype is established by the following expression:

$$\tau_m = \tau_p \tag{61}$$

$$\left(\frac{tv}{L}\right)_m = \left(\frac{tv}{L}\right)_p \tag{62}$$

Then $$\frac{t_m}{t_p} = \frac{L_m/L_p}{V_m/V_p} \tag{63}$$

Hence $$t_r = \frac{t_m}{t_p} = \frac{L_r}{V_r} \tag{64}$$

b. Reynolds Number The Reynolds Number can not be simultaneously scaled for water or sodium tests. As can be seen in Eqs. (51) to (53), the Reynolds Number only appears in the viscous term. For a large enough Reynolds Number, this term can be neglected. It is required that the Reynolds Number be sufficiently high to ensure turbulent flow. Verification of this modeling hypothesis will be given in Chapter IV where it is shown that the Reynolds Number is not important.

c. Peclet Number As mentioned earlier, application of the Peclet number would reveal the relative influence of conduction to convection of the fluid within the upper plenum. The highly convective flow nature at normal reactor scram renders the conductive heat transfer within the fluid negligible. It was for this reason that the Peclet number was not considered in the previous similitude studies. However, when the flow rate within the

upper plenum is further reduced to natural recirculation, heat transfer effects characterized by the Peclet number may become substantial. Under this condition, conservation of the Peclet numbers may be necessary.

1) Water as Test Fluid If water is employed as the test fluid, the conservation for both Ri and Pe requires that:

$$Ri_r = \left(\frac{\Delta\rho}{\rho}\right)_r \frac{L_r}{V_r^2} = 1 \tag{65}$$

$$Pe_r = \frac{V_r L_r}{\alpha_r} = 1 \tag{66}$$

It can be seen from Eq. (66) that since the ratio of the thermal diffusivities of water to sodium is about 1/430, $V_r L_r$ will have to change accordingly in order to maintain similitude.

Hence, it is difficult to match both Ri and Pe unless Vr, Lr and $(\Delta\rho/\rho)_r$ are made extremely small. Then the Reynolds Number would be too small to ensure proper simulation. Also, the temperature difference would be too small to obtain meaningful measurement.

2) Sodium as Test Fluid If sodium is used as the test fluid, α_r will be unity in Eq. (66). Then $V_r L_r$ will also be unity. Substitution of this value into Eq. (65) gives:

$$\left(\frac{\Delta\rho}{\rho}\right)_r = \frac{1}{L_r^3} \tag{67}$$

Hence, it is possible to match both Ri and Pe provided that L_r is not too small, otherwise $\Delta\rho/\rho$ would be too small and a meaningful temperature difference measurements would be difficult.

d. Density Ratio The density ratio is required to be matched in dimensional analysis. For most of LMFBR transients, the temperature change represents a 4% - 5% increase in sodium density. This density change is difficult to achieve for a water test. This density ratio requirement is not found in the governing equation approach. So it was is decided not to match the density ratio. Verification of this modeling hypothesis will be given in Chapter IV where it is shown that the density ratio is not extremely important.

III. SIMULATION OF CDS PHASE I: PLENUM MIXING STUDY

A. Introduction

The Phase I Conceptual Design Studies (CDS) upper plenum mixing was conducted by the Components Technology Division of Argonne National Laboratory [7].

Figure 2 shows ten different concepts which were under experimental study to identify and examine the geometrical dependence and influence upon mixing.

It is not the purpose of this work to present a comprehensive comparison of the different design features. However, certain information can be obtained in a particular design which would lead to better understanding of important laws governing the plenum mixing characteristics.

The particular design shown in Fig. 3(J) was selected for the PLENMIX code simulation. This design creates the sharpest hot-cold interface separating the cold fluid below from hot fluid above during normal reactor shutdown. This interface moves slowly upward and can be characterized by a large exit temperature gradient. The sharp temperature decrease could subject exposed components to excessive thermal stresses.

B. Problem Statement

This test was performed at 1/13 scale using water as the test fluid. It simulated a 2720 MW(t) LMFBR with a temperature drop across the reactor core of 134.2^{o}C and a reactor core coolant flow rate of 16.4 M^3/s. Flow coastdown was from 100% to 8%.

As shown in Figure 4, the upper plenum has six equal size Intermediate Heat Exchangers (IHXs). The reactor core coolant exit is located at the center of the pool. Since the thermal-hydraulic conditions are symmetric with respect to the vertical centerline, one needs to consider only 1/12 of the circular geometry.

Figures 5 and 6 show the axial, radial and azimuthal partitioning of the plenum. The axial direction is partitioned into twenty meshes. The radial direction is partitioned into five meshes and the azimuthal direction is partitioned into three equal 10^{o} angles.

The following assumptions were employed in this simulation:

i) The inlet velocity and temperature is uniform over the inlet cross-section.

ii) Turbulent eddy transport of energy and momentum is constant throughout the whole transient.

iii) The plenum wall inner surface is adiabatic while the IHXs surface is non-adiabatic.

From the steady-state operating conditions, a flow and temperature transient occurs at t = 120 sec. The inlet velocity

decreases to approximately 8% of its steady-state value in 8 seconds as shown in Figure 7. The inlet temperature decreases from 66.1^{o} C to 31.0^{o}C in 50 seconds as shown in Figure 6. Table 1 lists the parameters for the model and the corresponding prototype.

Table 1: Parameters Used in the CDS Simulation

Parameter	Prototype	Model
Fluid Type	Na	H_2O
Coolant Flow Rate	16.4 m^3/sec	0.0156 m^3/sec
Plenum Height	5.462 m	0.434 m
Effective Inlet Area	5.89 m^2	0.0349 m^2
Temperature Range	510^{o}C-375.8^{o}C	66.11^{o}C-31^{o}C
Initial Inlet Velocity	2.782 m/sec	0.4461 m/sec
Final Inlet Velocity	0.2228 m/sec	0.0357 m/sec
$\Delta\rho/\rho$	0.0365	0.0122
Initial Ri	0.2607	0.2607
Time Ratio	2.37	1

C. Simulation Results

In the PLENMIX code calculations, the numerical solution is performed over a 5 x 3 x 20 array containing 300 computational cells. These correspond to I = 1 to 5, J = 1 to 3 and K = 1 to 20 in Figures 5 to 6.

The simulation consists of first obtaining a steady-state solution, then a specified velocity and temperature transient is imposed at the plenum entrance. The transient is finally terminated when the time reaches 2700 sec.

As the transient proceeds, the flow rate and temperature are decreased. This causes the incoming cooler fluid to move to the botton while the warmer fluid will become stagnant at the top.

The test facility contains two water-supply tanks. A 2000-gallon tank supplied the hot flow prior to and during the initial stage of the flow transient. Cold flow was introduced from a 320-gallon tank in due time to create the required flow and temperature transients. The flow and temperature transients were controlled by a microprocessor whose directives are sent to the relays causing valve movements. Temperature variations in the plenum were recorded by a grid of bare bead thermocouples which were located on a vertical plane bisecting the test model as shown in Fig. 5.

The computational results are compared with all available temperature measurements. Figures 9-23 show the comparisons of the

PLENMIX calculations and the measured temperature transients. As can be seen, the temperature variations on most of the figures show reasonably good agreements throughout the whole transient.

Figures 24 to 33 present the isothermal line of the plenum vertical cross-section at various time intervals. The temperature difference for isothermal lines is $3^{o}C$. As the inlet velocity decreases, the cooler fluid at the inlet can no longer reach the top, then the cooler part of the plenum fluid falls to the bottom as a result of buoyancy effects and the stratified flow is then formed. These figures clearly show the existence of a hot-cold interface.

D. Summary and Discussion

The previous section has presented the computational results from PLENMIX simulations of a reactor upper plenum under reactor scram conditions. Reasonably good agreement has been shown for all comparisons between experimental and calculated temperatures. Disagreement, when present, may be due to the coarseness of the mesh. This may be investigated by using a finer mesh partitioning; however, it would increase the computation time and cost.

During the period of analyzing these plenum transients, some physical models have been investigated and improved. Modeling of the thermal iteraction between the coolant and the IHXs outer surface was found to be important. The heat loss through convective

heat transfer between coolant and the IHXs outer surface is not negligible. It would change the temperature field as well as the speed of the hot-cold interface movement. Without this heat loss term, the speed of the hot-cold interface upward movement would be much slower. This will be shown in the next chapter.

In summary, the PLENMIX computer code has been successfully employed in providing a reasonably good prediction of temperatures at each of the thermal couple locations.

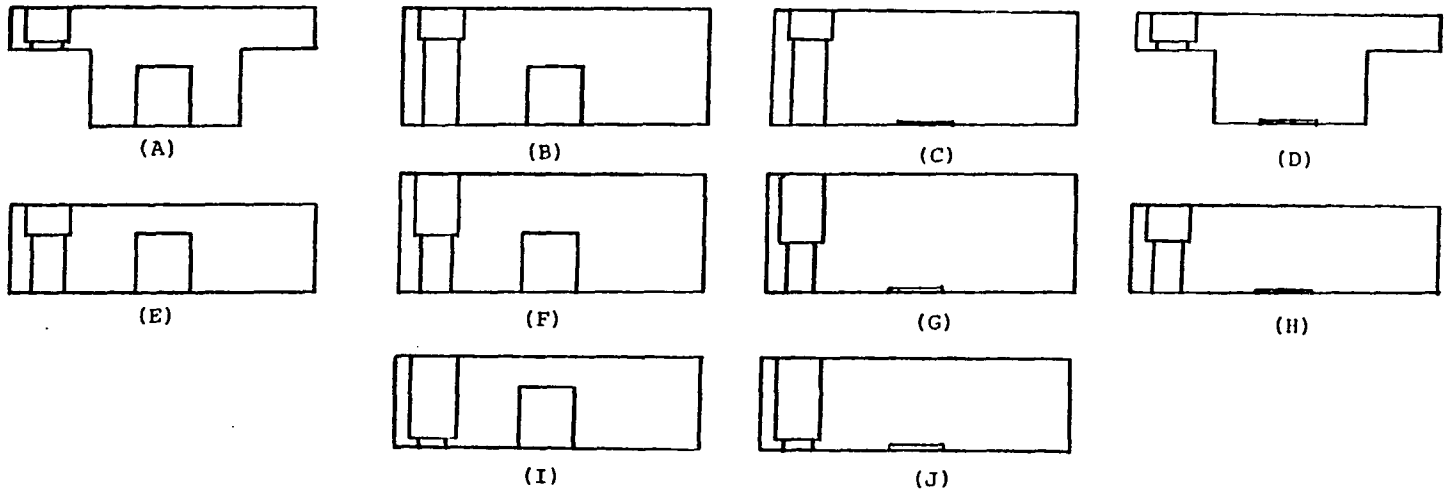

Figure 3. CDS upper plenum mixing text matrix (side view)

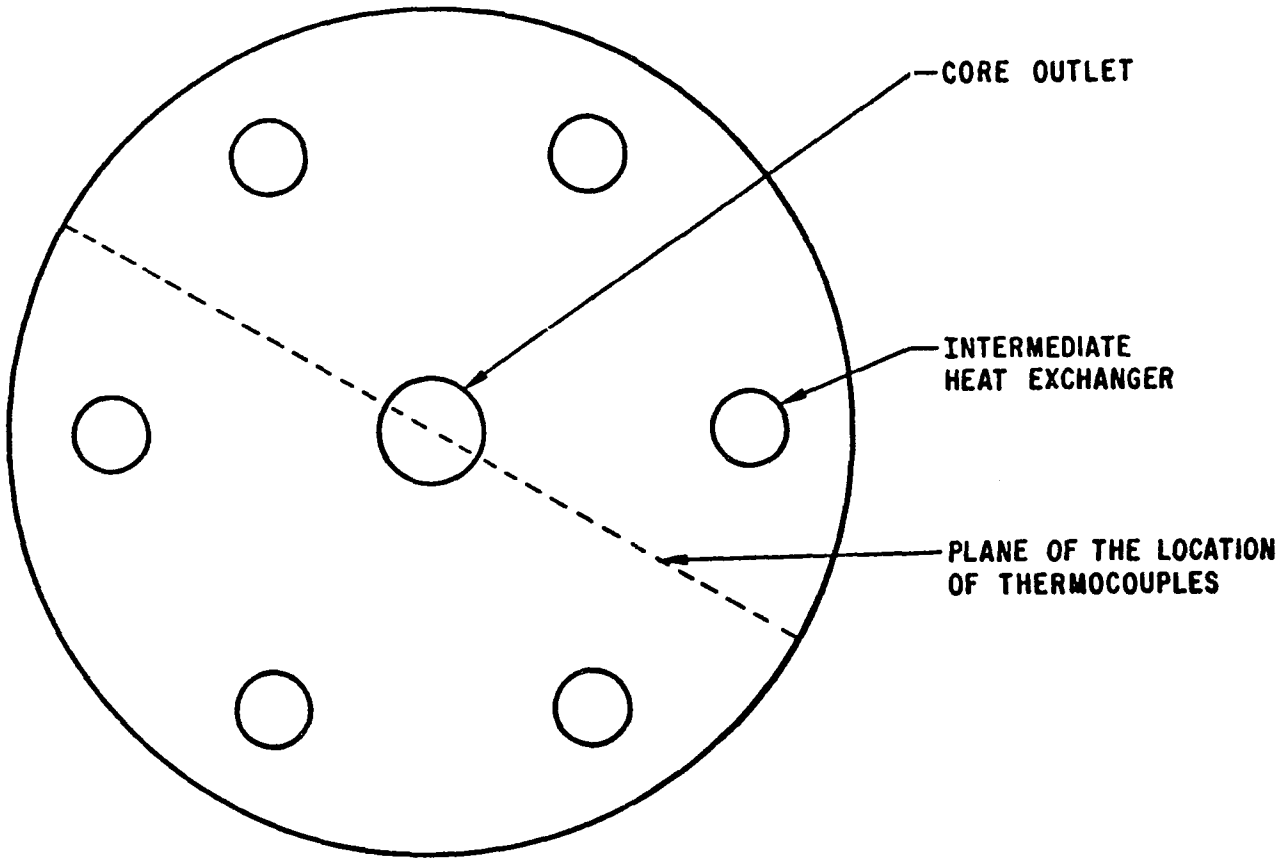

Figure 4. Top view of CDS upper plenum mixing test matrix

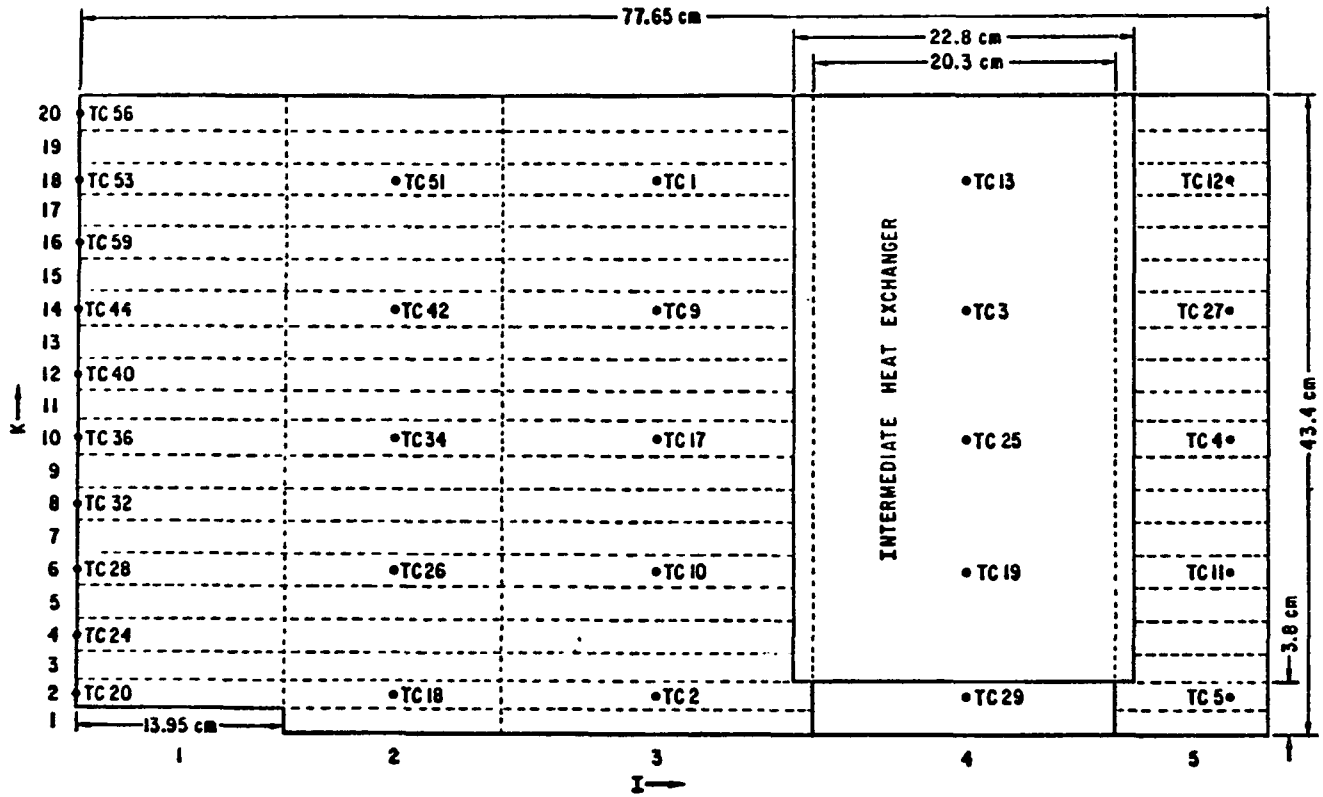

Fixture 5. Axial and radial partitioning of PLENMIX code simulation

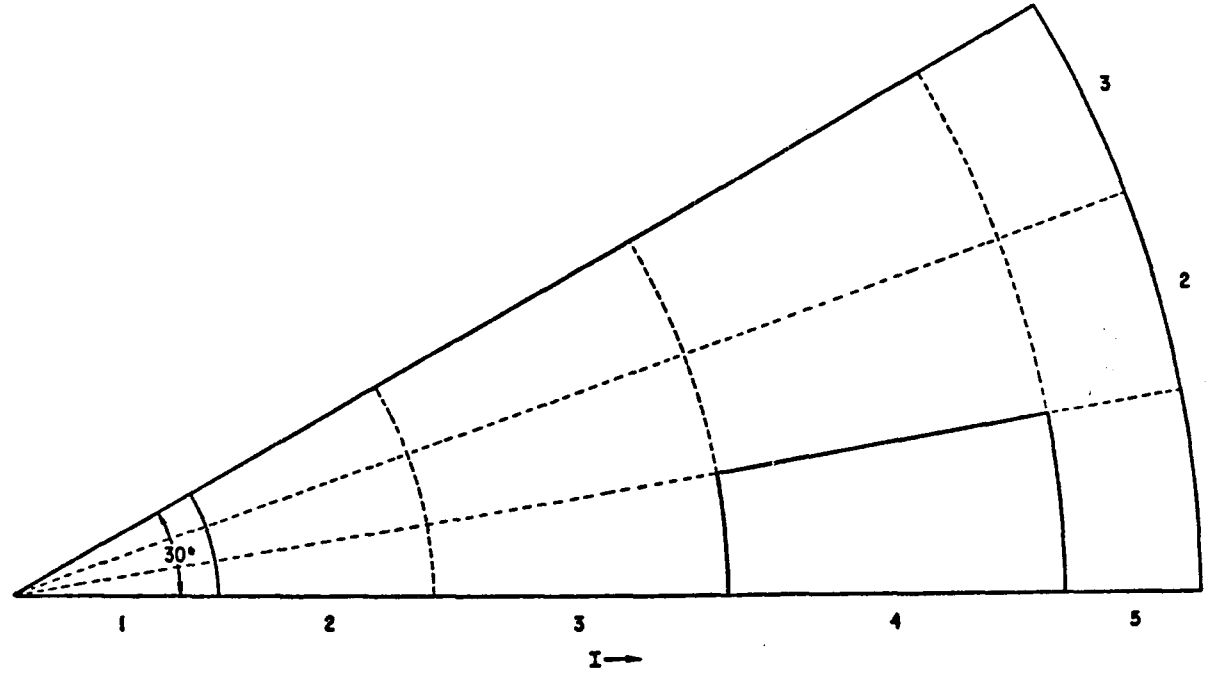

Figure 6. Axial and azimuthal partitioning of PLENMIX code simulation

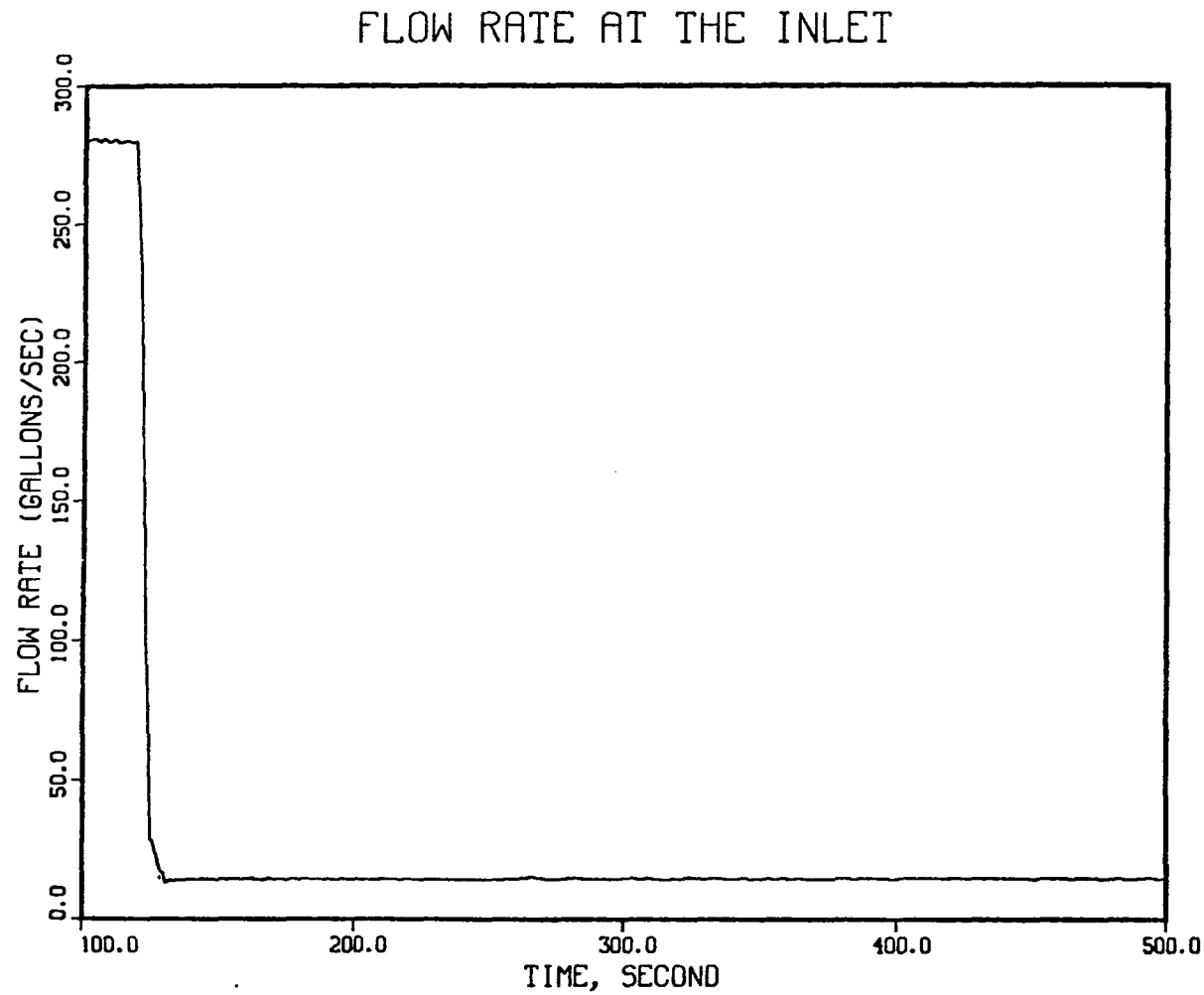

Figure 7. Inlet flow transient for mixing experiment

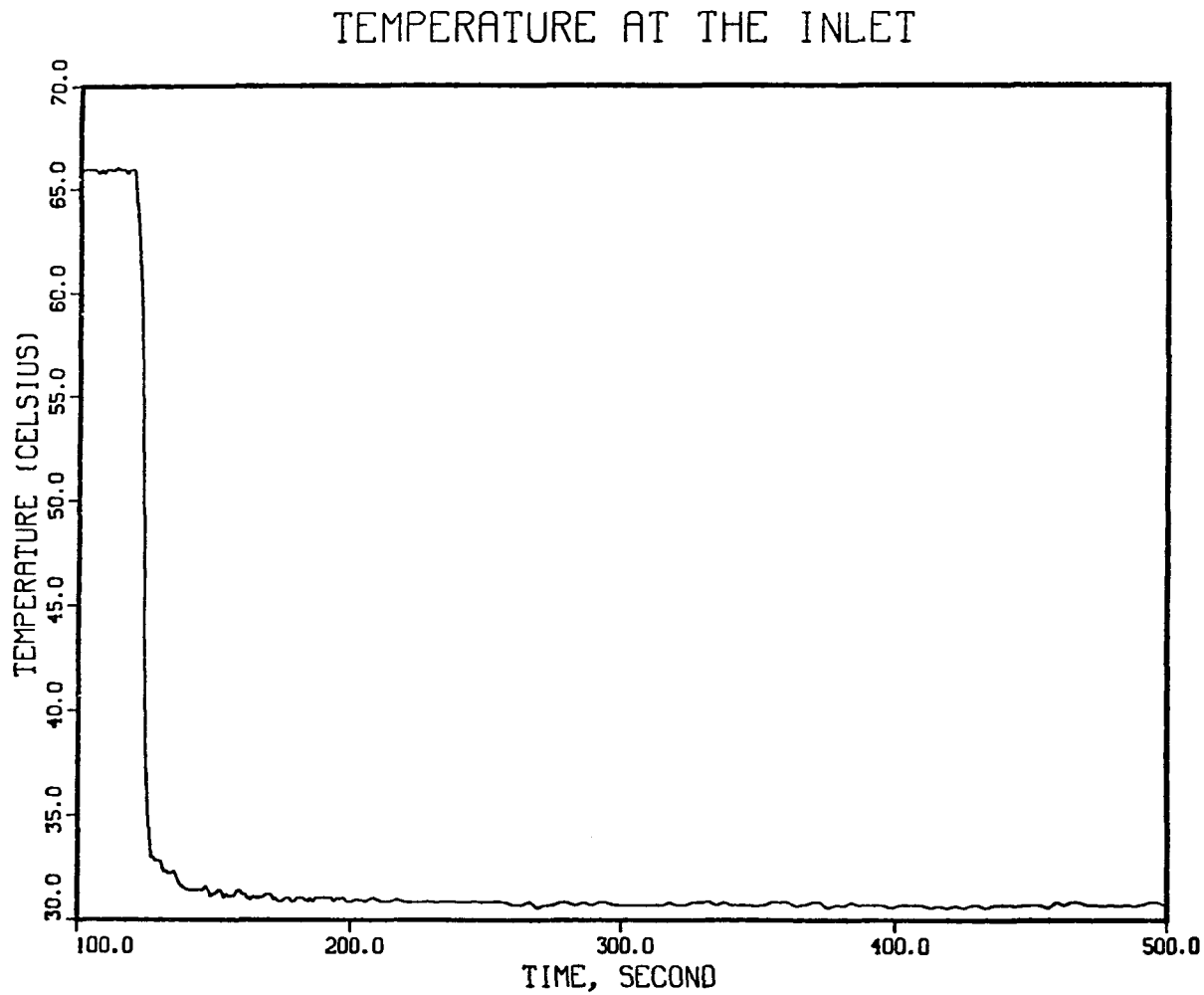

Figure 8. Inlet temperature transient for mixing experiment

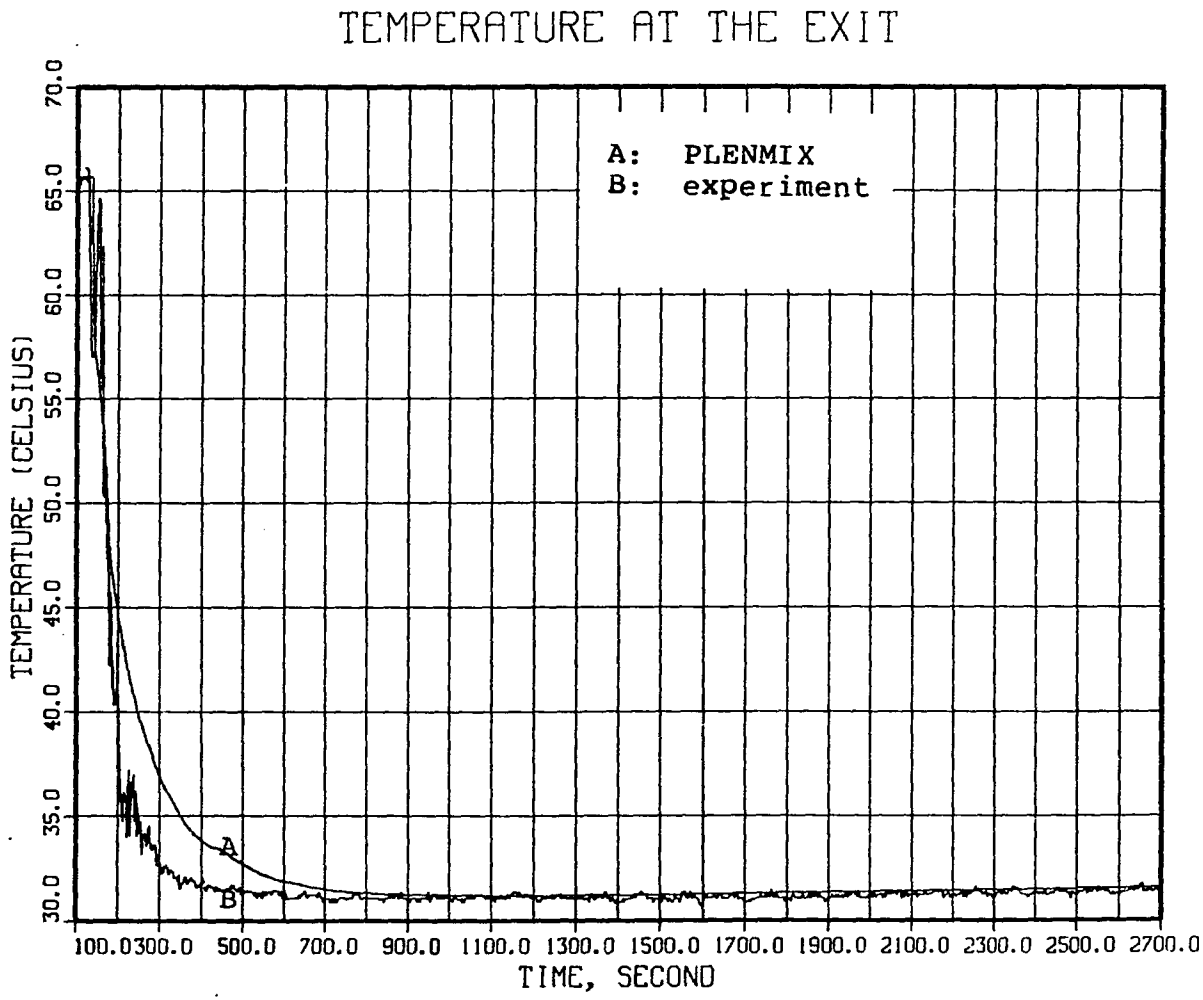

Figure 9. Temperature transient at the plenum exit

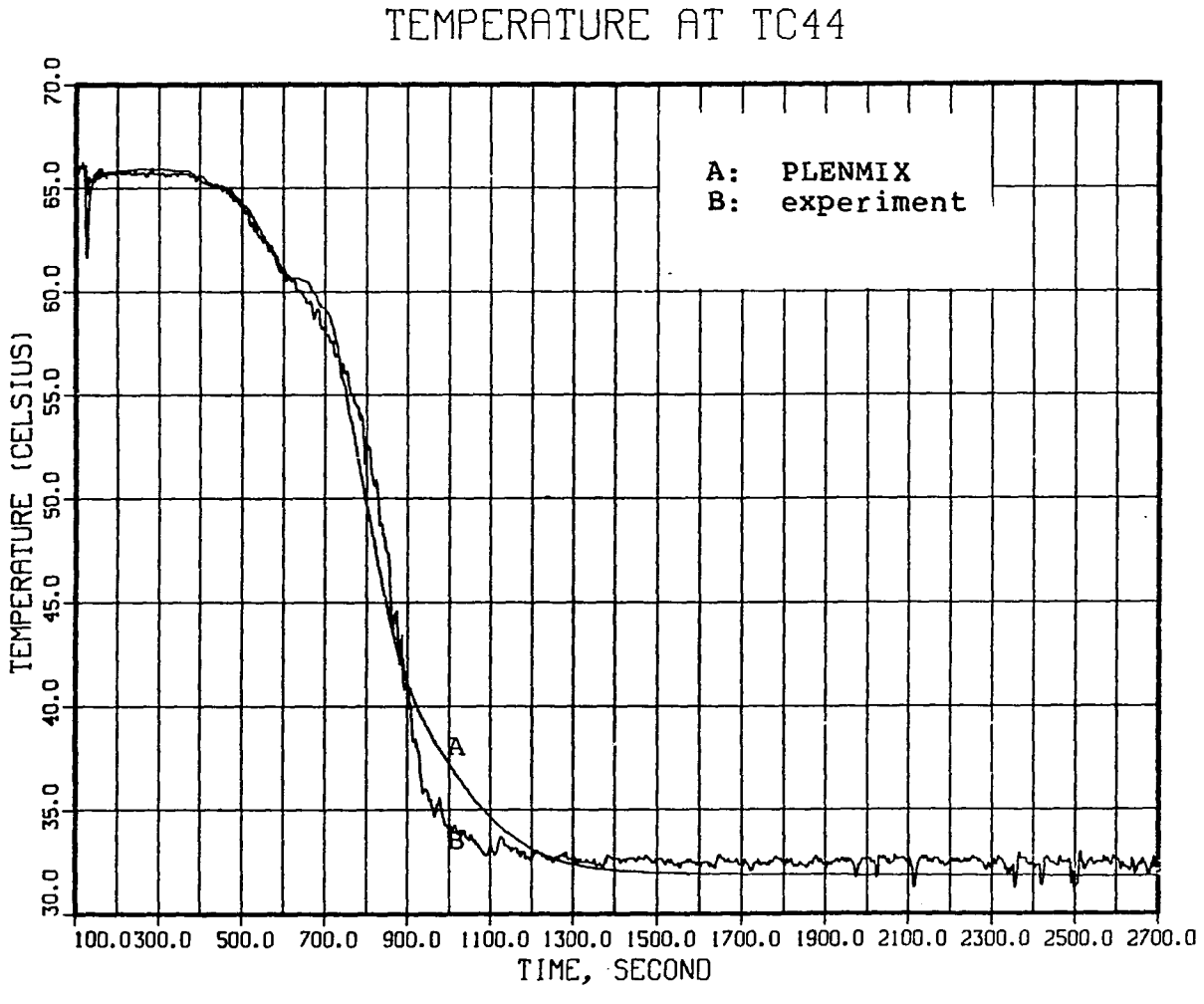

Figure 10. Temperature transient at TC44

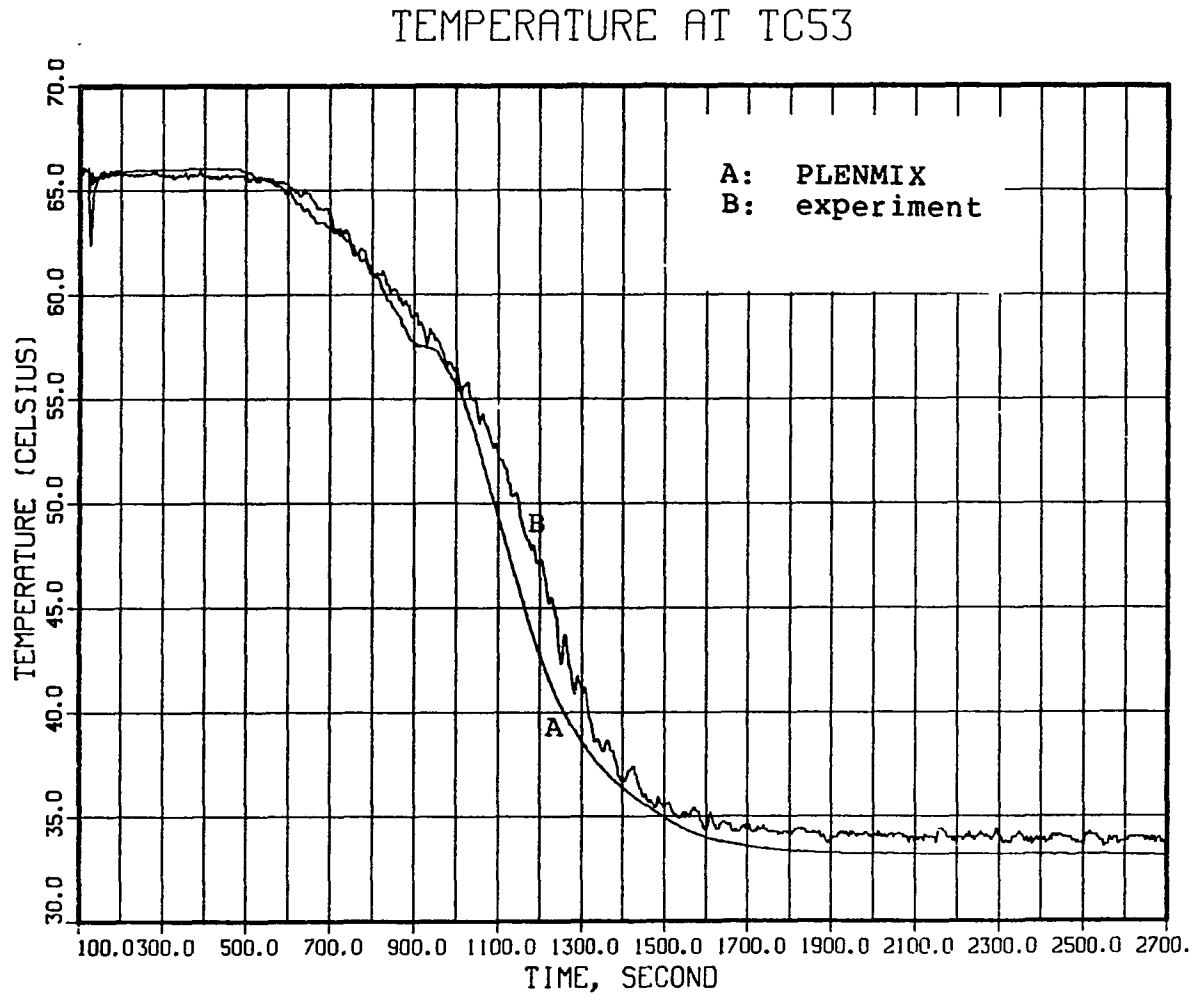

Figure 11. Temperature transient at TC53

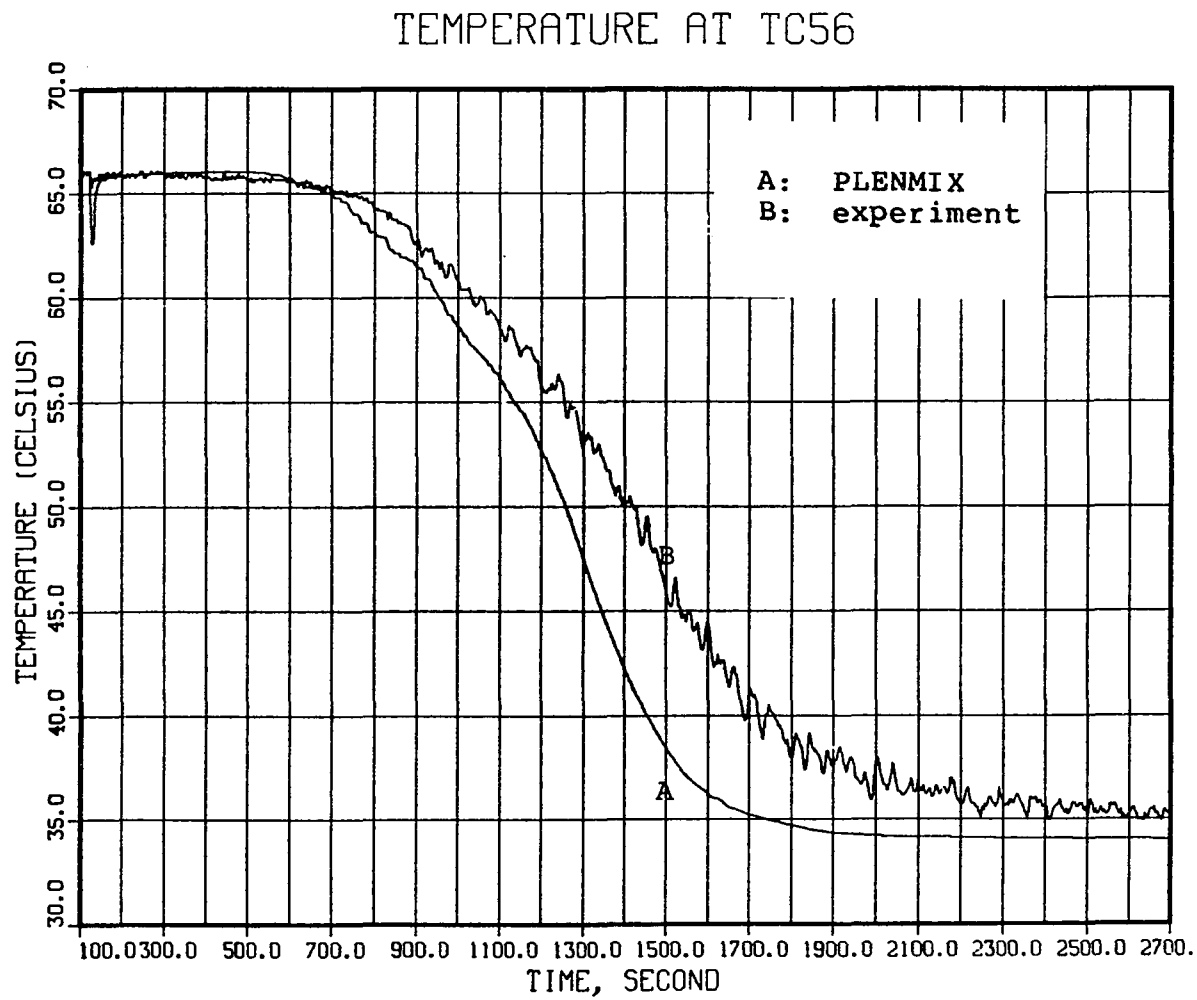

Figure 12. Temperature transient at TC56

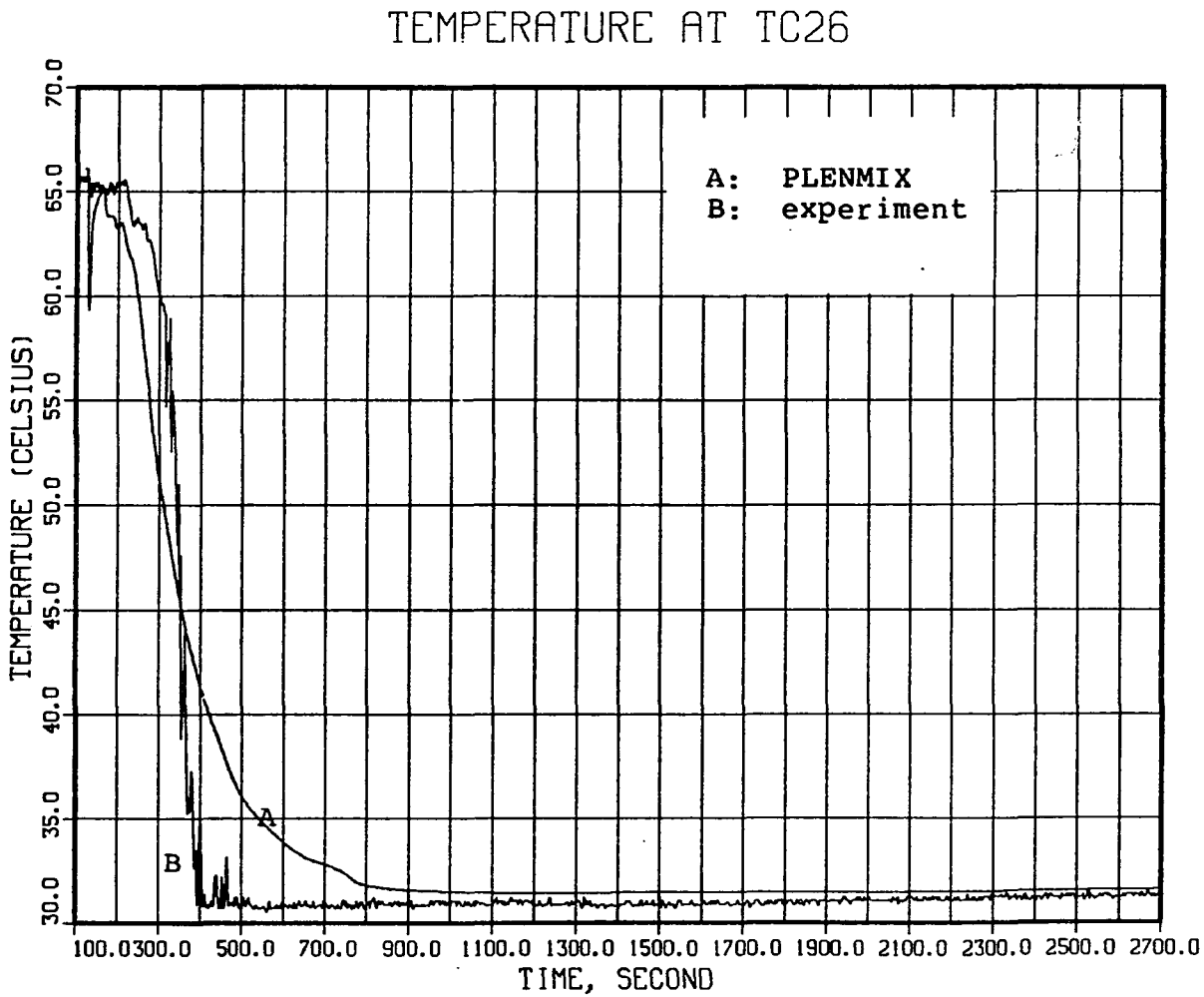

Figure 13. Temperature transient at TC26

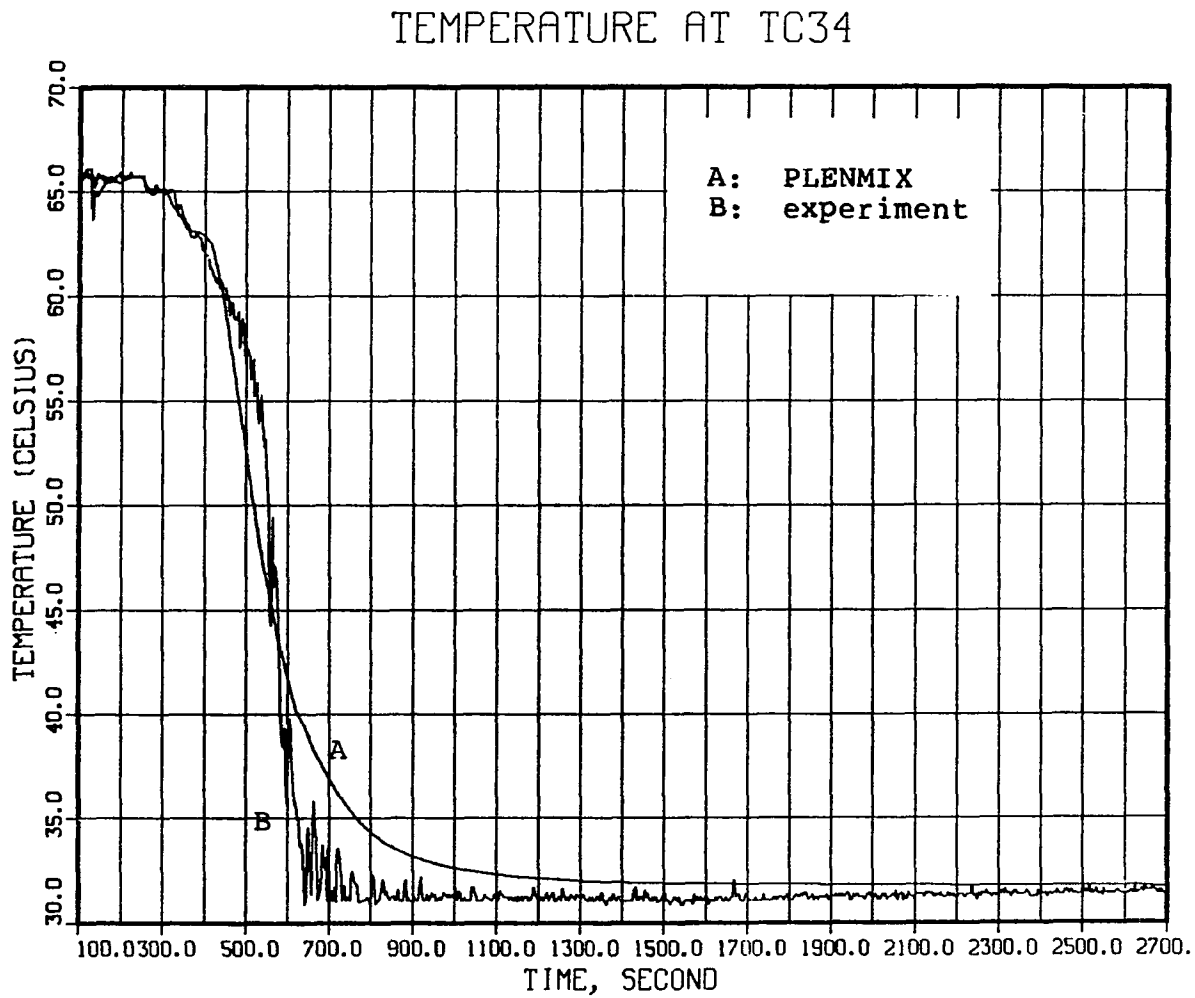

Figure 14. Temperature transient at TC34

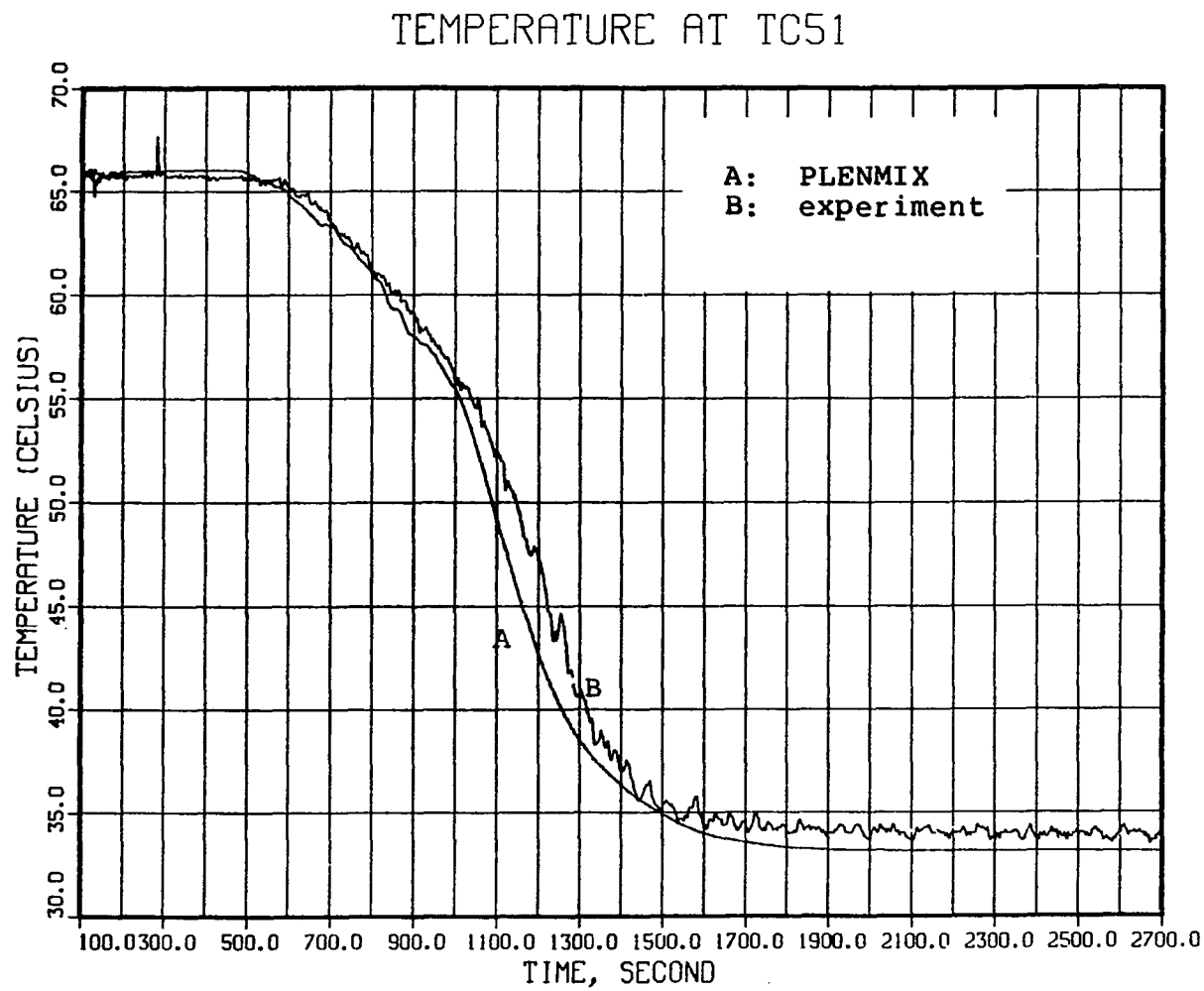

Figure 15. Temperature transient at TC51

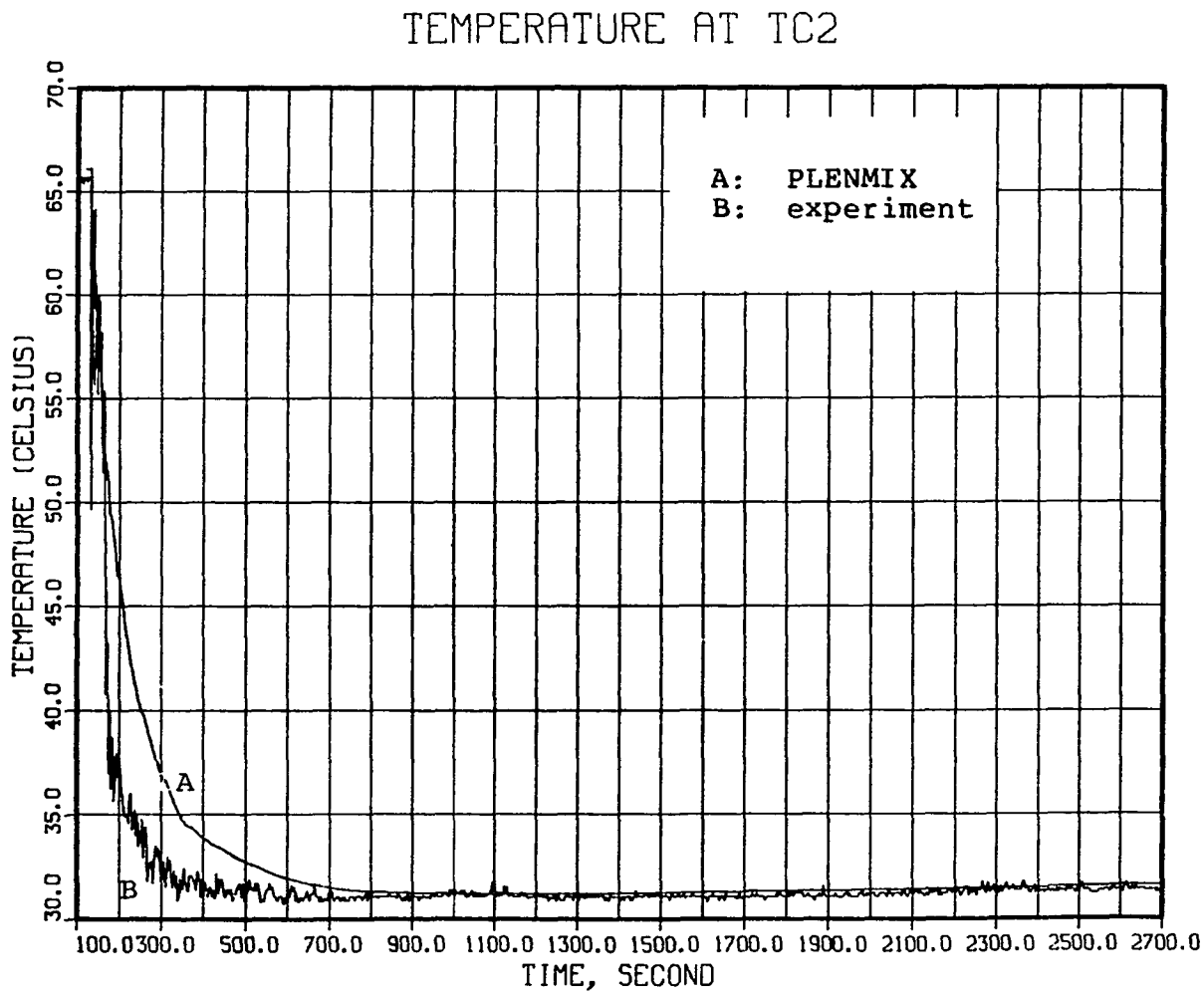

Figure 16. Temperature transient at TC2

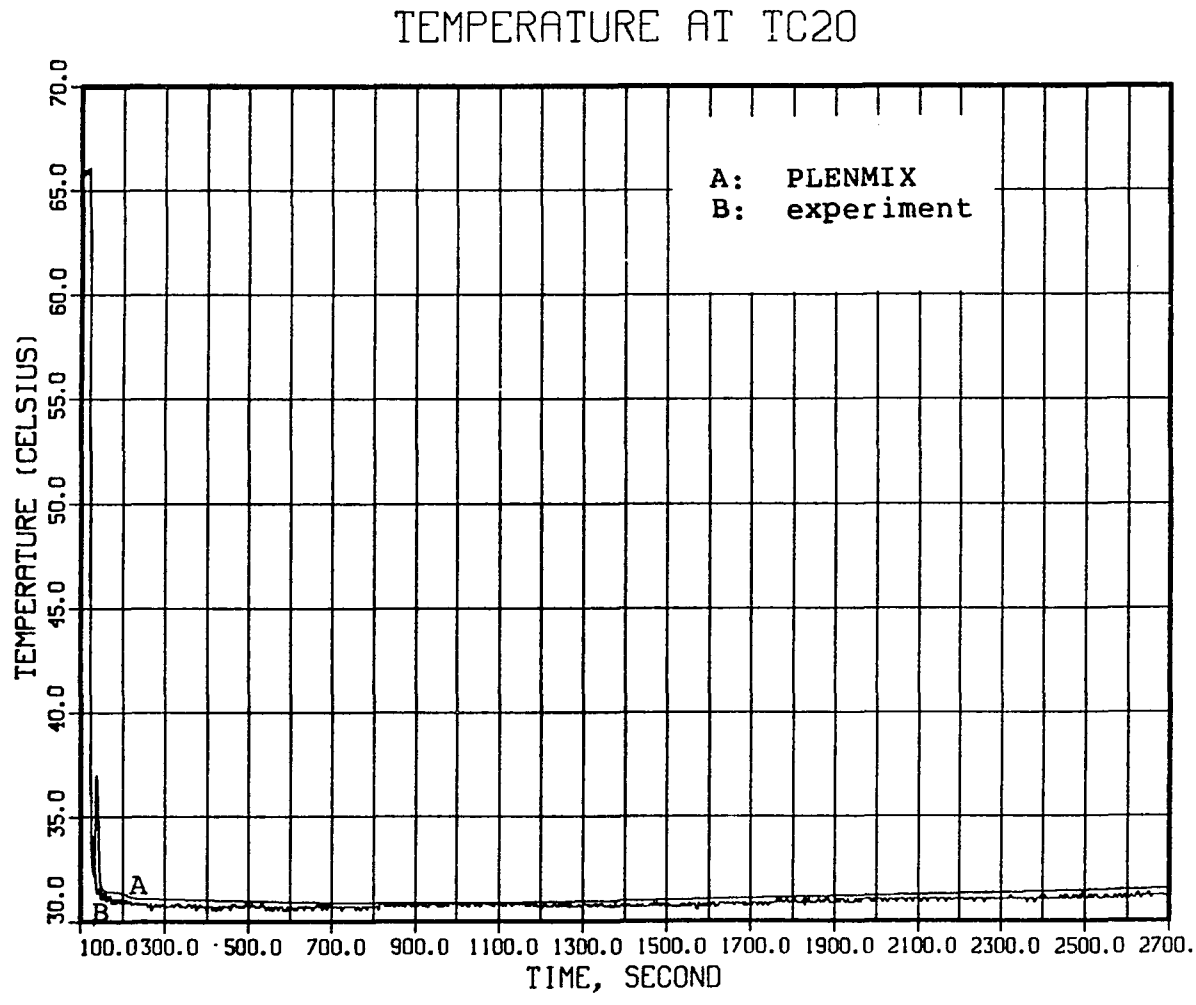

Figure 17. Temperature transient at TC20

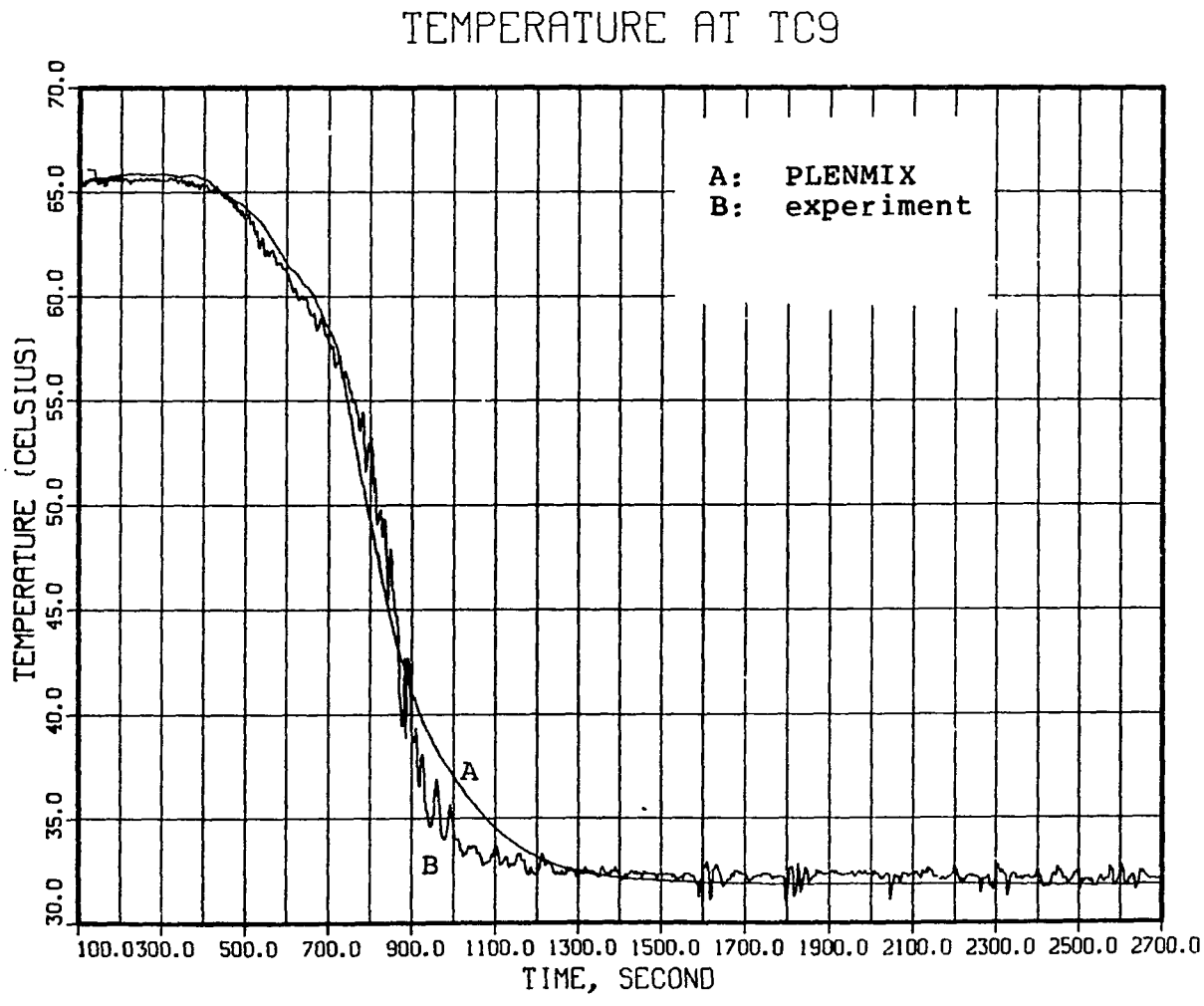

Figure 18. Temperature transient at TC9

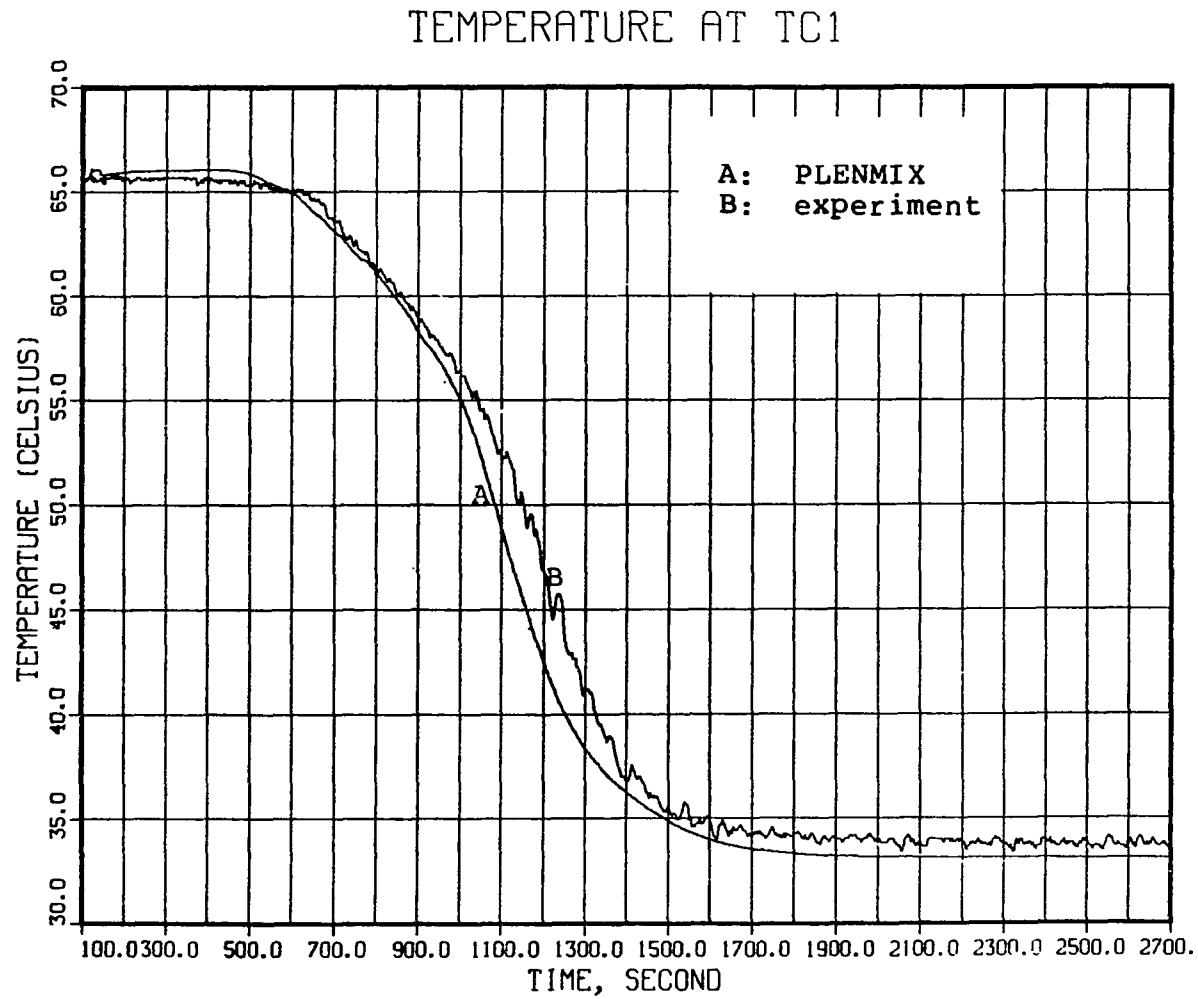

Figure 19. Temperature transient at TC1

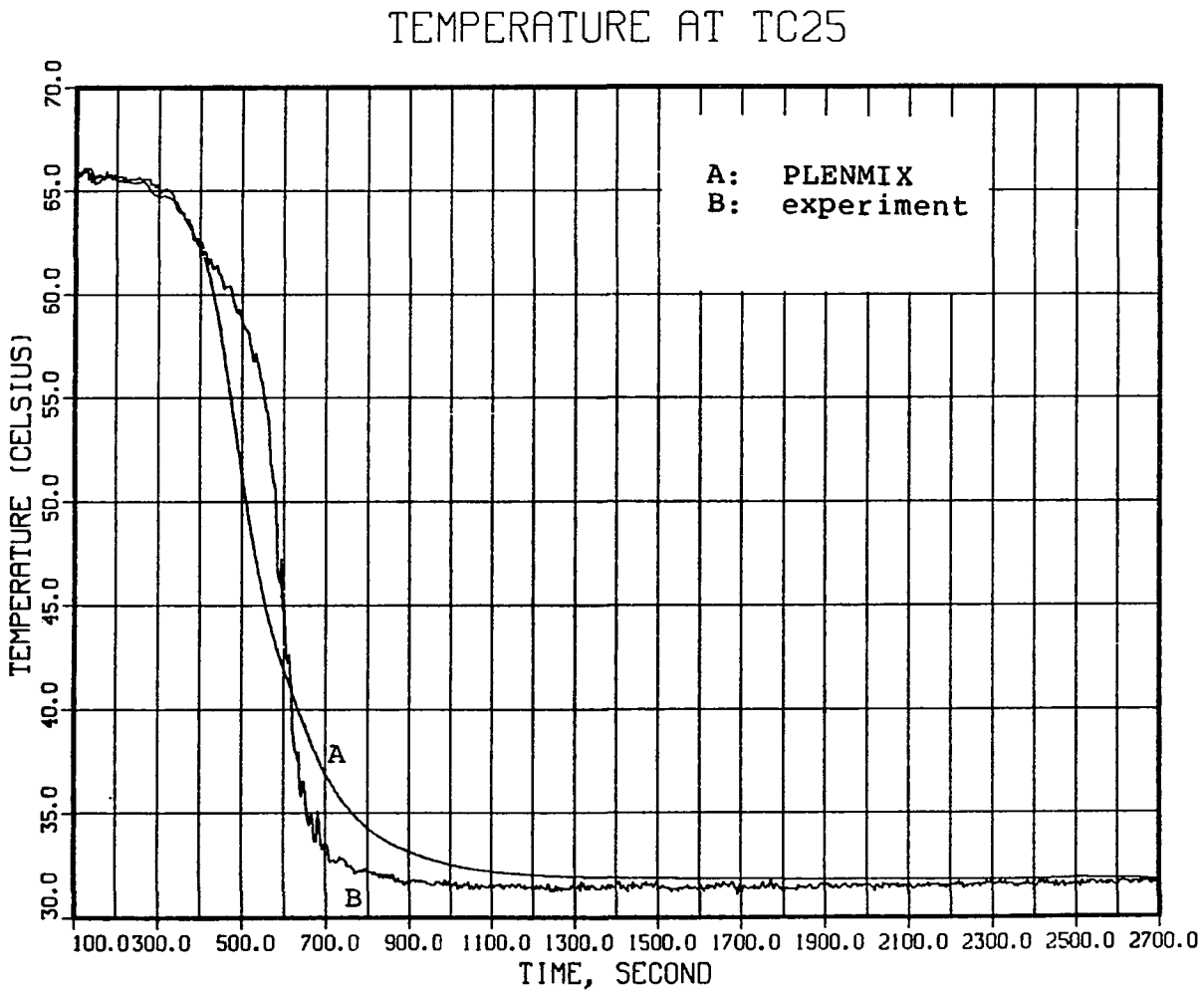

Figure 20. Temperature transient at TC25

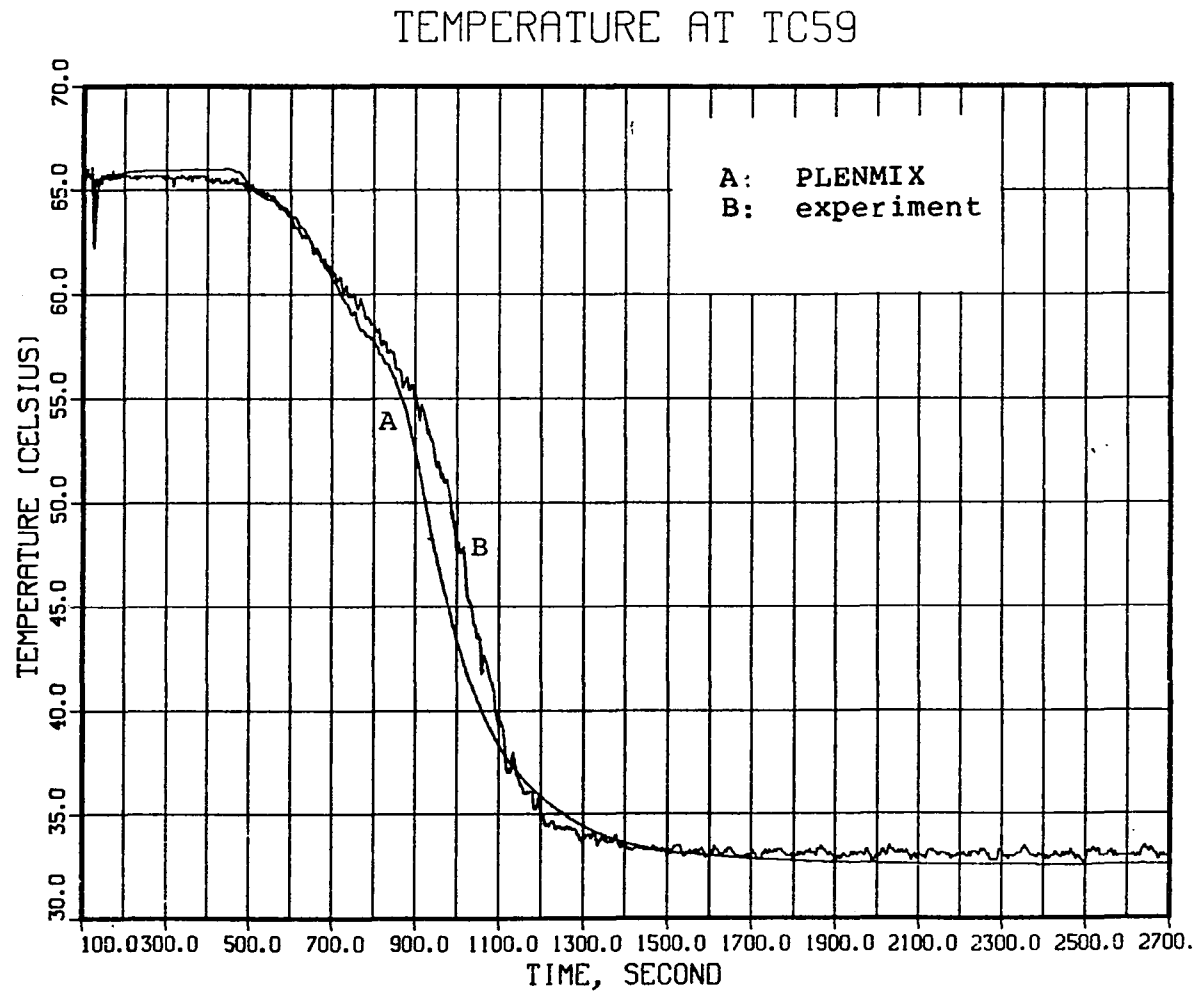

Figure 21. Temperature transient at TC59

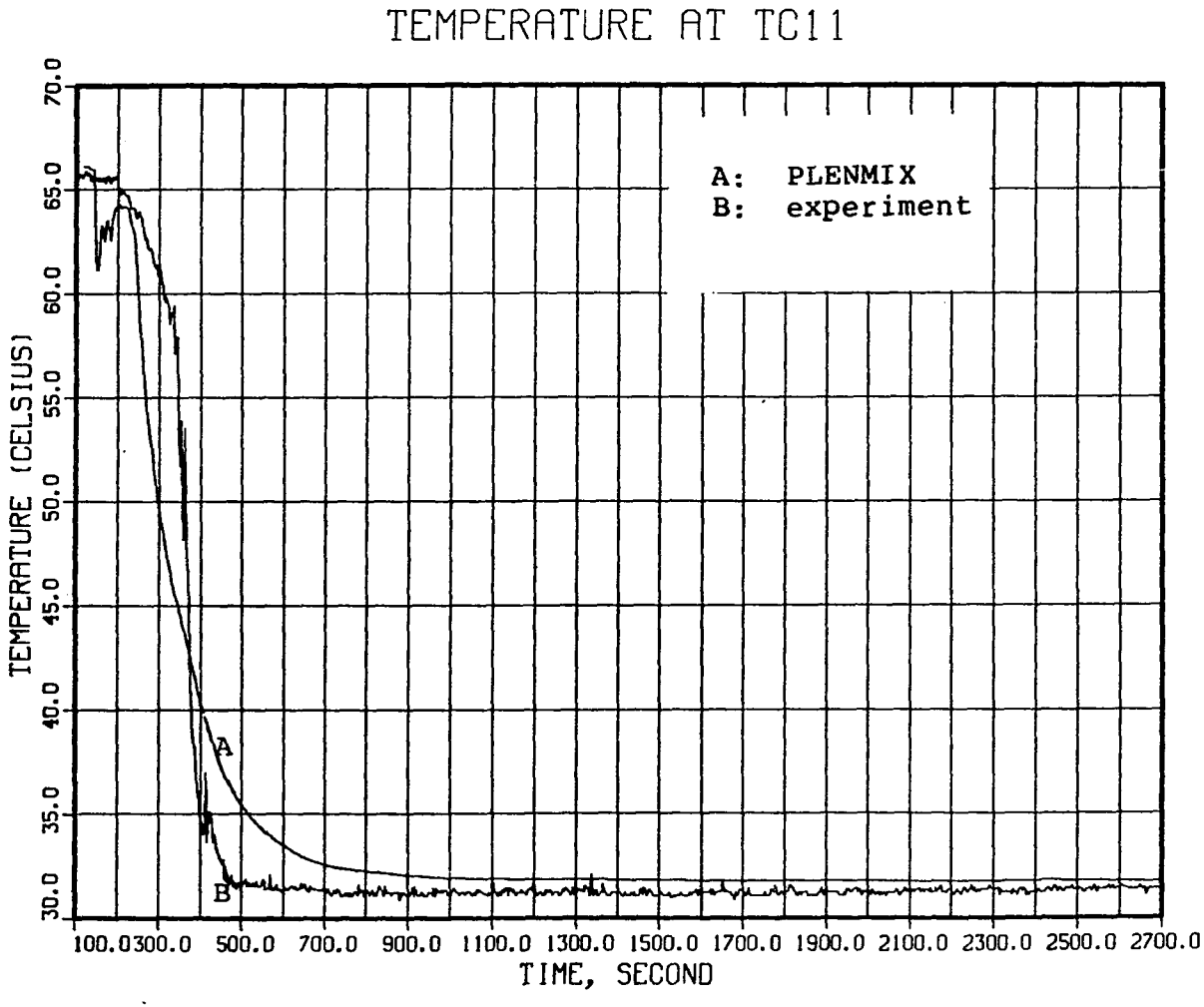

Figure 22. Temperature transient at TC11

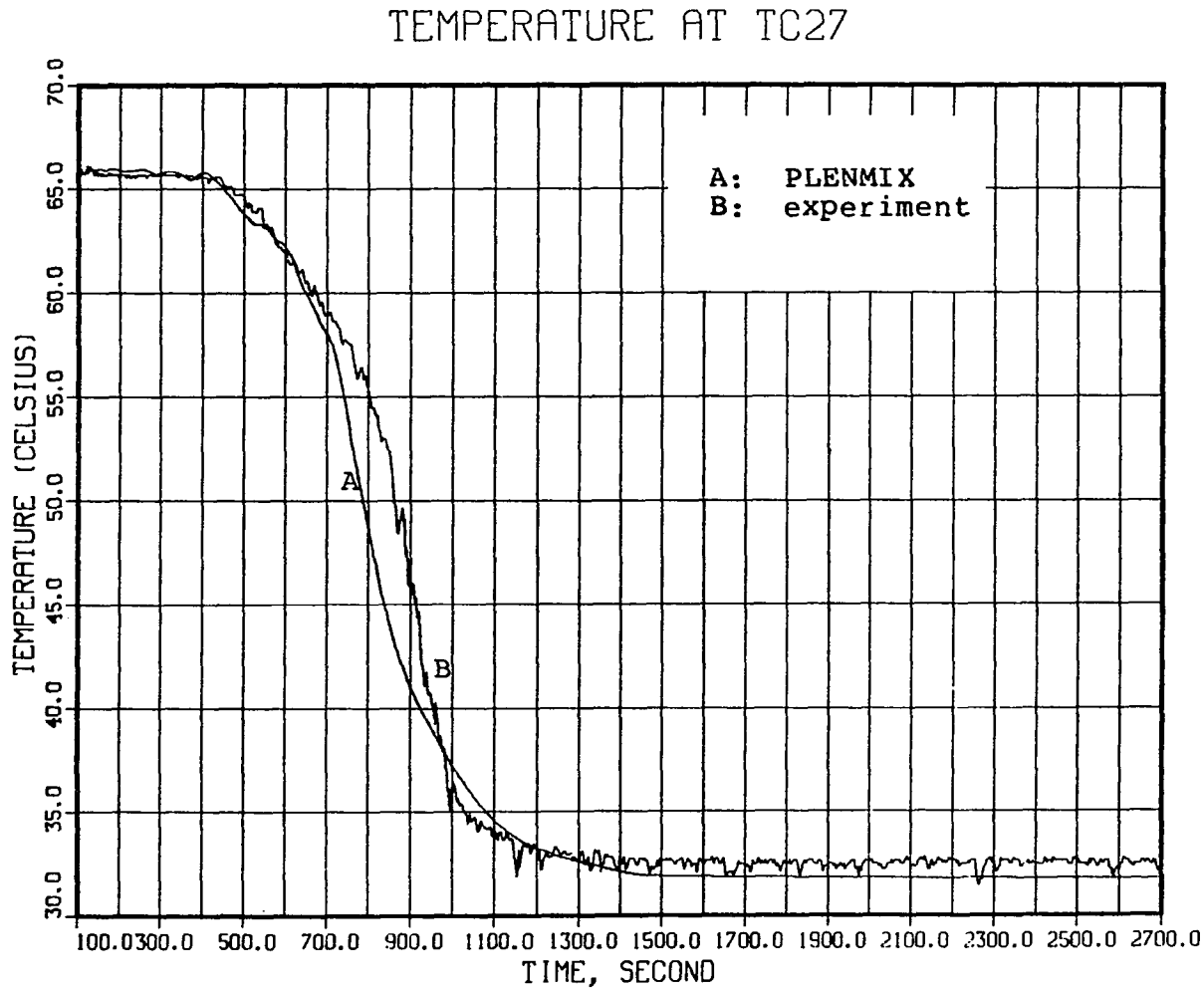

Figure 23. Temperature transient at TC27

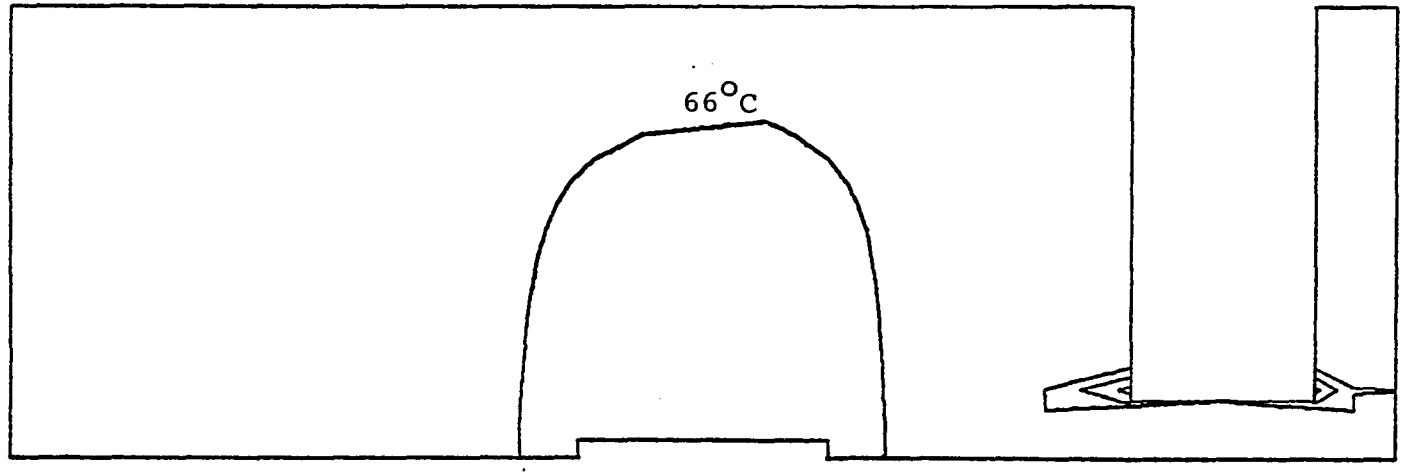

Figure 24. Isothermal lines of vertical cross section at t = 121.2 sec

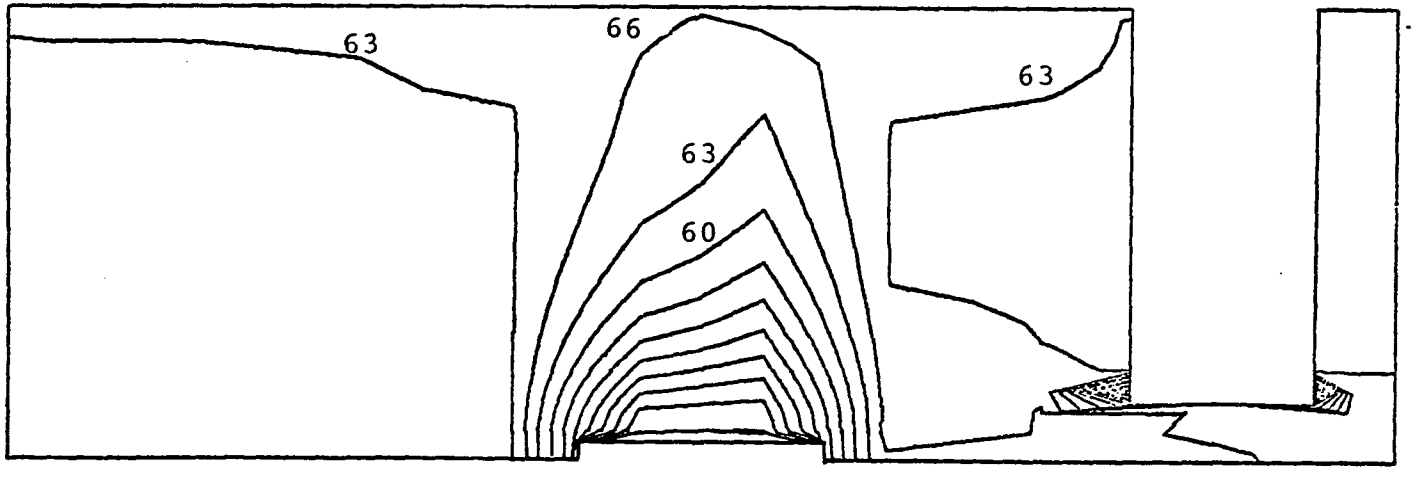

Figure 25. Isothermal lines of vertical cross section at t = 124.7 sec

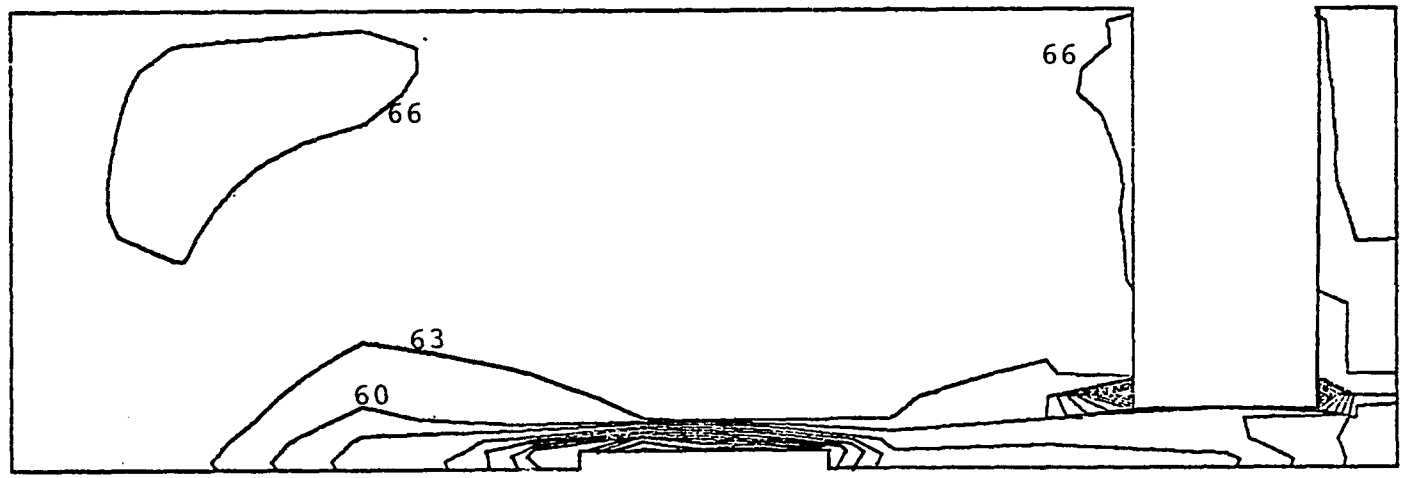

Figure 26. Isothermal lines of vertical cross section at t = 137.6 sec

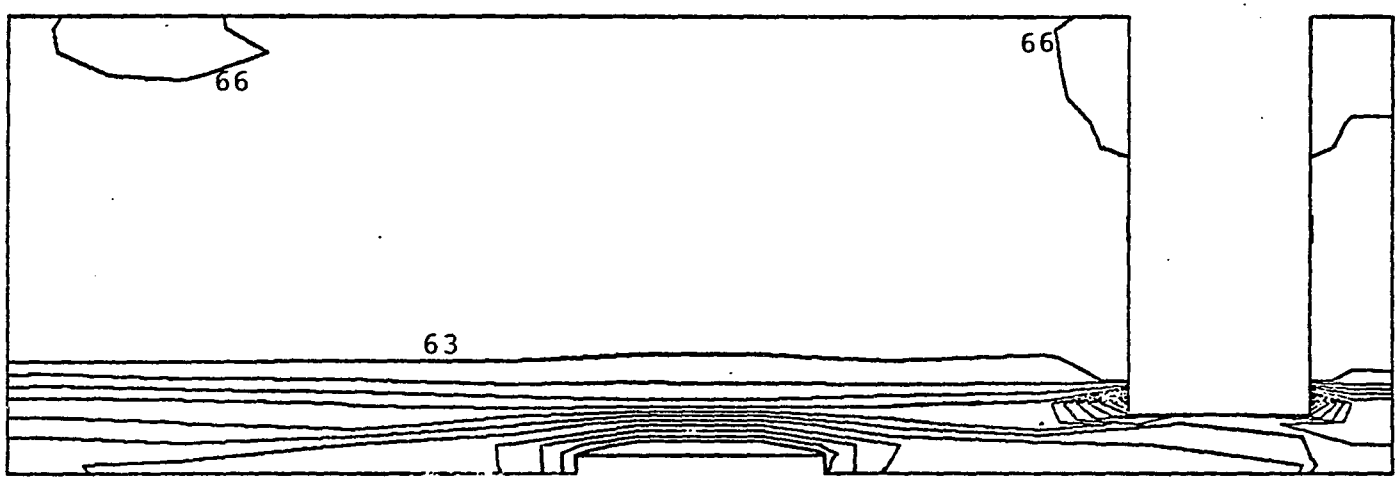

Figure 27. Isothermal lines of vertical cross section at t = 209.4 sec

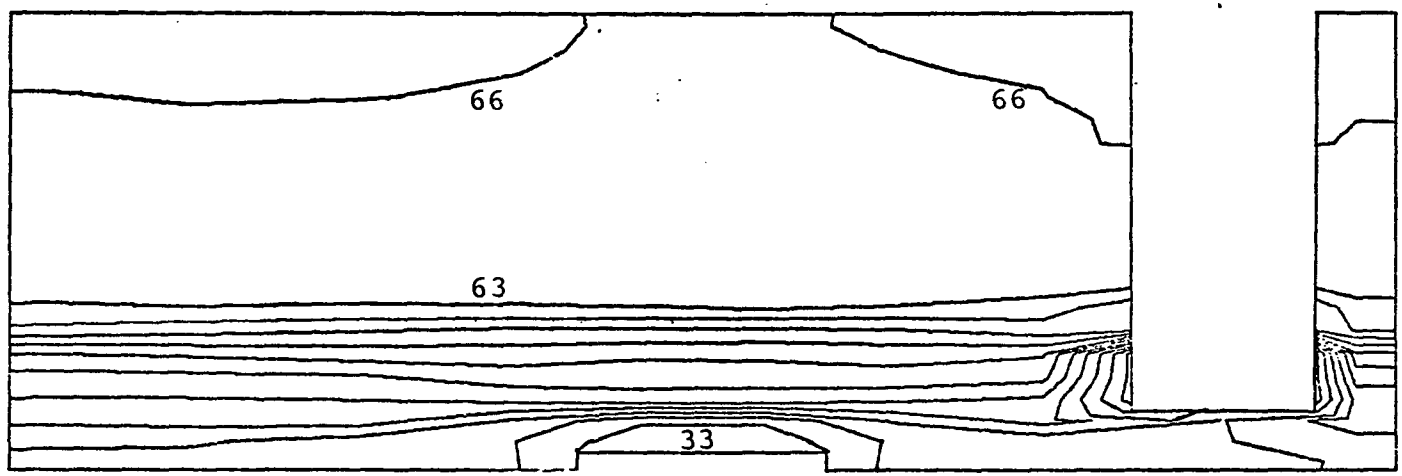

Figure 28. Isothermal lines of vertical cross section at t = 290.2 sec

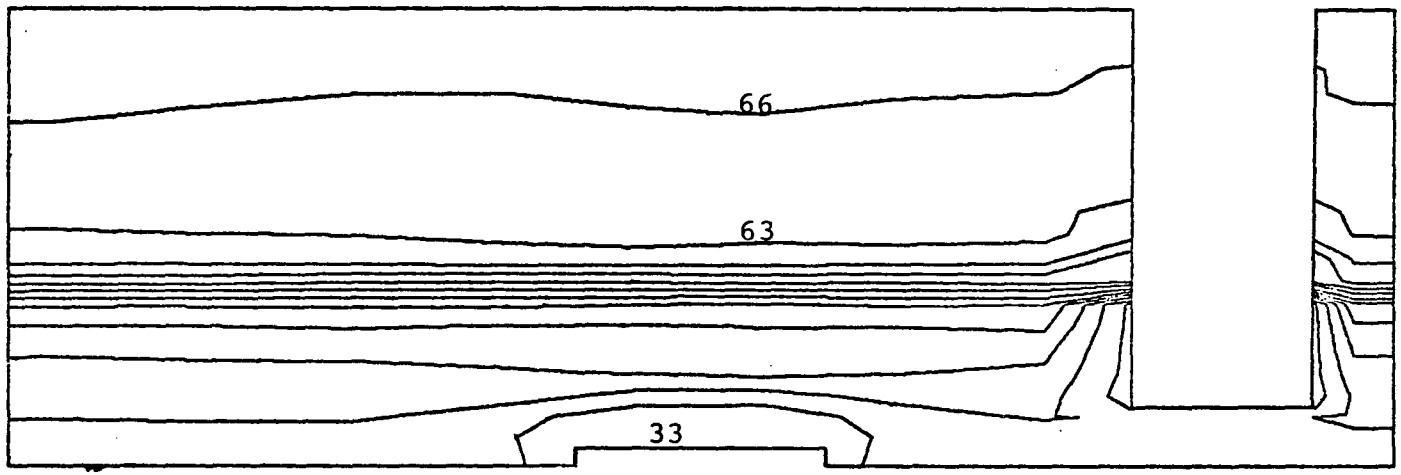

Figure 29. Isothermal lines of vertical cross section at t = 371.2 sec

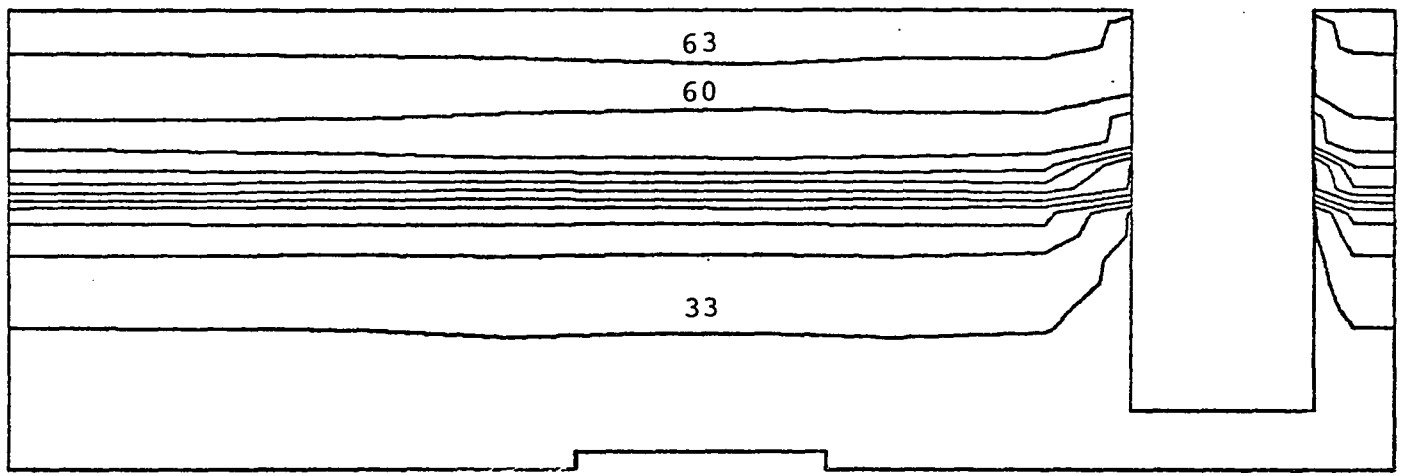

Figure 30. Isothermal lines of vertical cross section at t = 736.3 sec

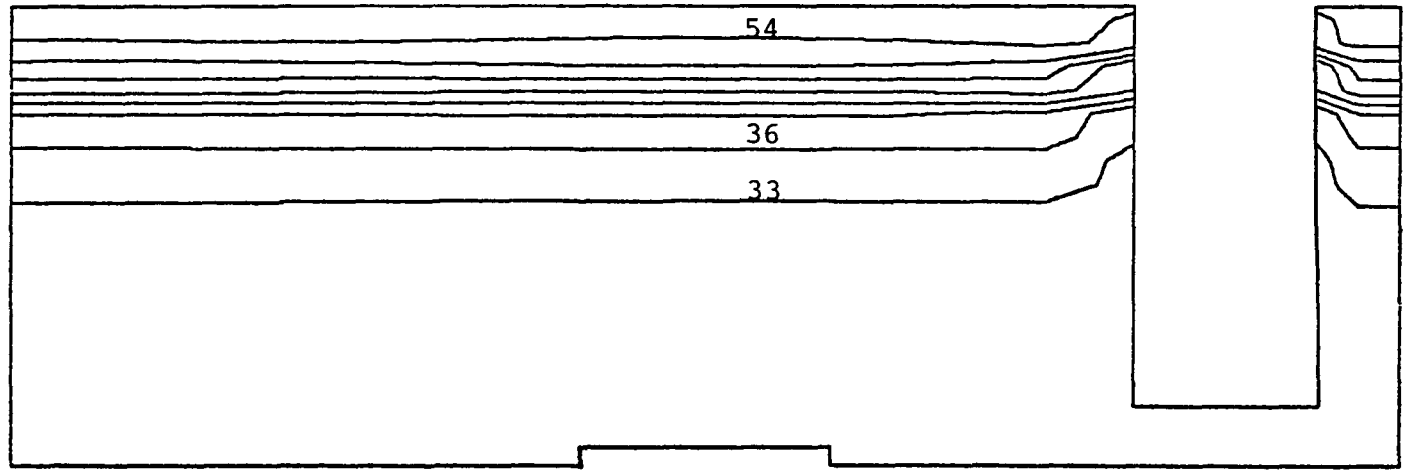

Figure 31. Isothermal lines of vertical cross section at t = 1076.1 sec

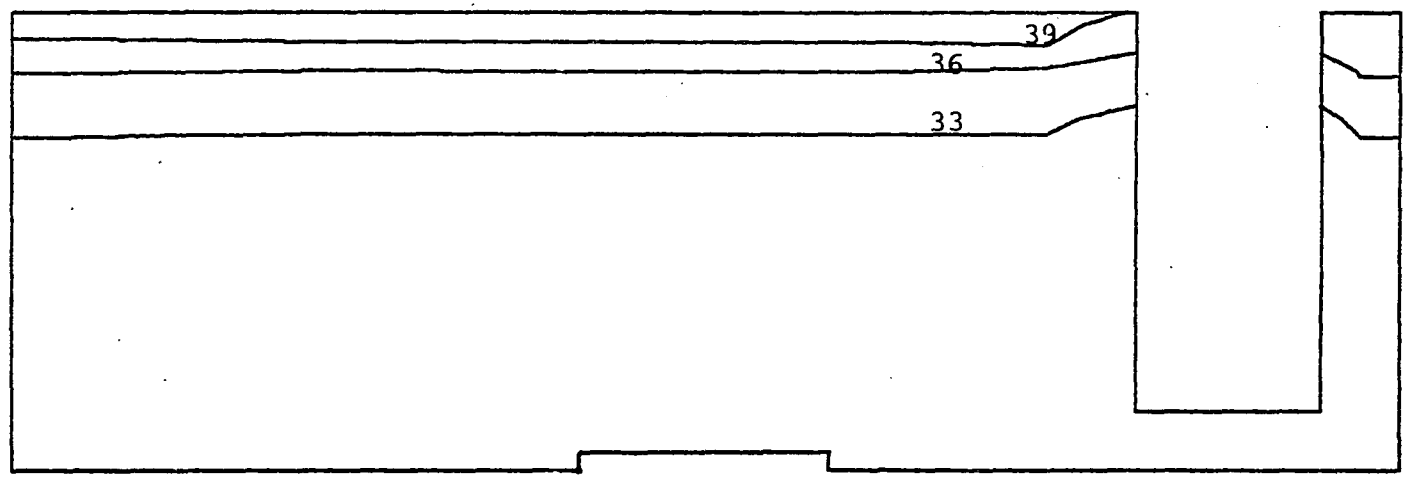

Figure 32. Isothermal lines of vertical cross section at t = 1424.7 sec

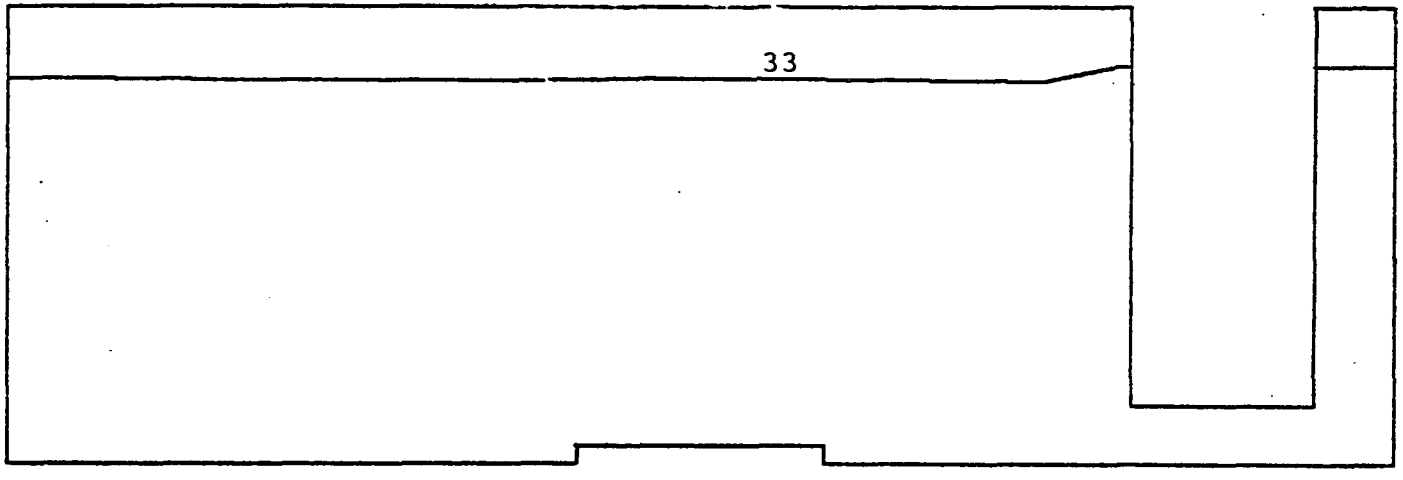

Figure 33. Isothermal lines of vertical cross section at t = 2700.0 sec

IV. SIMILITUDE REQUIREMENT

A. Scaling Problems

In order to establish specific scaling laws for determining the test facility requirements for upper plenum testing, an assessment of scaling requirements is presented in this chapter. The projection of the model test data for prediction of the full-scale plenum behavior is discussed. Since it is impossible to match all the similarity parameters, the sensitivity of the the system to various parameters is considered in some detail.

The task of selecting an appropriate scale for the test facility is a complex one. This work can not be done through any scale experiments because the influence of weak governing laws can not be identified. Also it can not be done by simplified mathematical models due to the same reason. This task can be done by a reliable, detailed, three-dimensional thermal hydraulic mathematical model. The PLENMIX code was found to be an excellent tool for this purpose.

The prime coolant candidates for the experimental facility are sodium and water. Water has the potential for increased flexibility at lower cost. Therefore, an evaluation was conducted on the adequacy of water and sodium for natural convective experiments involving the upper plenum

In comparison of water with sodium, it is obvious that water is more advantageous from the standpoint of cost and operating ease. It has been used successfully in a number of forced-convective flow hydraulic studies of the plenum. Table 2 lists the physical property data for sodium and water.

The thermal conductivity, the density, the specific heat, the thermal diffusivity, the viscosity and the Prandtl number of sodium differ significantly from water. Therefore, a question has been raised whether water is an adequate fluid to simulate sodium for a full-scale plenum operating condition. It may be necessary to construct a scale test facility using sodium as the test fluid.

Table 2. Physical properties of sodium and water

	Water (50°C)	Sodium (350°C)
Density, ρ kg/m	983	868
Viscosity, μ kg/m-sec	5.62×10^{-4}	2.96×10^{-4}
Specific heat, C_p J/kg - K	4190	1290
Thermal conductivity k, J/m-sec-K	0.6245	74.05
Kinematic viscosity, ν m^2/sec	5.72×10^{-7}	3.41×10^{-7}
Thermal diffusivity, α m^2/sec	1.52×10^{-7}	6.61×10^{-5}
Prandtl number, Pr	3.77	5.16×10^{-3}

B. Case Study I: 100%-10% Flow Transient

In the process of comparing sodium and water, computer simulation began with a hypothetical 100%-10% flow transient. The temperature and flow transients for both sodium and water are shown in Figure 34. The plenum geometry for both coolants is identical to that in Figs. 2-4, which is 1/13 of the prototype scale.

In order to investigate the influence of thermal conduction between the hot and cold layers of the stratified flow, the following assumptions were made:

i) The IHX's outer surface is adiabatic.

ii) The plenum wall inner surface is adiabatic.

iii) Turbulent eddy transport of energy and momentum is constant.

iv) The inlet velocity and temperature is uniform over the inlet cross-section.

Table 3 lists the parameters for both water and sodium simulations based on the conservation of the Richardson Number.

Table 3. Parameters used in the 100%-10% flow transient simulation

Parameter	Sodium	Water
Size	1/13 Scale	1/13 Scale
Coolant flow rate	.0269 m^3/sec	.0177 m^3/sec
Temperature range	510.0°C - 375.83°C	66.11°C-31.0°C
Reference temperature	375.83°C	31.0°C
Initial inlet velocity	0.7716 m/sec	0.4461 m/sec
Final inlet velocity	0.07716 m/sec	0.04461 m/sec
$\Delta\rho/\rho$	0.0365	0.0122
Time ratio	0.578	1
Initial Ri	0.2607	0.2607
Initial Re	5.86×10^5	5.67×10^5
Initial Pe	2.2×10^6	2.93×10^3

The normalized exit temperature transient for both sodium and water are plotted on Figure 35. The normalized temperature (see Eq. 33) is defined as:

$$\phi = \frac{\text{Transient Temp. - Reference Temp.}}{\text{Steady State Temp. - Reference Temp.}} \tag{53}$$

The time scale is adjusted accordingly to Eq. (49). The agreement between these two simulations is excellent. Figures 36 to 45 also present the comparison of temperature transients at various (I, J, K) locations. The agreement for all locations is good. This implies that both water and sodium scale testing will give accurate prediction for prototype behavior in a 100 -10 flow transient. This also implies that the Richardson Number is the only parameter needs to be matched.

C. Case Study II: 100%-1% Flow Transient

The next important case examined was a 100%-1% flow coastdown simulation. Under this condition, the temperature field may be influenced by conduction between the hot fluid in the plenum top with the cold fluid in the plenum bottom as pointed out by Heisler and Singer [3]. Therefore, the accuracy in the extrapolation of the water scale test data to a full-scale prototype LMFBR has been questioned, and a sodium test facility has subsequently been proposed [3].

Various scales and test fluids have been employed to simulate this 100%-1% flow transient. These are:

(1) Prototype, sodium

(2) 1/13 scale, water

(3) 1/13 scale, sodium

(4) 1/7 scale, sodium

(5) 1/3 scale, sodium

Table 4 lists the parameters used in these simulations. Figure 46 shows the temperature and flow transient forcing function.

The plenum exit transient temperature is given in Figure 47. It shows that the agreement between the prototype and the 1/13 scale water simulation is excellent. The scale sodium simulation is not as good and deviates even more as the scale becomes smaller. Figures 48 to 55 show the transient temperatures at various locations. All the figures show good agreement between the prototype and the 1/13 scale water simulation. However, the scale modeling using sodium is not as good as the water results.

The discrepancy of the exit temperature changing rate between the prototype and the 1/13 scale sodium model is significant. This means that if small-scale sodium test data are extrapolated for prediction of a full-scale LMFBR plenum natural convection behavior, the components could be exposed to unwarranted thermal stresses. Also, it takes a much longer time for the reactor upper plenum to cool down than the prediction of the sodium model.

In summary, scale water test can predict full scale prototype thermal behavior while scale sodium test can't for low flow condition. The good agreement between the prototype and the 1/13 scale water simulation implies that the Richardson Number is the only parameter that needs to be matched.

Table 4. Parameters used in the 100%–1% flow transient simulation

Parameter	Prototype	1/13 Scale Water	1/13 Scale Sodium	1/7 Scale Sodium	1/3 Scale Sodium
Temperature (°C)	510.–375.83	66.11–31.0	510.–375.83	510.–375.83	510.–375.83
Reference temperature (°C)	375.83	31.0	375.83	375.83	375.83
Initial inlet velocity (m/sec)	2.782	0.4461	0.7716	1.052	1.606
Final inlet velocity (m/sec)	0.02782	0.004461	0.007716	0.01052	0.01606
$\Delta\rho/\rho$	0.0365	0.0122	0.0365	0.0365	0.0365
Time ratio	1.0	0.48	0.277	0.378	0.577
Coolant flow rate	16.4	0.0156	0.0269	.1265	1.052

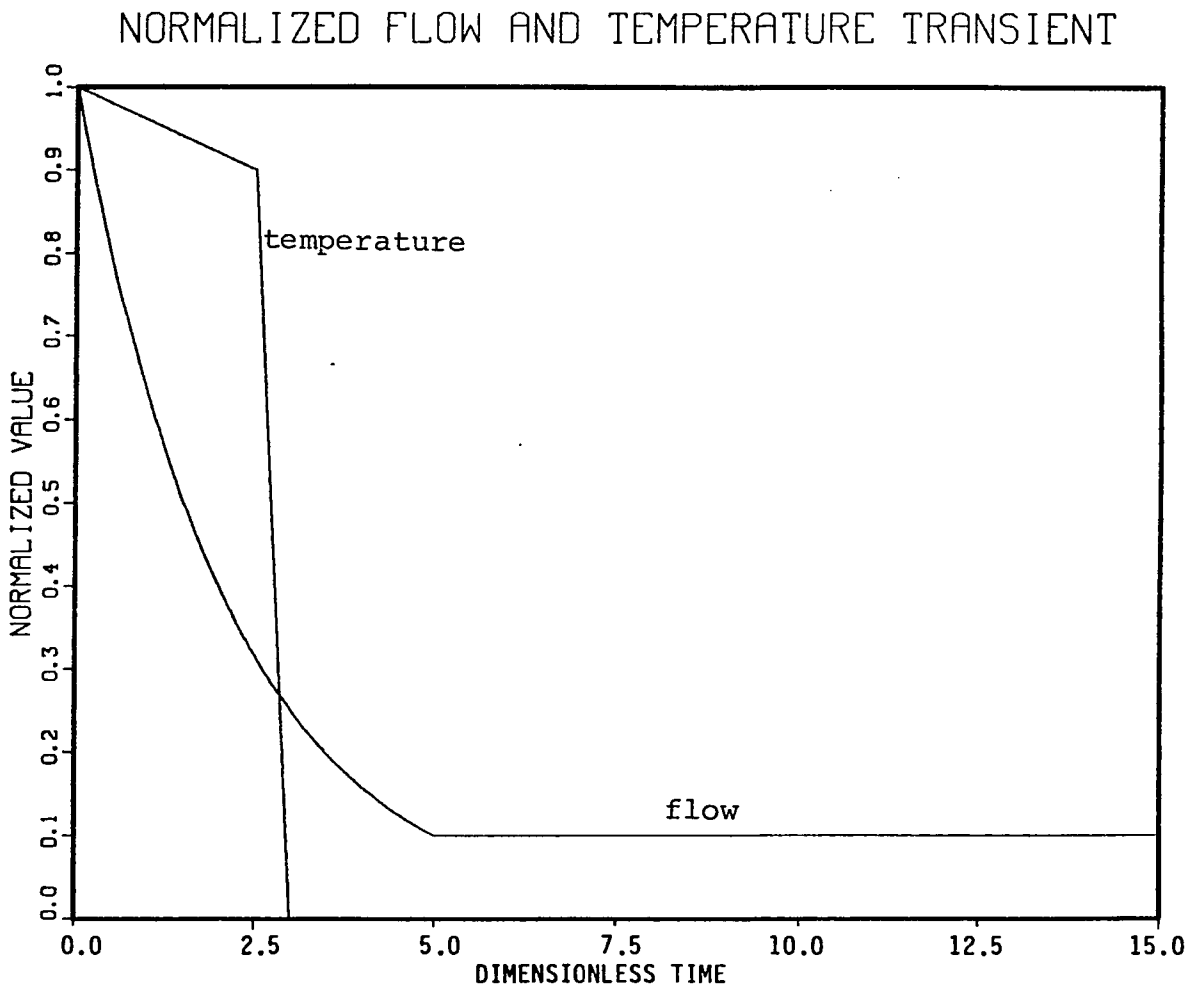

Figure 34. Normalized flow and temperature transient for case I

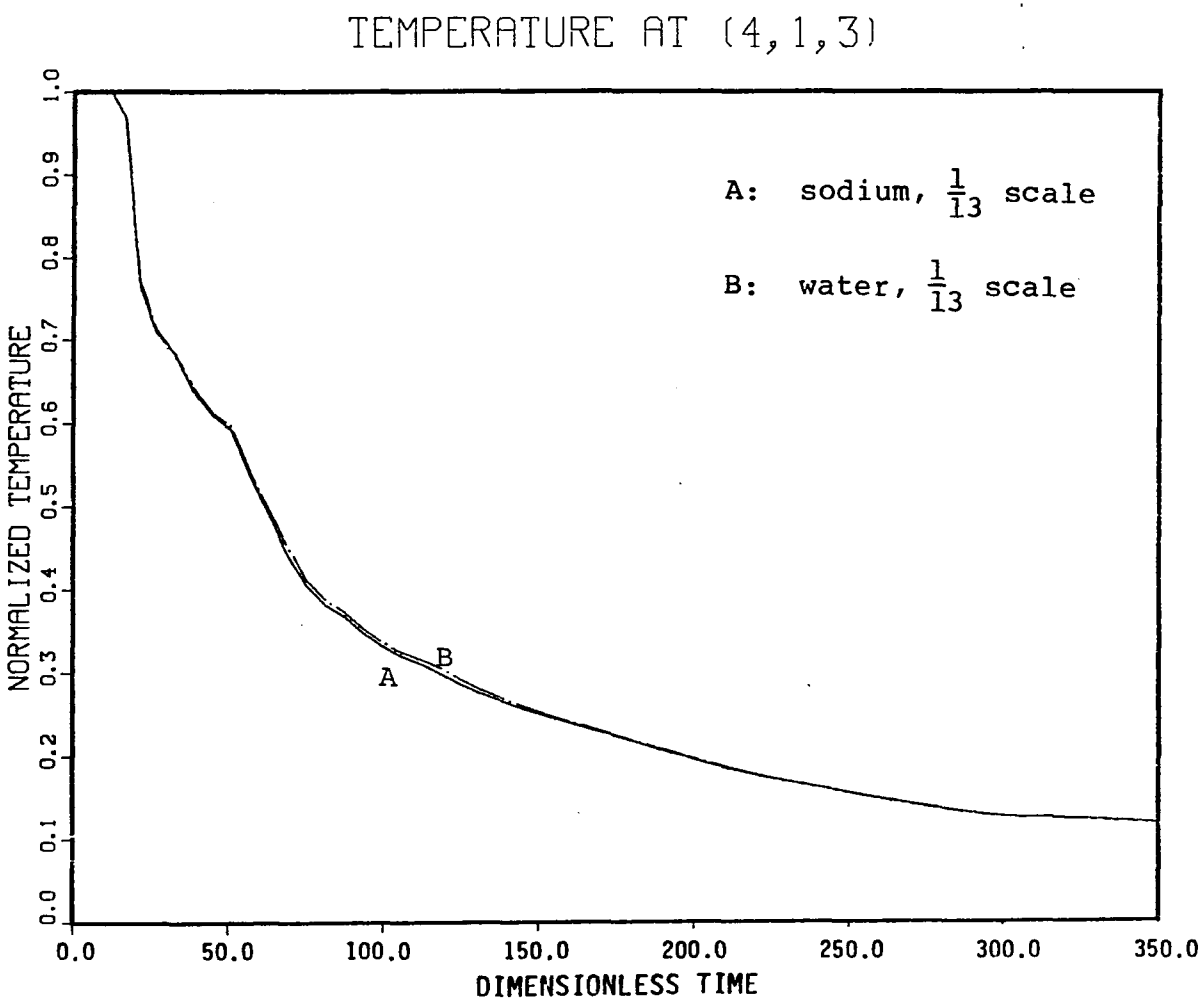

Figure 35. Normalized exit temperature transient for case I

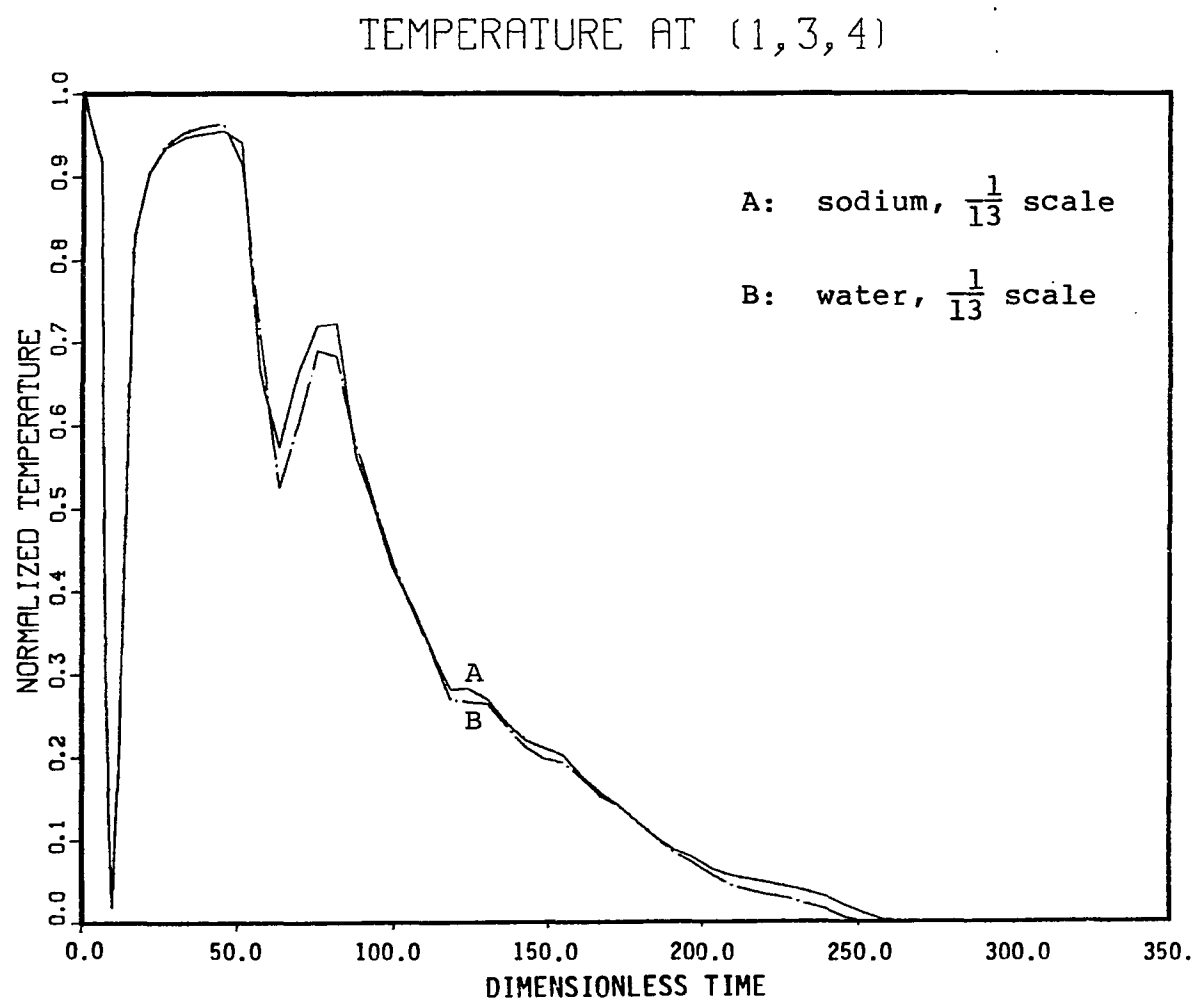

Figure 36. Normalized temperature transient at (1,3,4) for case I

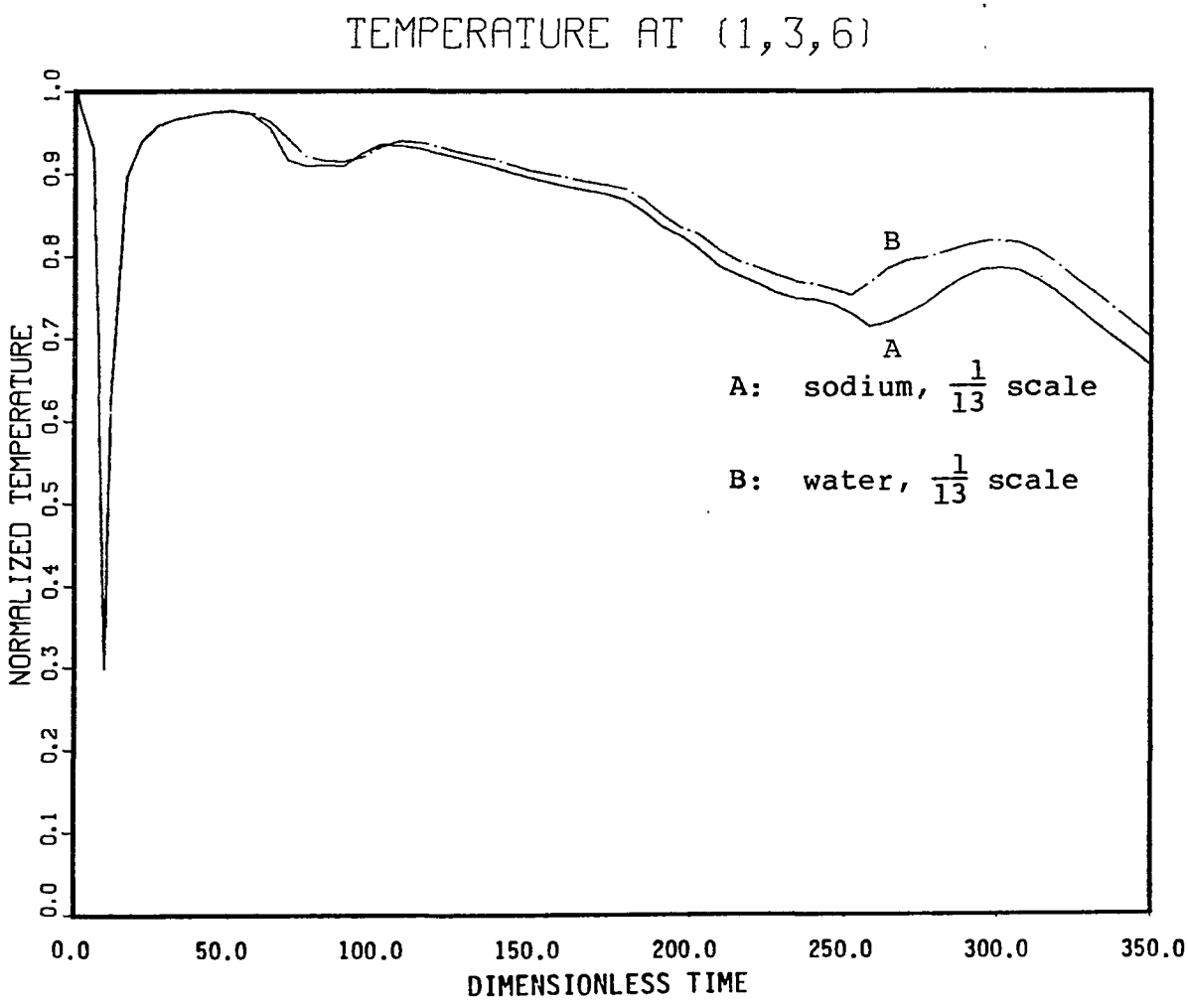

Figure 37. Normalized temperature transient at (1,3,6) for case I

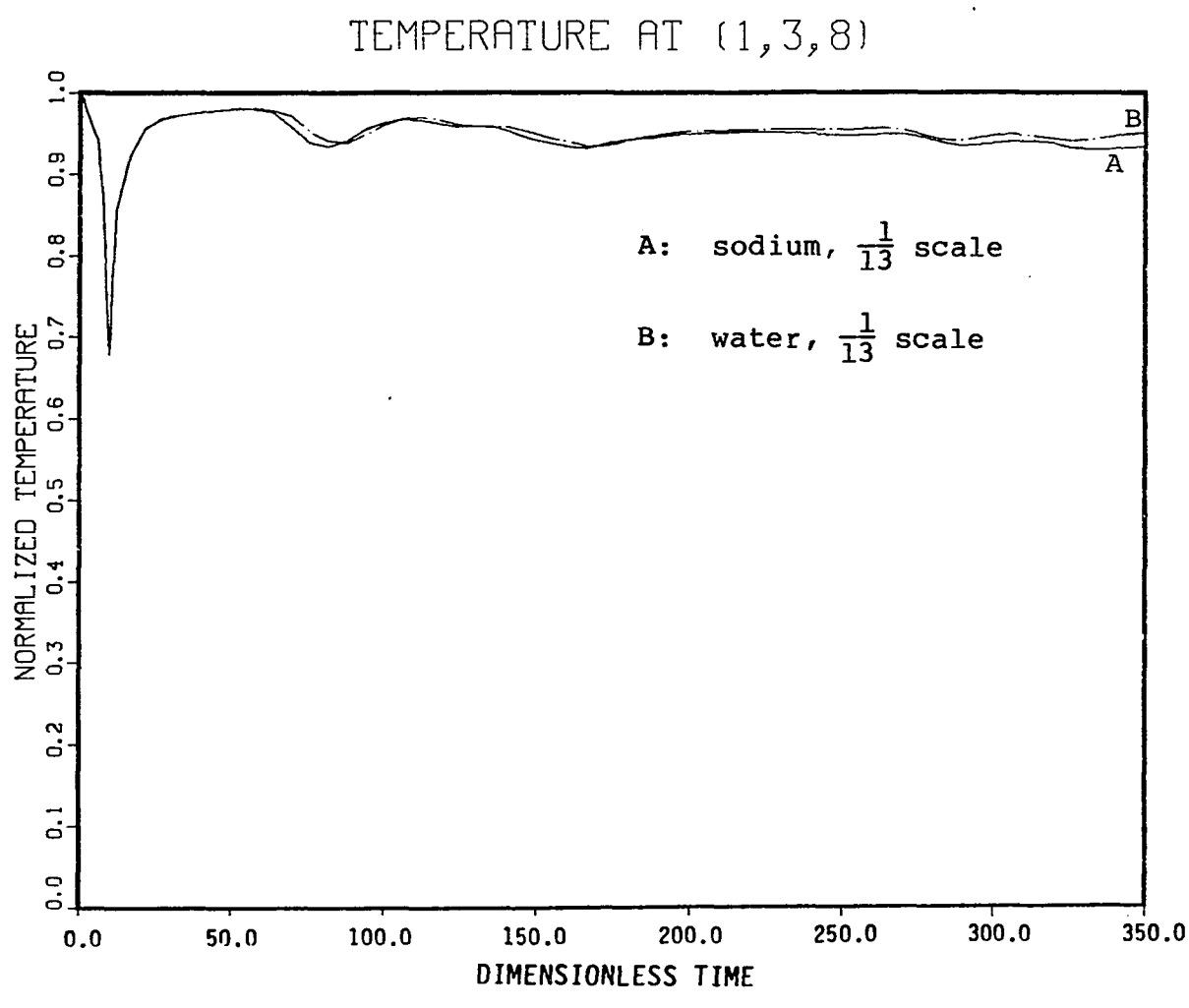

Figure 38. Normalized temperature transient at (1,3,8) for case I

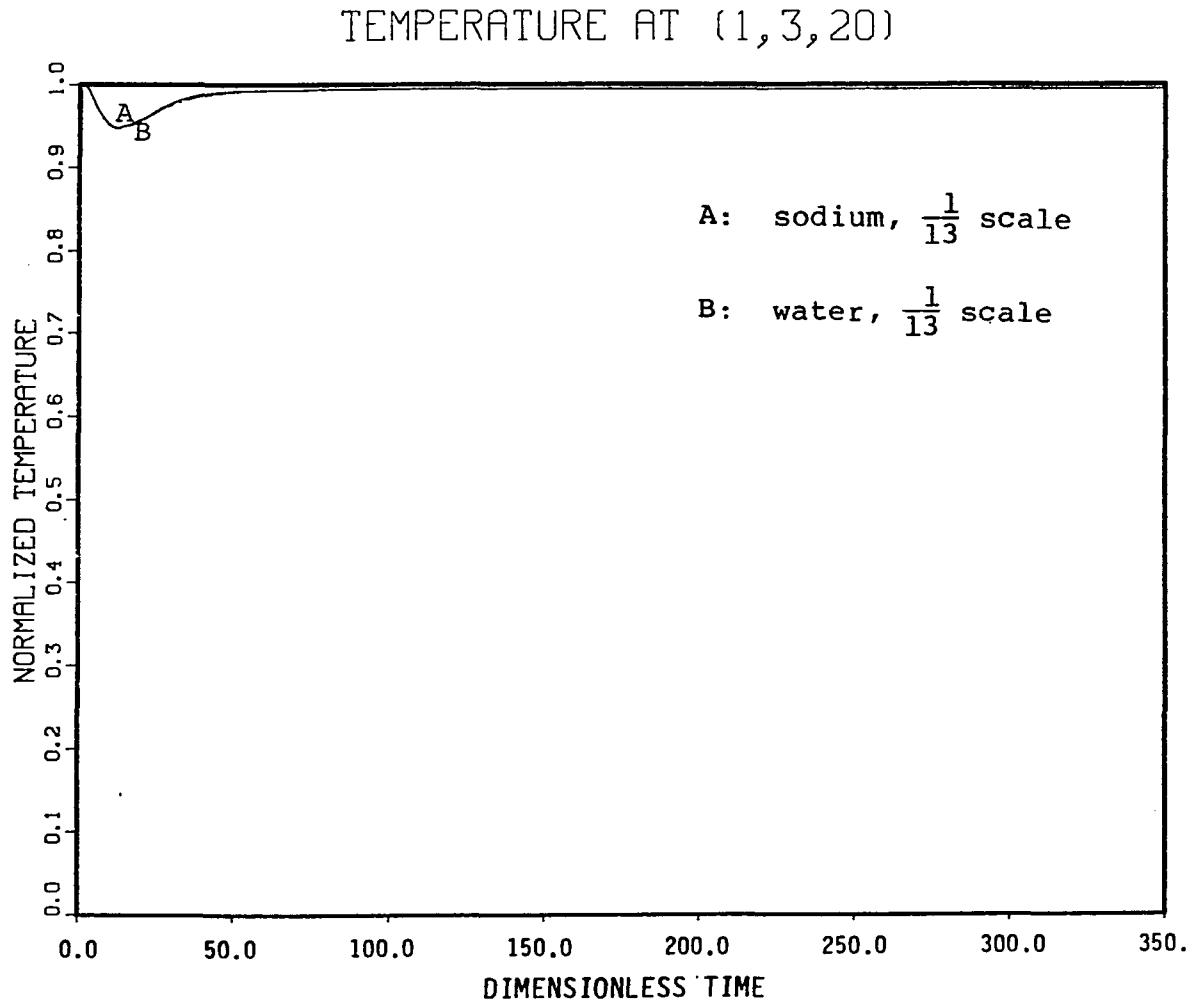

Figure 39. Normalized temperature transient at (1,3,20) for case I

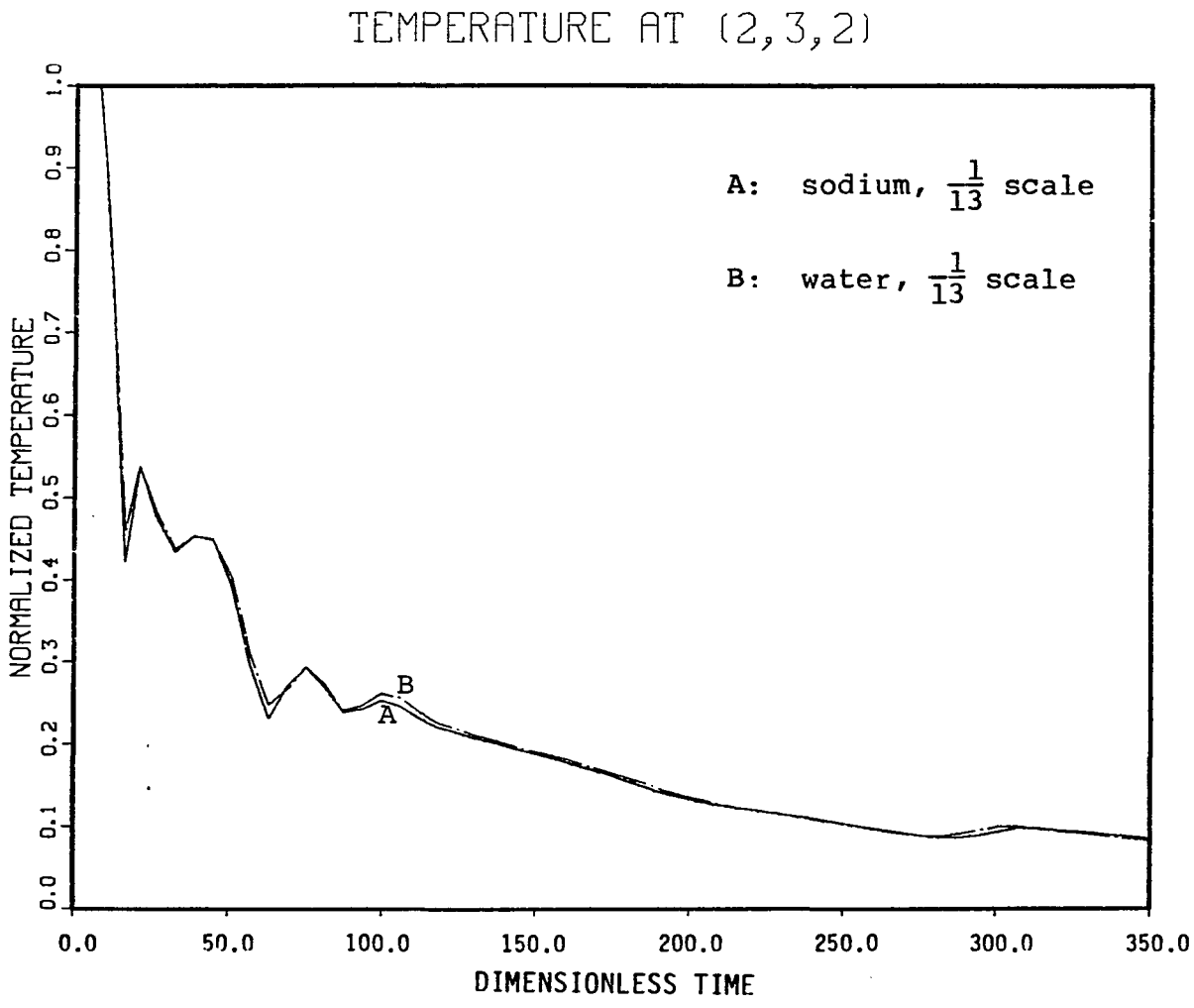

Figure 40. Normalized temperature transient at (2,3,2) for case I

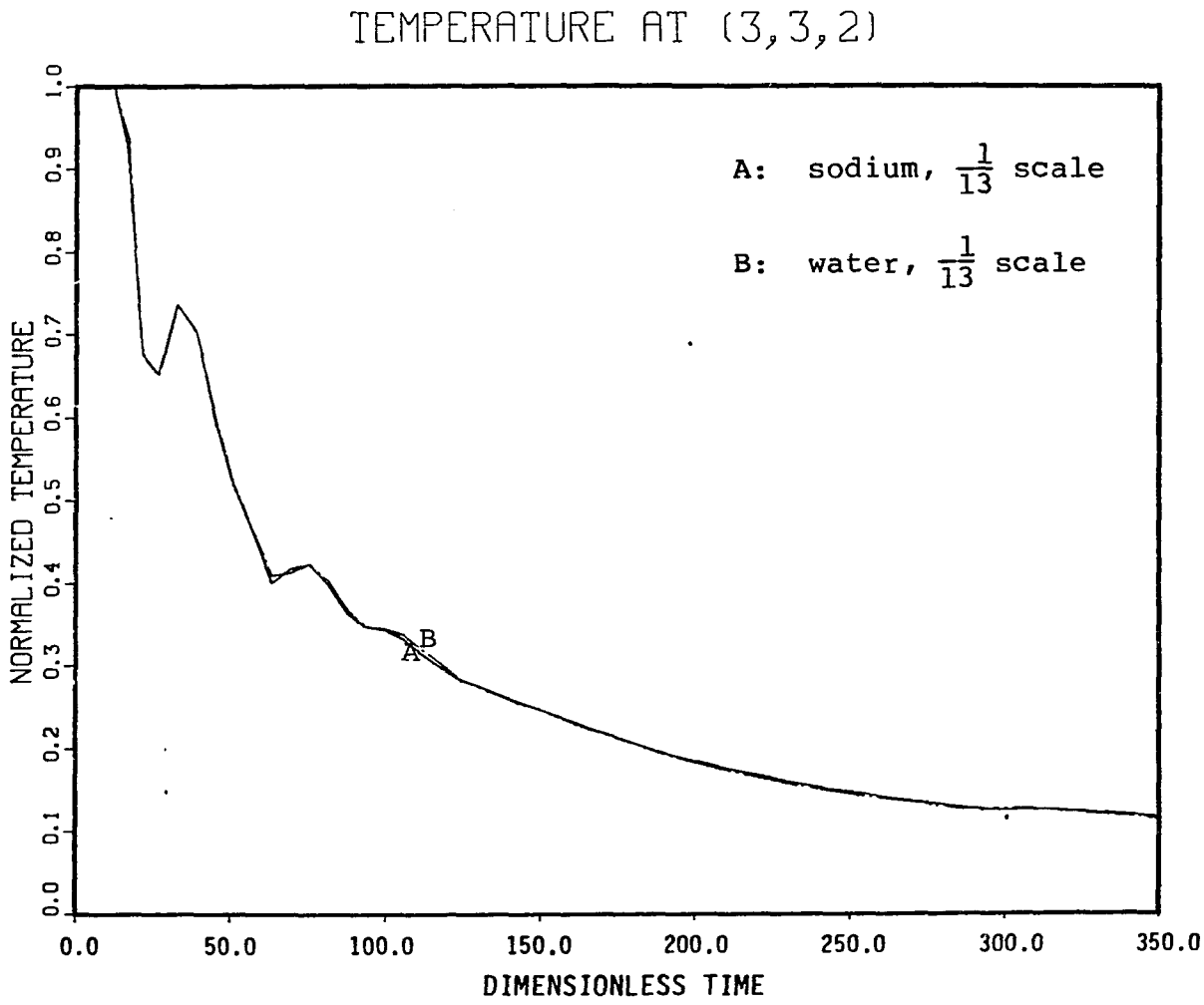

Figure 41. Normalized temperature transient at (3,3,2) for case I

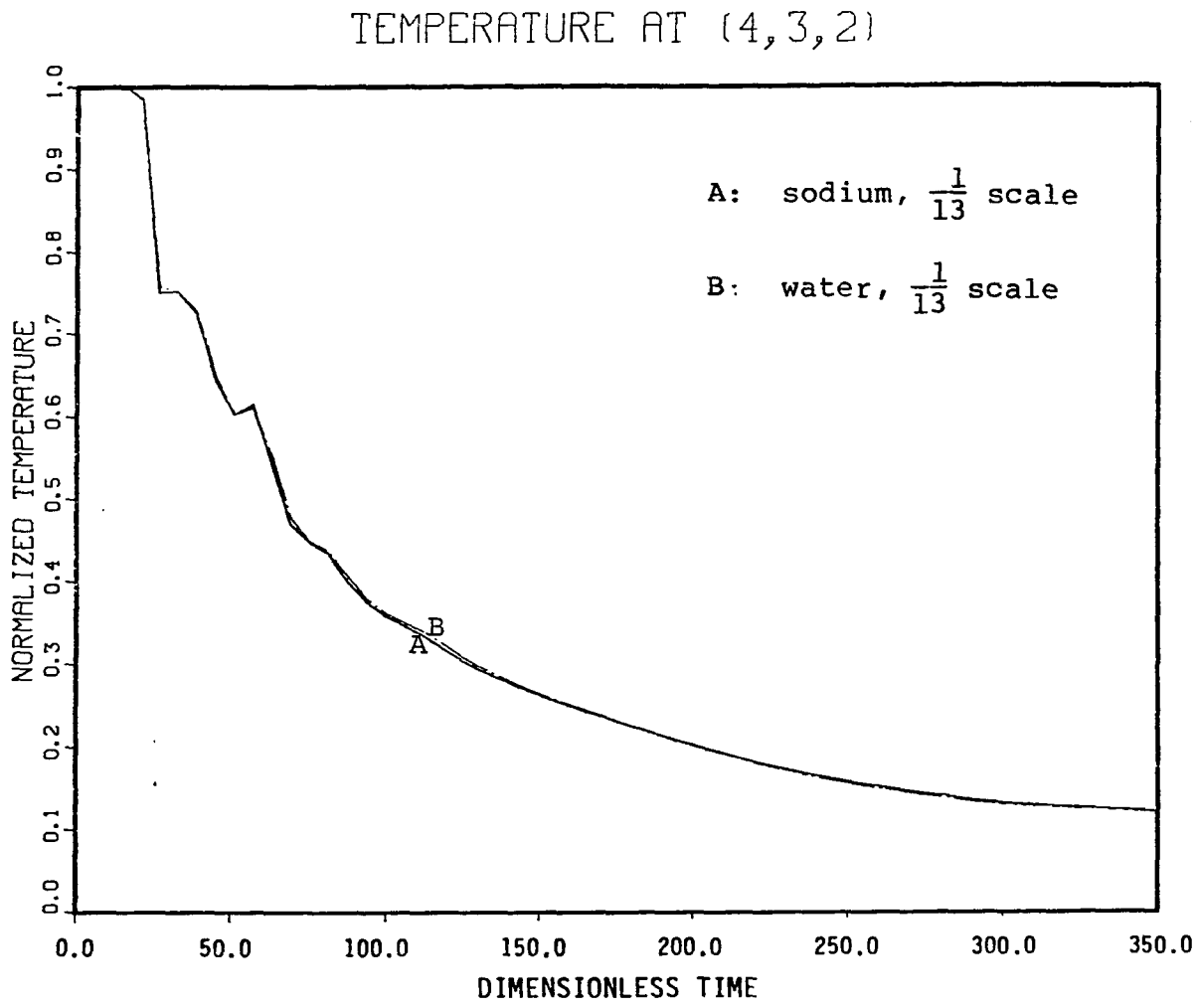

Figure 42. Normalized temperature transient at (4,3,2) for case I

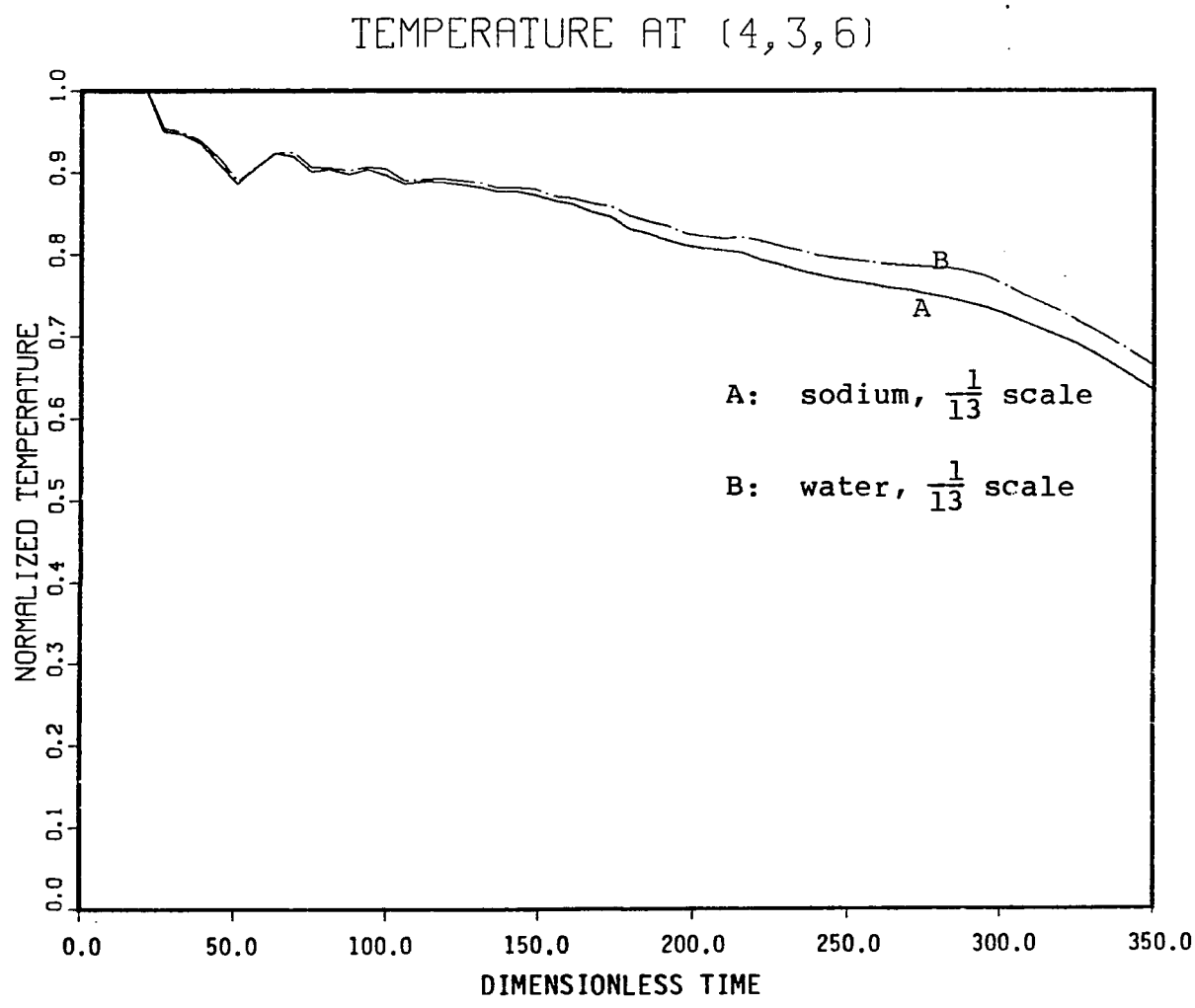

Figure 43. Normalized temperature transient at (4,3,6) for case I

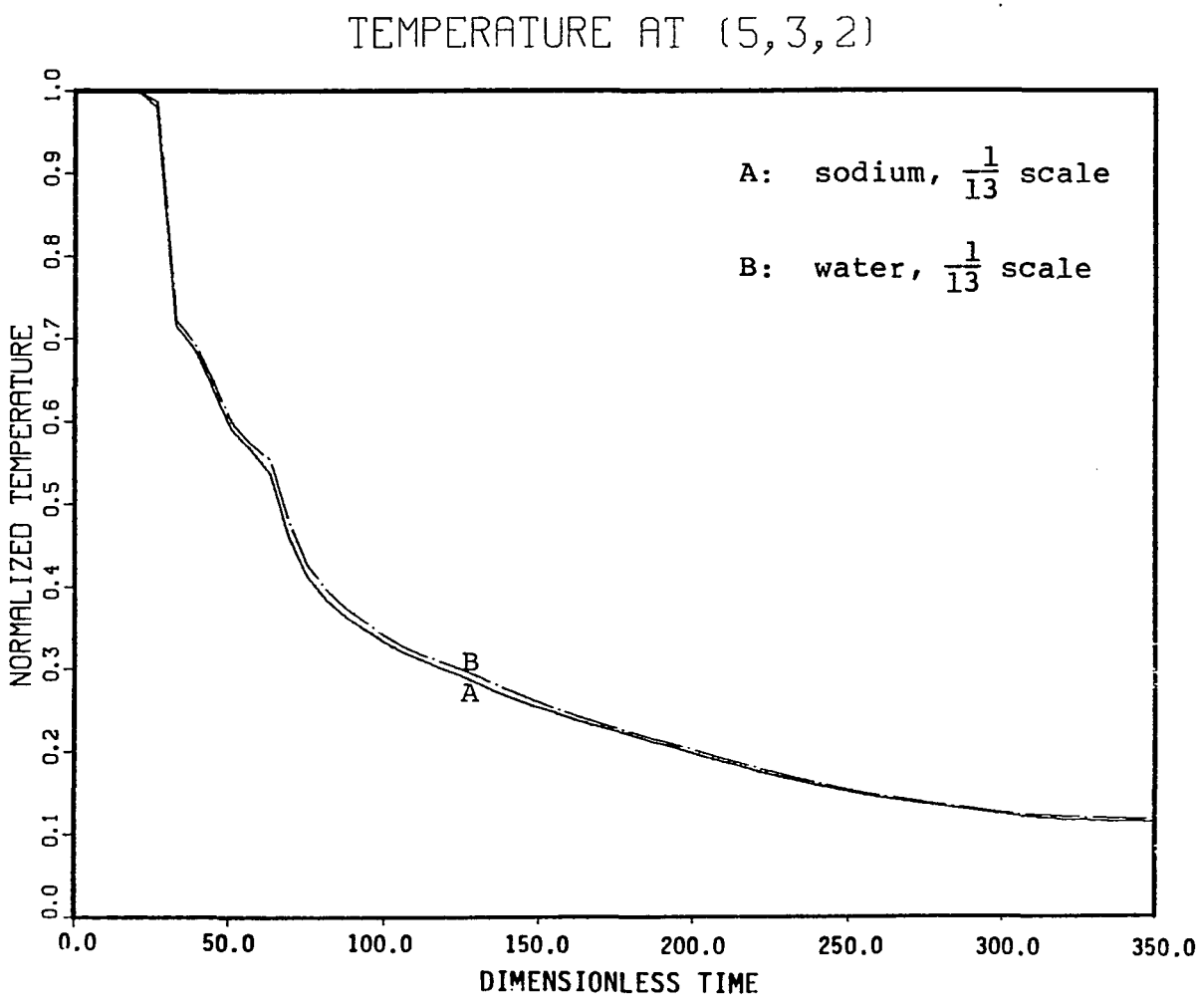

Figure 44. Normalized temperature transient at (5,3,2) for case I

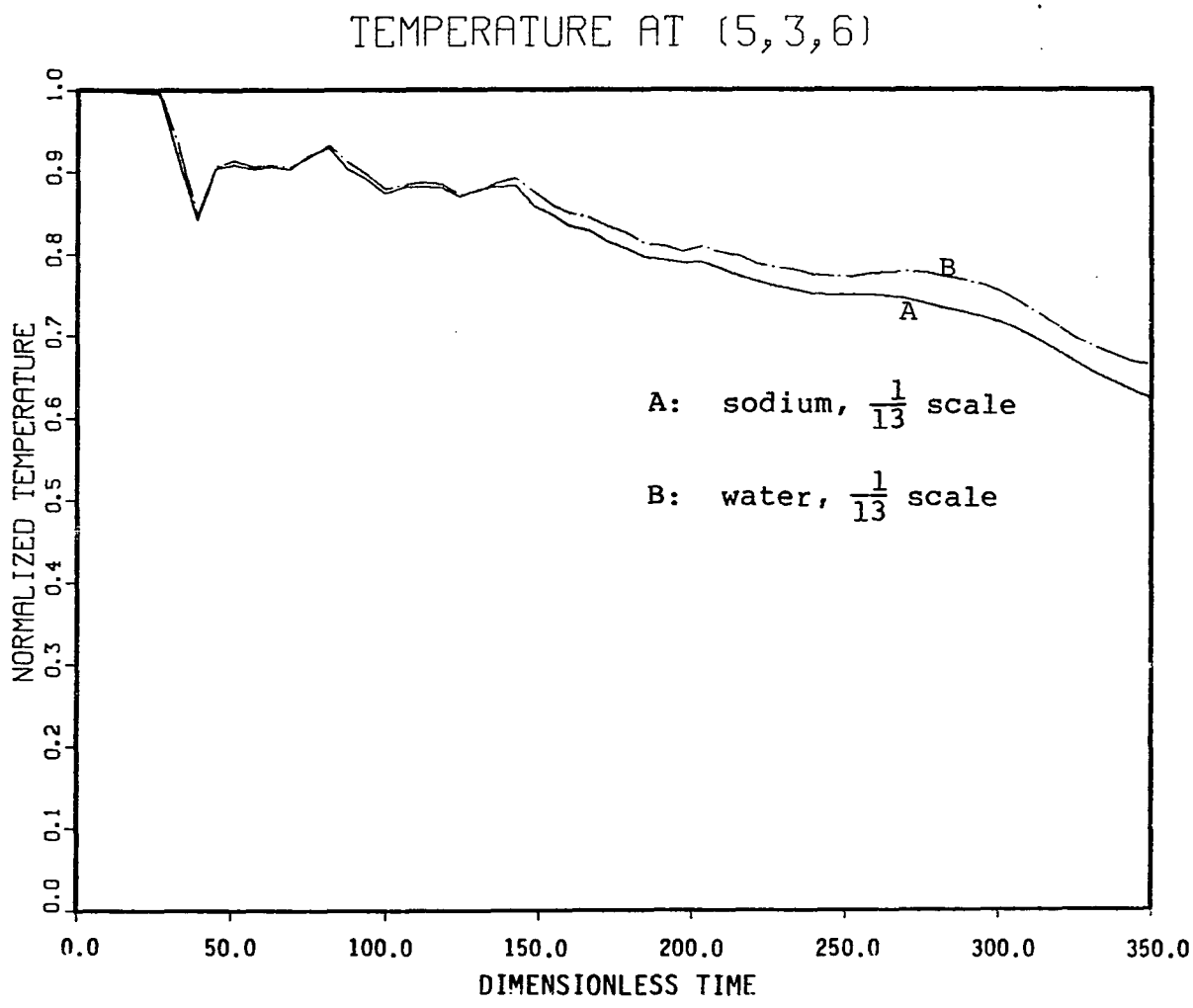

Figure 45. Normalized temperature transient at (5,3,6) for case I

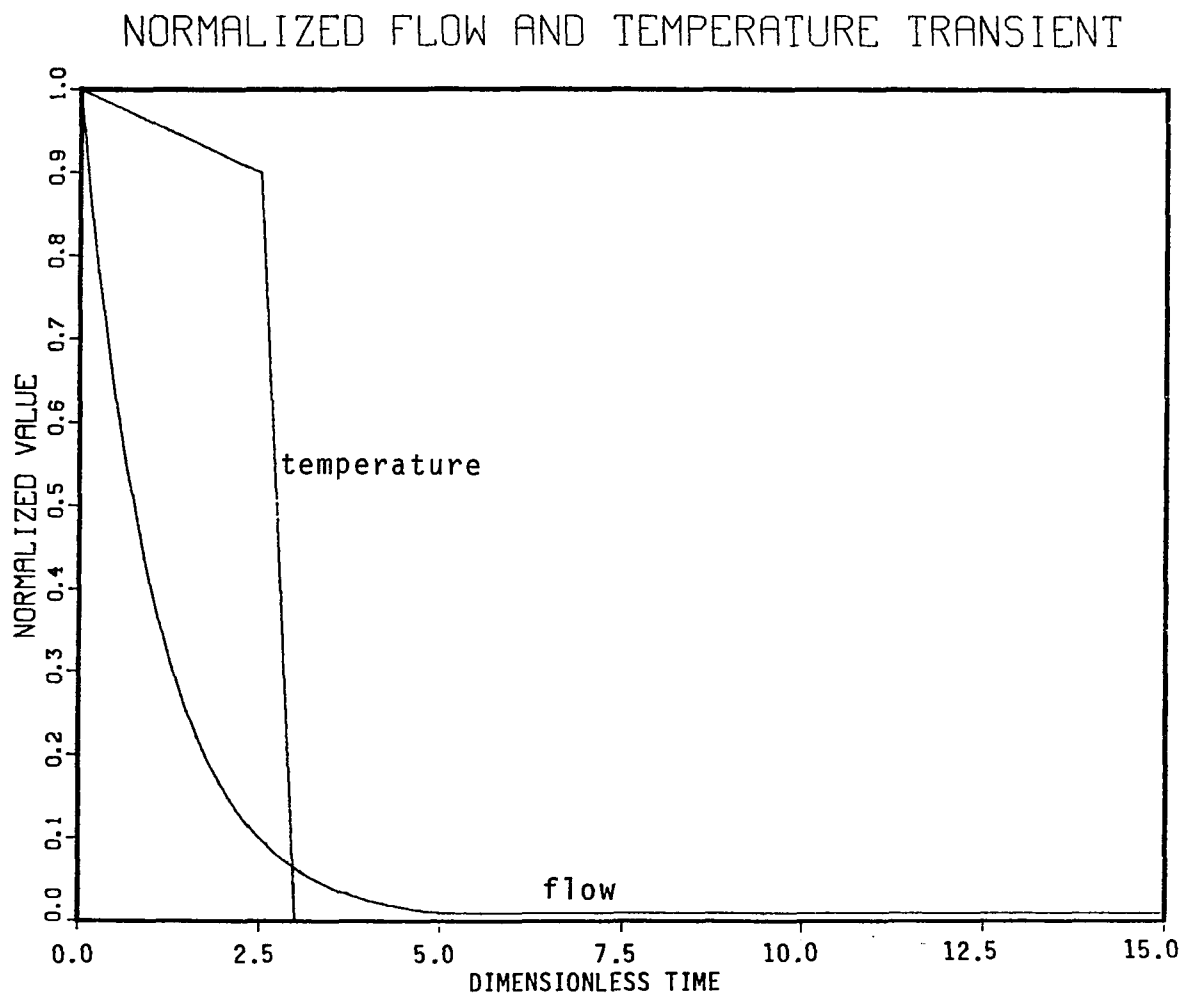

Figure 46. Normalized flow and temperature transient for case II

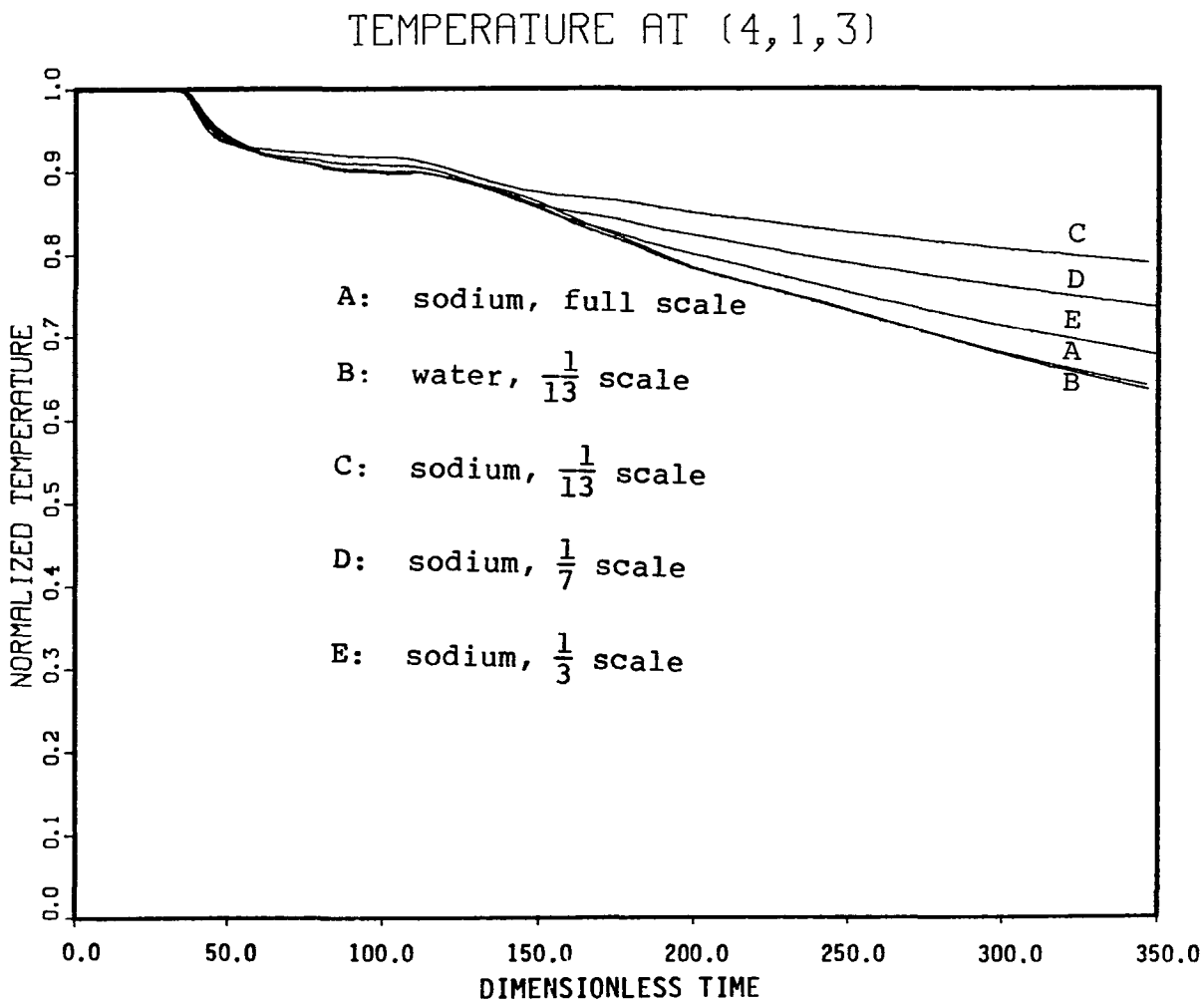

Figure 47. Normalized exit temperature transient for case II

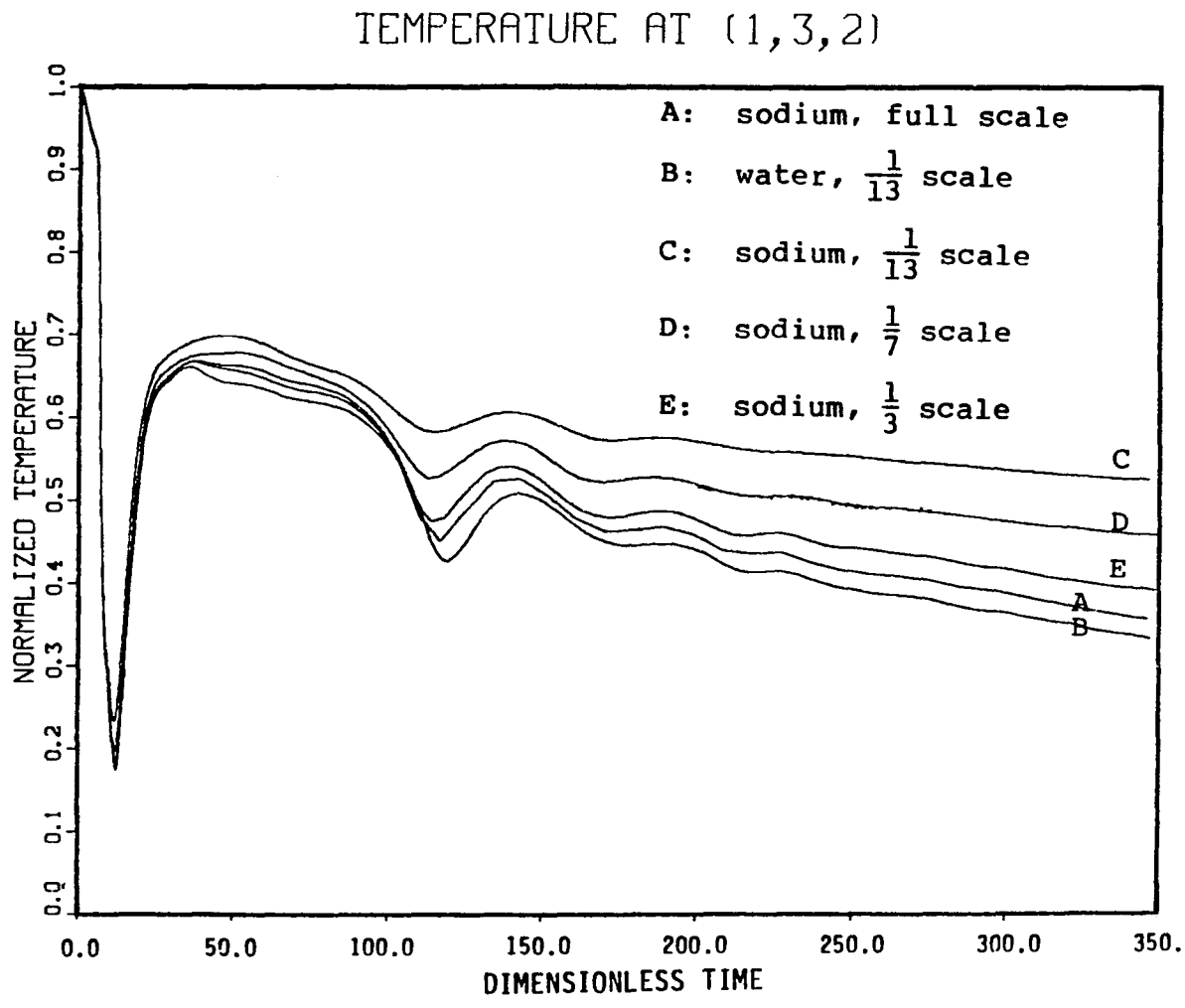

Figure 48. Normalized temperature transient at (1,3,2) for case II

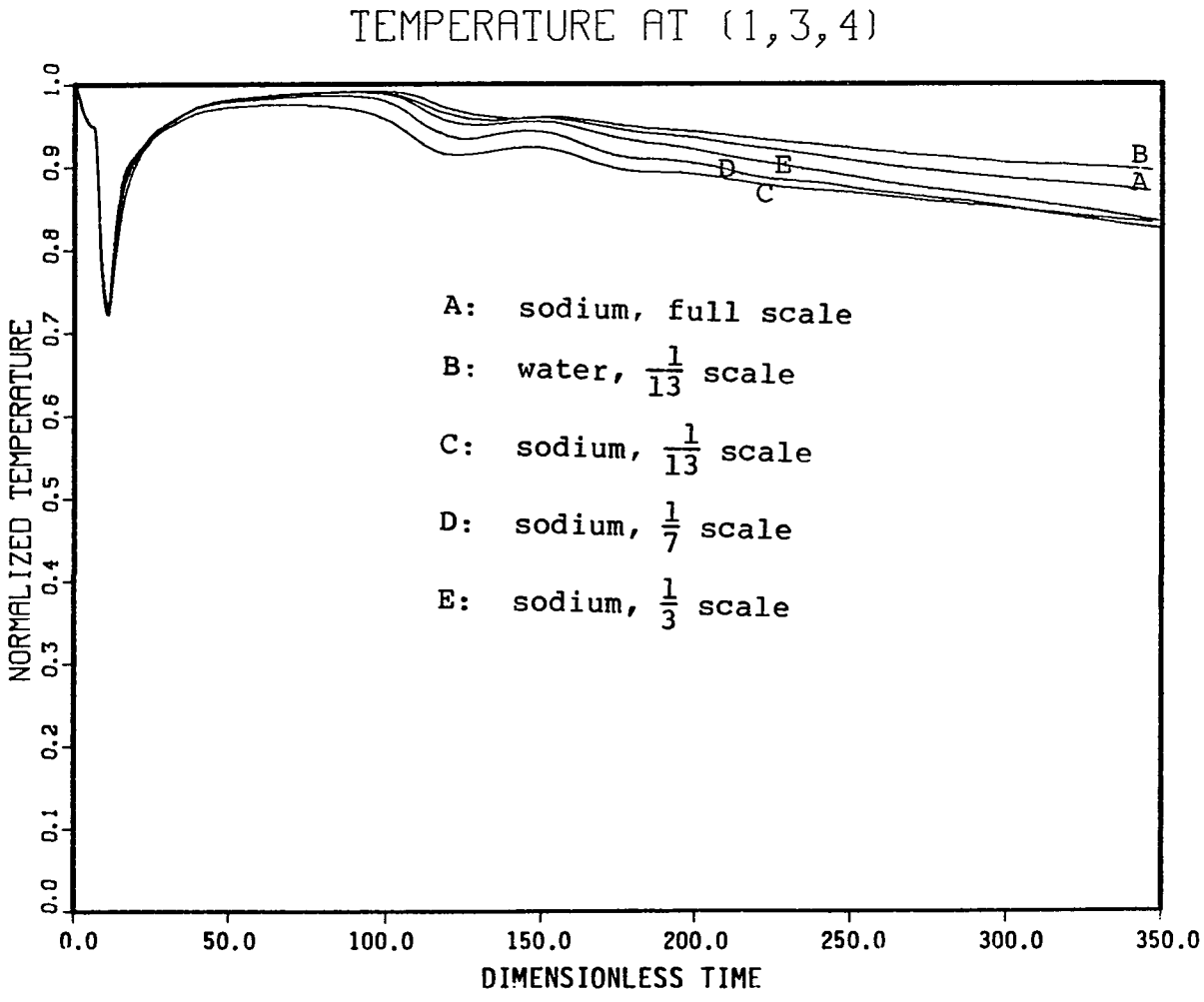

Figure 49. Normalized temperature transient at (1,3,4) for case II

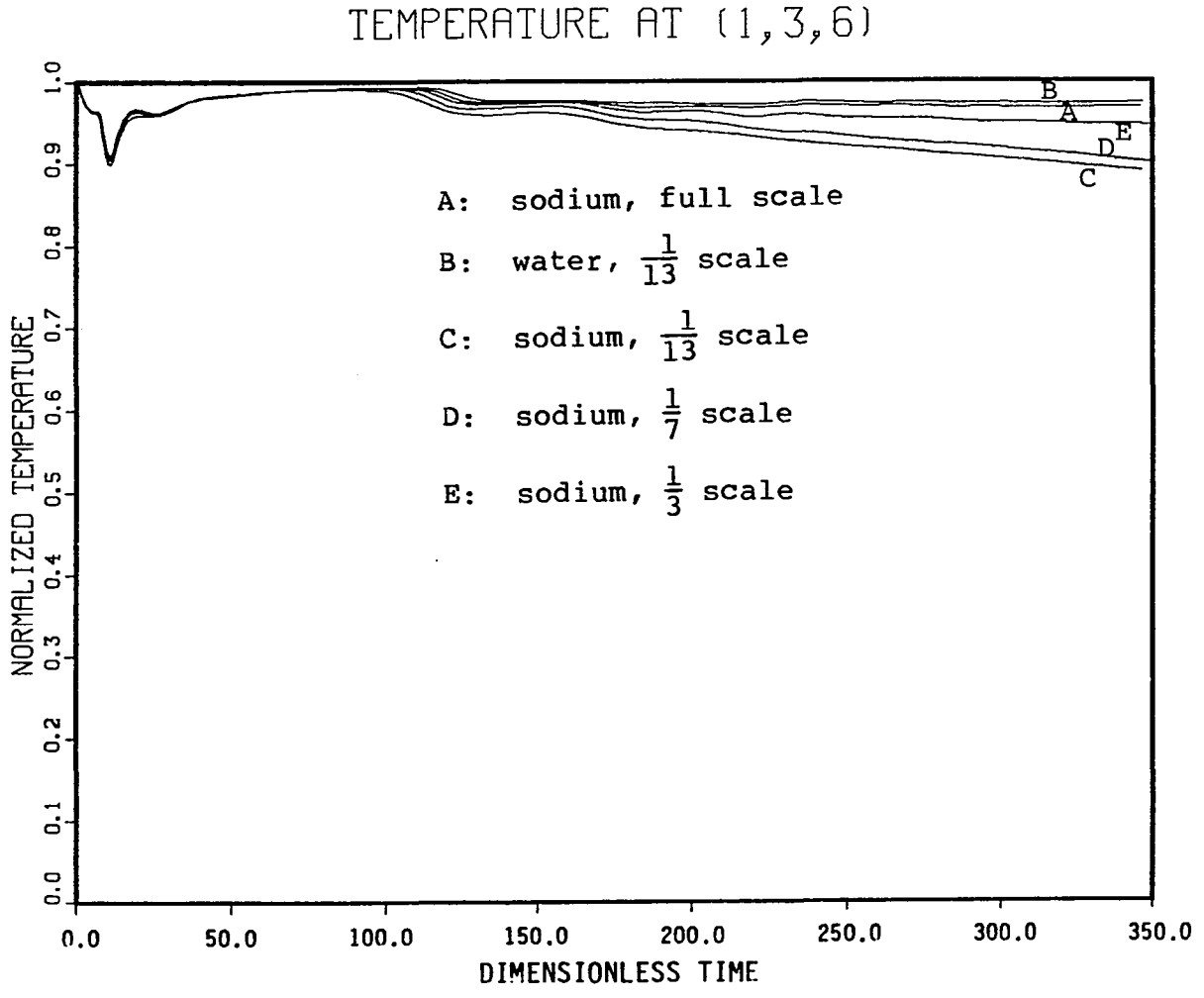

Figure 50. Normalized temperature transient at (1,3,6) for case II

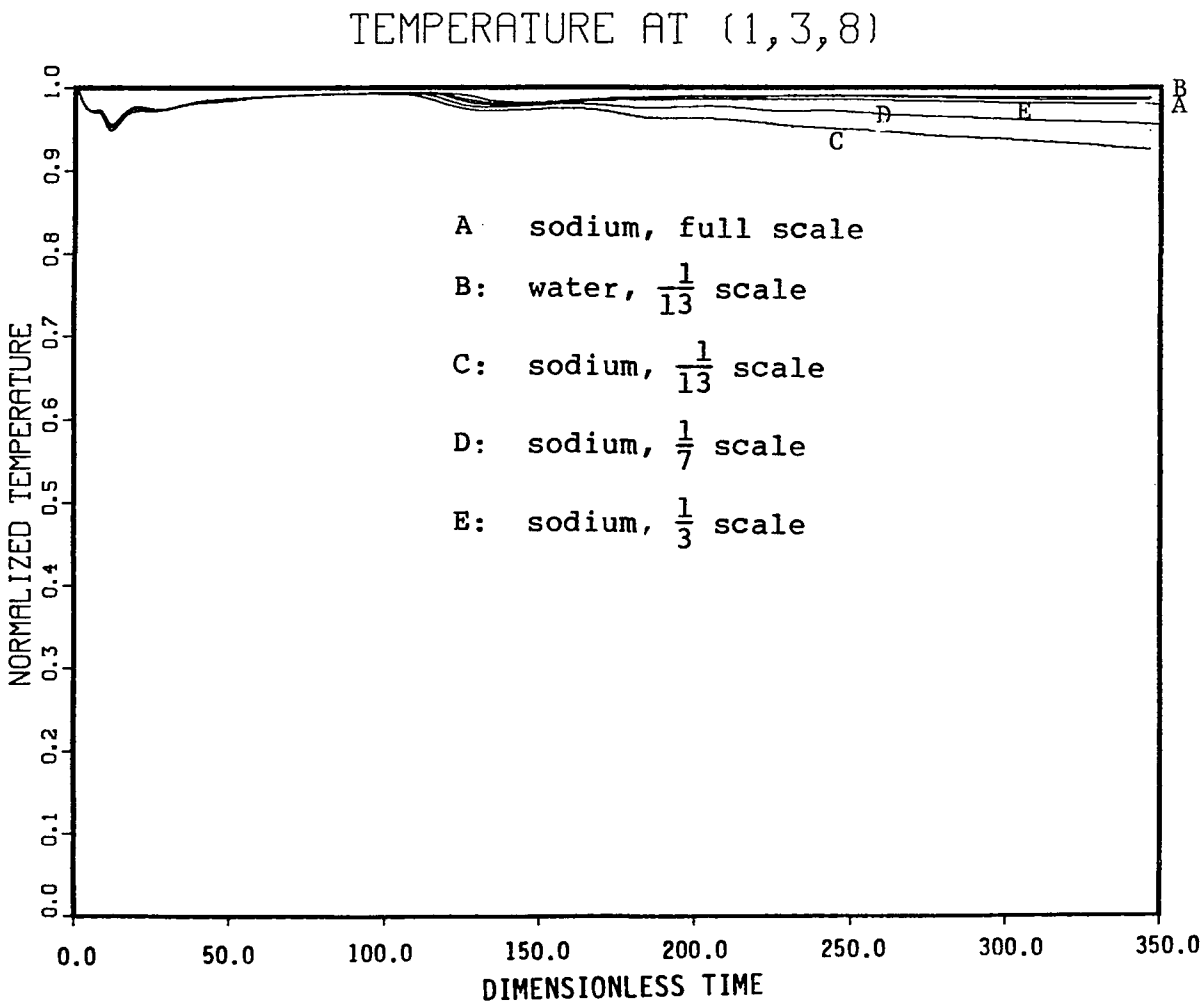

Figure 51. Normalized temperature transient at (1,3,8) for case II

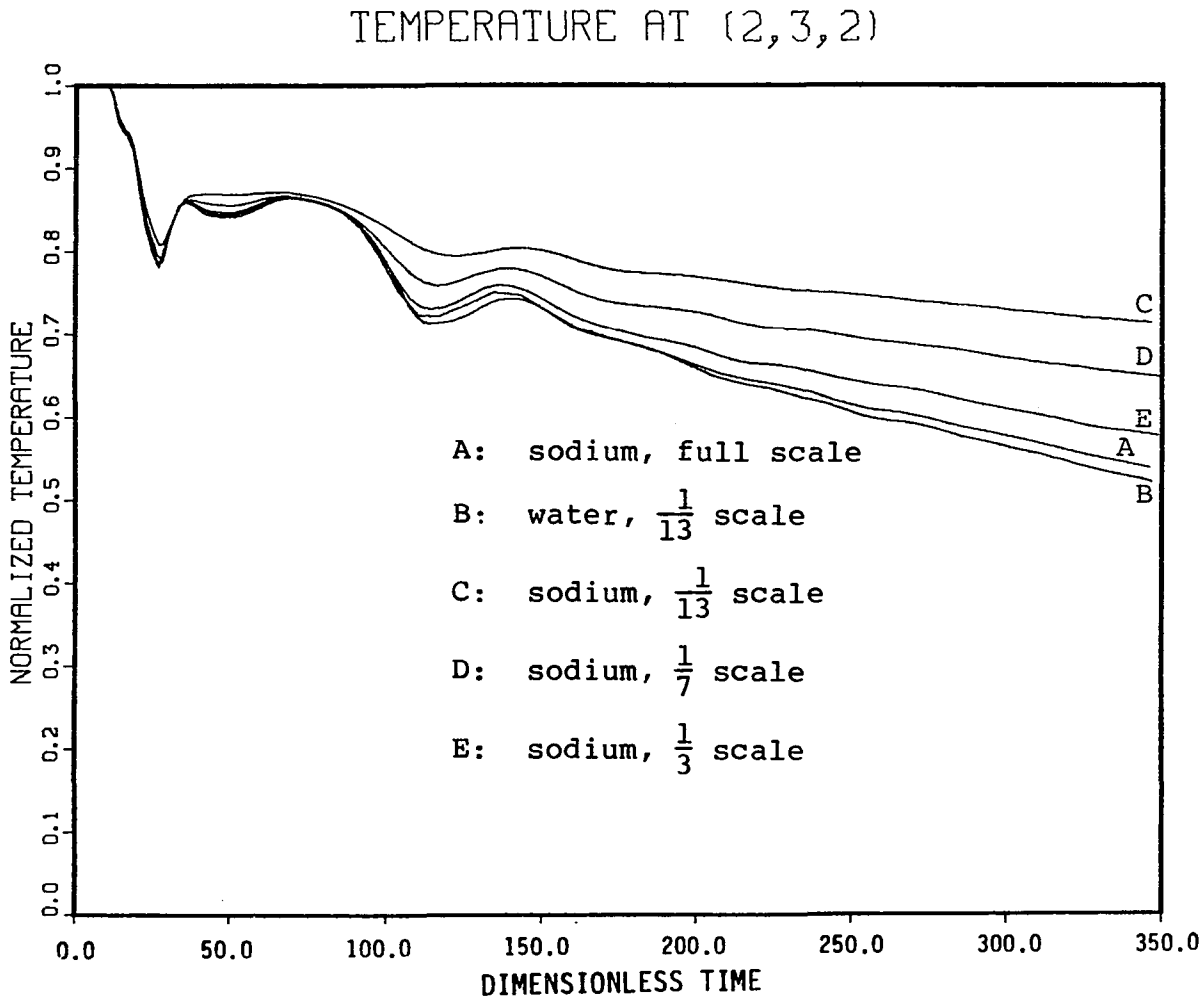

Figure 52. Normalized temperature transient at (2,3,2) for case II

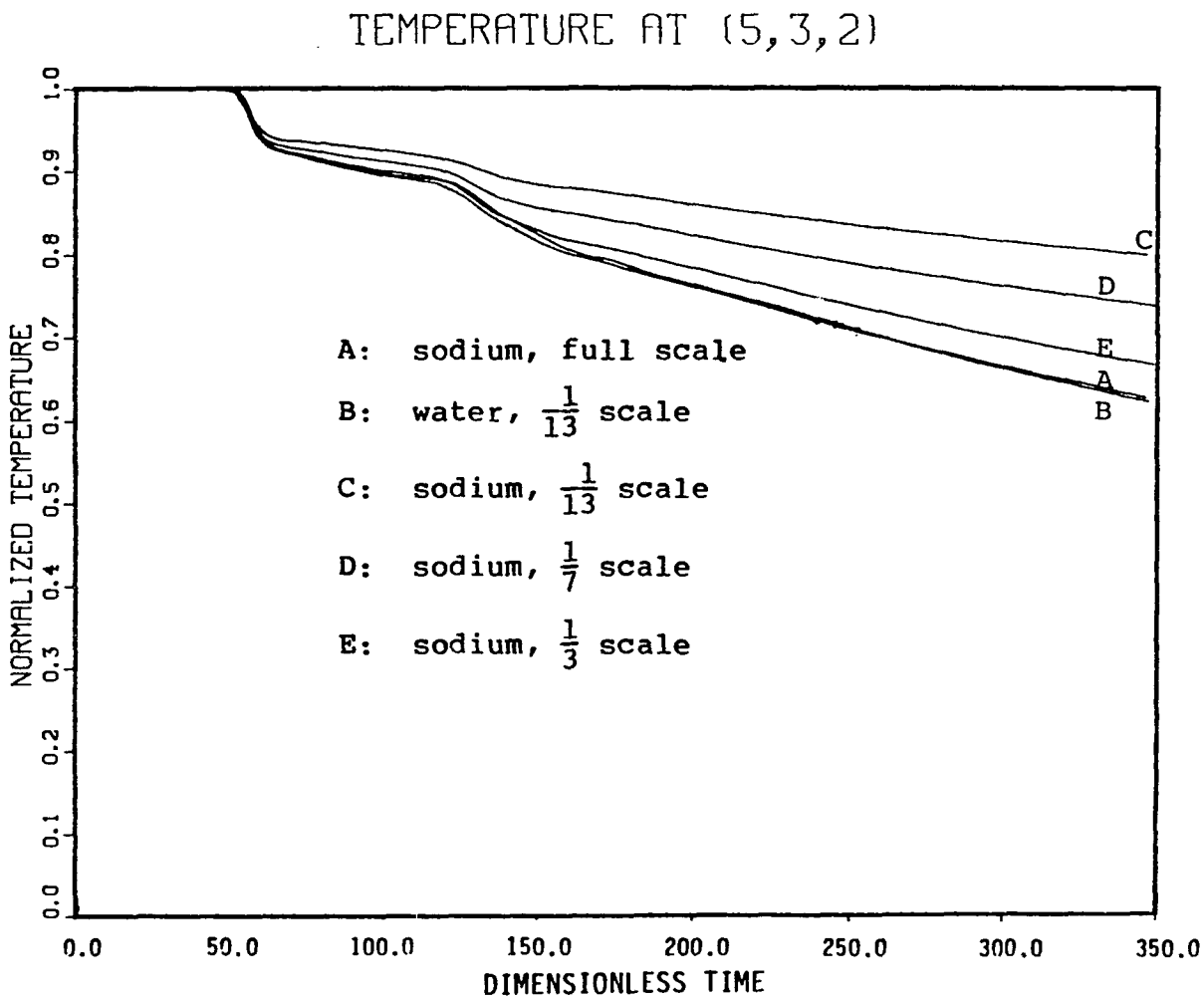

Figure 53. Normalized temperature transient at (5,3,2) for case II

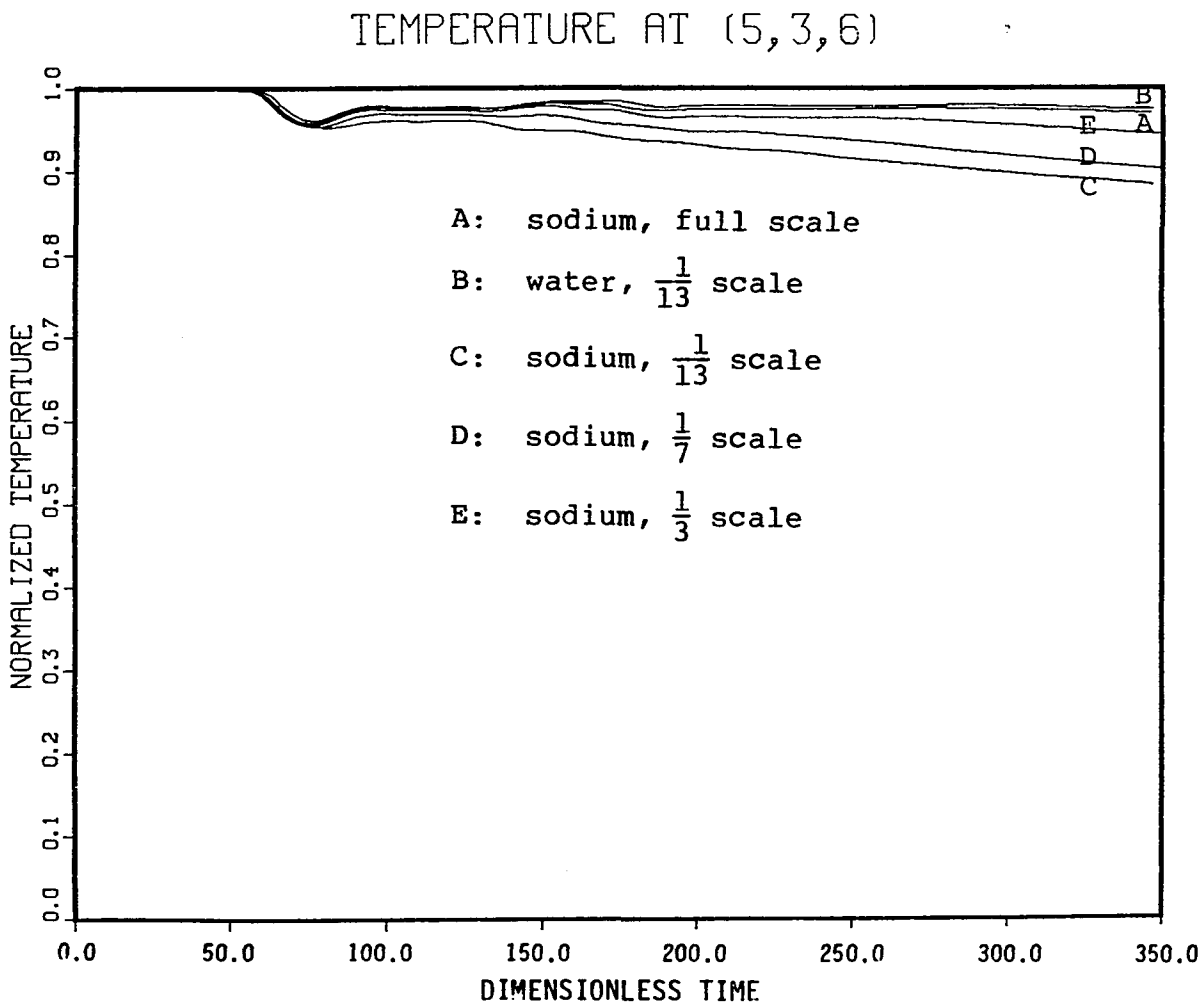

Figure 54. Normalized temperature transient at (5,3,6) for case II

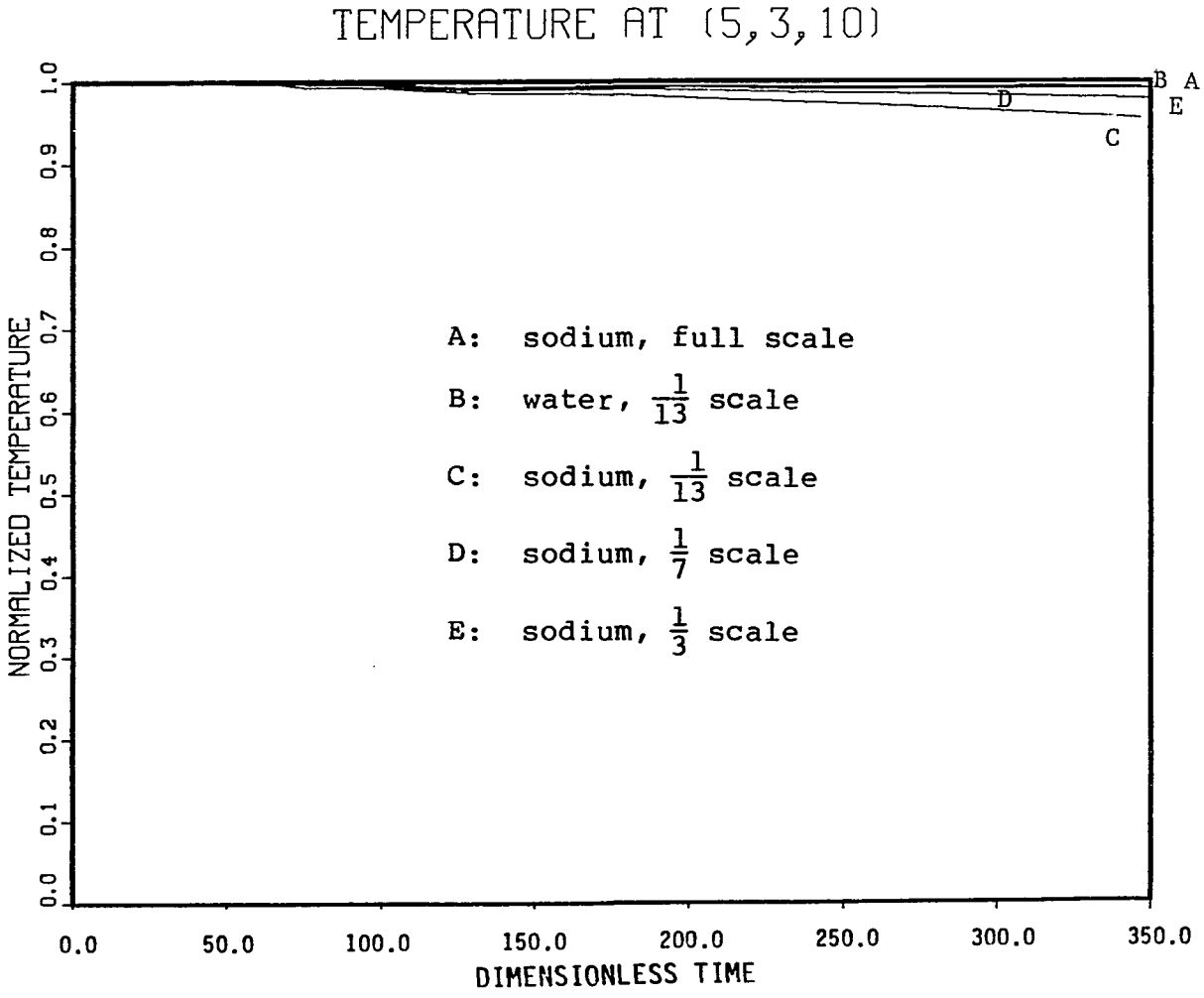

Figure 55. Normalized temperature transient at (5,3,10) for case II

D. Peclet Number and the Scaling Laws

In order to determine the threshold Peclet number below which heat transfer is influenced by conduction, a simplified, one-dimensional analysis is presented.

Under stratified, low flow conditions, the temperature pattern is mainly influenced by:

(1) Thermal conduction between hot and cold layers.

(2) Convection due to incoming flow

Consider a tank which is isothermal. Now if cold fluid is pumped into the tank from the bottom and the hot fluid is drawn out from the top of the tank, the heat transfer process between the hot and cold layers in the tank can be expressed approximately by the equation:

$$\rho C v \frac{\partial T}{\partial Z} = -k \frac{d^2 T}{dZ^2} \tag{68}$$

where

T = temperature of the fluid

ρ = density of the fluid

C = specific heat of the fluid

v = velocity

k = thermal conductivity

Z = axial coordinate

t = time

The ratio of conductive to convective heat transfer is given by R, where

$$R = kL \frac{\partial T}{\partial \eta} \Big/ (\rho c v T) \tag{69}$$

where $\eta = \frac{Z}{L}$

L = characteristic length

A solution of eg. (68) for a unit step change in temperature over a small length L is:

$$T = \frac{\exp\ (-\ cvL\eta/k)\ -\ 1}{\exp\ (-\ cvL/k)\ -\ 1} \tag{70}$$

Here CvL/k is defined as the Peclet number, Pe.

$$\text{Hence } T = \frac{\exp\ (-Pe\eta)\ -\ 1}{\exp\ (-Pe)\ -1} \tag{71}$$

Inserting Eq. (70) into Eq. (69), one has the following expression for the ratio of conductive to convective heat transfer in the stratified flow:

$$R = \frac{\exp\ (-Pe\eta)}{1\ -\ \exp\ (-Pe\eta)} \tag{72}$$

The heat transfer ratio R for $\eta = 0.5$ is plotted in Figure 56. As can be seen, the ratio of conduction to convection heat transfer increases as the Peclet number decreases.

Consider the Case I study where the flow decreased from 100 to 10 . The Peclet numbers for the sodium and the water models were 11 and 2620 respectively. The corresponding ratio of conduction to

convection is relatively small for both fluids. Hence, the conservation of the Richardson Number only will give accurate predictions for a prototype under a 100%-10% flow transient.

Table 5 gives the Peclet numbers and the corresponding conduction to convection ratios for the Case II 100%-1% flow transient. The magnitudes of R for both the prototype and the 1/13 water model are small while all scales of the sodium model give relatively large R values. The large R value implies that the temperature field is influenced by conduction.

As can be seen in Figure 56, the influence of conduction can not be ignored as the Peclet falls below 10.

It should be noted that Eqs. (68) to (72) only provide an estimate of relative importance of conduction to convection for one-dimensional, low velocity flow. For highly turbulent flow, Eqs. (68) to (72) are not applicable. The heat transfer correlation of axisymmetric stagnant flow can be found in Reference [18] and are not discussed here.

Table 5. Convection to connection ratio for the 100%-1% flow transient simulation

Parameter	Prototype	1/13 Scale Water	1/13 Scale Sodium	1/7 Scale Sodium	1/3 Scale Sodium
Final Inlet velocity (m/sec)	2.782×10^{-2}	4.461×10^{-3}	7.716×10^{-3}	1.052×10^{-2}	1.606×10^{-2}
Final flow rate (m^3/sec)	1.64×10^{-1}	1.56×10^{-4}	2.69×10^{-4}	1.265×10^{-3}	1.052×10^{-2}
Effective upper plenum cross-sectional area (m^2)	287.3	1.7	1.7	5.86	31.9
Hot-cold interface velocity (m/sec)	5.7×10^{-4}	9.18×10^{-5}	1.6×10^{-4}	$2,16 \times 10^{-4}$	3.3×10^{-4}
Characteristic length (m)	5.642	0.434	0.434	0.806	1.881
Final Peclet Number	49	262	1.1	2.7	9.5
R-Ratio	2×10^{-11}	$1. \times 10^{-57}$	1.4	0.35	8.7×10^{-4}

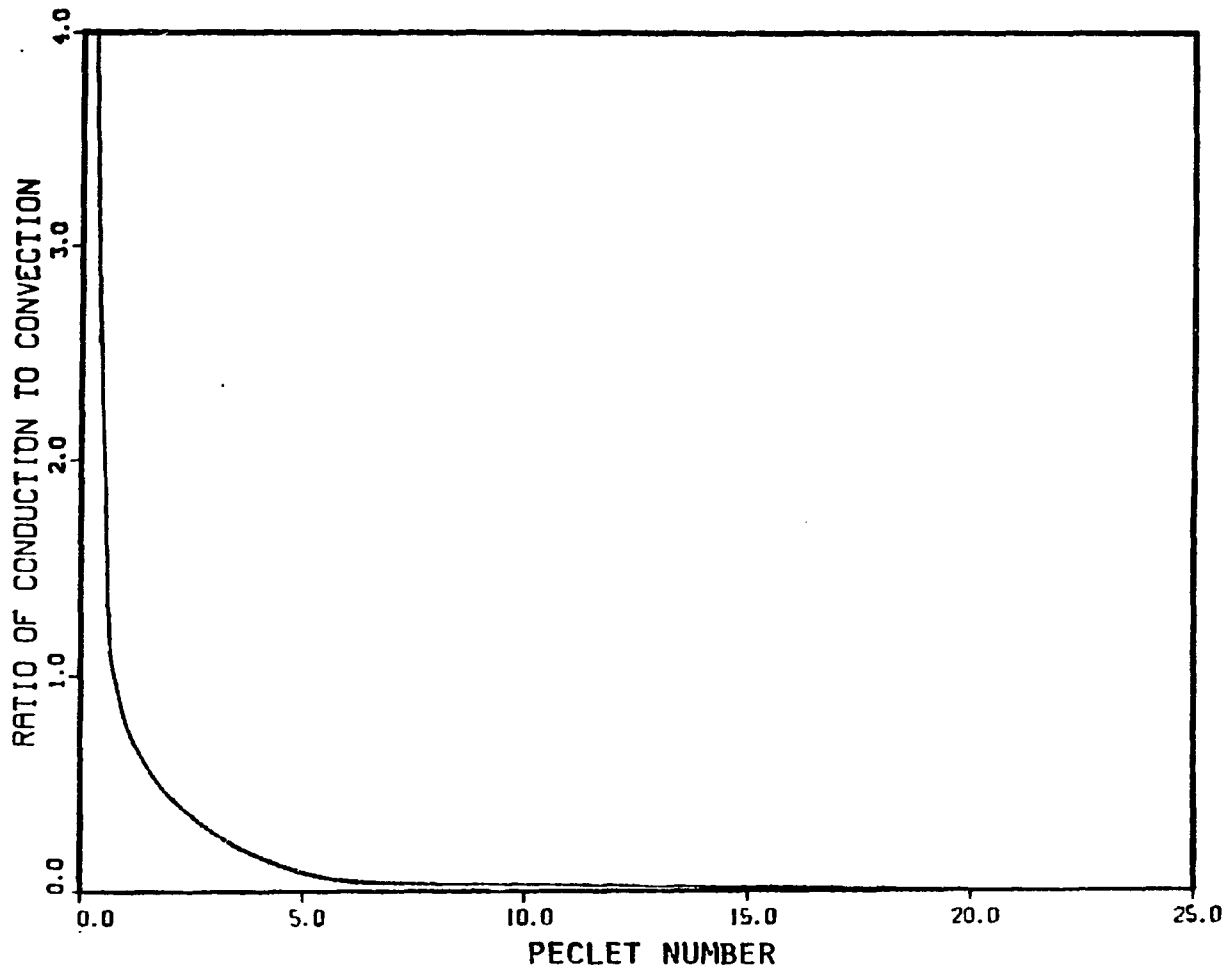

Figure 56. Ratio of conduction to convection

V. CONCLUSION

Scale model experiments are usually faster and cost less than full-scale experiments. Yet, if properly designed and executed, they yield sufficient information for correct engineering decisions.

The fundamental requirement of scale modeling is that the model and prototype must be governed by the same physical laws. Hence, before a model can be designed, the physical laws governing the prototype must be known.

Based on this study, it was found that the importance of each similitude parameter can be determined by a detailed, three-dimensional transient computer simulation for low-flow, stratified conditions.

To extend water test data to prototype behavior under such conditions was once questioned due to the low thermal conductivity of water. This work, however, concluded that water test is adequate for the prediction of full scale LMFBR upper plenum thermohydraulic behavior under such conditions. It was also found that the results of reduced-scale sodium simulation could be misleading because of the temperature distortion due to heat conduction between hot and cold layers. The discrepancy of the rate of exit temperature change could be as high as 50 . If the scaled sodium simulation is applied, the components could be exposed to unwarranted thermal stresses. Also, it takes a much longer time for the reactor upper

plenum to cool down than the prediction of the sodium model. Hence, there is no benefit of using a costly reduced-scale sodium test facility.

It is also concluded that the threshold Peclet number above which convection dominates the heat transfer is estimated to be about 10. If the Peclet number is smaller than 10, the influence of conductive heat transfer can not be ignored.

This study also revealed that the PLENMIX code can be a powerful tool in parametric and optimization studies of reactor upper plenum design and hence reduce any investments in experimental facilities.

VI. SUGGESTIONS FOR FUTURE STUDY

As has been shown, the three-dimensional computer code PLENMIX can give accurate results of the actual transient behavior of a LMFBR upper plenum. These simulations can reduce costly experiments. However, further work should be done in the following areas:

(1) Parametric studies should be run which show the influence of the plenum wall heat capacity, density, thermal conductivity and heat transfer coefficient upon the temperature pattern.

(2) Application of the method presented in this report could be used on a reactor lower plenum, on reactor piping and on other components.

(3) Similitude studies of the upper plenum thermohydraulic transients using NaK as a test fluid can be investigated. Since the thermal conductivity of NaK is smaller than sodium, there is a possibility that a reduced scale NaK test can accurately predict the full-scale prototype under buoyancy dominated, natural convective flow conditions.

VII. REFERENCES

1. P.A. Howard and K. K. Shiu, "Mixing Studies for Geometric Variations of a 1/15 Scale Loop - Type Plenum," ANL-CT-80-6, Nov. 1979.

2. P. A. Howard and J. A. Haried, "Mixing in a Pool-Type PLBR after a Scram," ANL-CT-79-36, June 1979.

3. M. Heisler and R. Singer, "Facility Requirement for Natural Convection Shutdown Heat Removal System Specialist Meeting on Natural Convection Heat Transfer," Brookhaven National Laboratory, Nov. 1980.

4. J. J. Lorenz, R. D. Carlson, and P. A. Howard, "An Investigation of LMFBR Outlet Plenum Thermal-Hydraulic Behavior During Reactor Scram Transients," ANL-CT-76-18, Sept. 1979.

5. J. A. Carr and L. J. Flanigan, "CRBR Outlet Plenum Flow Stratification Study," Battelle-Columbus Laboratory Report, Dec. 1975.

6. J. J. Lorenz, R. D. Carlson and P. A. Howard, "The Influence of Scale Size and Fluid Thermal Properties in Simulating LMFBR Outlet Plunum Behavior," AICHE Paper No. 34, 1976. National Heat Transfer Conference, St. Louis, July, 1976.

7. P. A. Howard and K. K. Shiu, " Conceptual Design Studies: Phase I: Plenum and Pool Mixing Studies," ANL-CT-79-17, Feb. 1979.

8. H. M. Domenus, "COMMIX-1A: A Three Dimensional Transient Single Phase Component Computer Program for Thermal-Hydraulic Analysis," to be published by ANL.

9. P. A. Howard and J. J. Carbajo, "Plenum-2A: A Program for Transient Analysis of LMFBR Outlet Plenum," ANL-CT-79-17, Feb. 1979.

11. W. C. Rivard and M. D. Torrey," K-Fix: A Computer Program for Transient Two-Dimensional Two-Fluid Flow," LA-NUREG-6623, Nov. 1976.

11. G. H. Golden and J. V. Tokar, "Thermophysical Properties of Sodium," ANL-7323, Aug. 1967.

12. J. H. Keenan, F. G. Keyes, P. G. Hill and J. G. Moore, Steam Tables (John Wiley and Sons, Inc., New York, 1969).

13. R. Nijsing and W. Eifler, "Temperature Fields in Liquid Metal Cooled Assemblies," Prog. Heat Mass Transfer 7.115 (1973).

14. W. T. Sha and B. E. Launder, "A General Model for Turbulent Momentum and Heat Transport in Liquid Metals," ANL-77-78, Nov. 1977.

15. S. J. Kline, Similtude and Approximation Theory, (McGraw-Hill Book Company, New York, 1965)

16. D. J. Schuring, Scale Models In Engineering, (Pergamon Press, New York, 1977).

17. G. Murphy, "Similitude in Engineering," (Ronald Press, New York, 1950).

18. W. M. Rohsenow and J. P. Hartnett, "Handbook of Heat Transfer," (McGraw-Hill Book Company, New York, 1973).

VIII. ACKNOWLEDGMENTS

The author wishes to express his gratitude to Dr. Alfred F. Rohach for his guidance and encouragement through his graduate study.

The author wishes to acknowledge the late Professor Paul Barcus for his review and valuable suggestions.

The author also wishes to thank Dr. Paul A. Howard of Argonne National Laboratory and Dr. Alvin T. Shih of General Electric Company for their valuable discussions and suggestions.

The author extends thanks to Argonne National Laboratory which gave him support.